Evaluation of the City of Scottsdale Loop 101 Photo Enforcement Demonstration Program

Final Report AZ-684

Prepared by:
Simon Washington, Ph.D.
Kangwon Shin
Ida van Schalkwyk
Arizona State University
Department of Civil & Environmental Engineering
Tempe, AZ

November 2007

Prepared for:
Arizona Department of Transportation
206 South 17th Avenue
Phoenix, Arizona 85007
in cooperation with
U.S. Department of Transportation
Federal Highway Administration

Technical Report Documentation Page

1. Report No. AZ-07-684	2. Government Accession No.	3. Recipient's Catalog No.
4. Title and Subtitle Evaluation of the City of Scottsdale Loop 101 Photo Enforcement Demonstration Program		5. Report Date November 2007 6. Performing Organization Code
7. Authors Dr. Simon Washington, Kangwon Shin, and Ida van Schalkwyk		8. Performing Organization Report No.
9. Performing Organization Name and Address Arizona State University Department of Civil & Environmental Engineering Tempe, AZ 85287-5306		10. Work Unit No. 11. Contract or Grant No. T0749A0022
12. Sponsoring Agency Name and Address Arizona Department Of Transportation 206 S. 17th Avenue, Phoenix, Arizona 85007		13.Type of Report & Period Covered Final Report 14. Sponsoring Agency Code

15. Supplementary Notes

Prepared in cooperation with the U.S. Department of Transportation, Federal Highway Administration

16. Abstract

Speeding is recognized as one of the most important factors causing traffic crashes. In 2005, 30% of all fatal crashes were speeding-related (National Highway Traffic Safety Administration 2005). According to NHTSA, the cost of speed-related crashes is estimated to be $40.4 billion per year (National Highway Traffic Safety Administration 2005). Intelligent Transportation Systems (ITS) now exist to reduce speeding-related crashes by enforcing speed limits with camera-based technologies. These enforcement technologies are generically called "speed cameras" and have been effective on municipal streets and arterials in Arizona.

The City of Scottsdale began automated enforcement efforts in December of 1996. On October 25, 2005, the Scottsdale City Council approved the nine-month *speed enforcement camera demonstration program* on a 7.8-mile stretch of the SR 101 segment within Scottsdale. The speed enforcement program (SEP) began on January 22, 2006 and ended on October 23, 2006. The demonstration program on the SR 101 freeway segment in Scottsdale is the first use of the fixed-site photo enforcement equipment on a freeway in Arizona and is believed to be the first in the nation.

This study was conducted to estimate the impact of the SEP on traffic safety, speed, speeding behavior, and daily travel time uncertainty. More specifically, the objectives were to estimate: the impact of the SEP on speeding behavior; the changes in mean speed due to the SEP; the impact of the SEP on traffic safety in the enforcement zone; the total travel time impacts; and the economic impacts of the safety effects.

17. Key Words	18. Distribution Statement	23. Registrant's Seal
Photo enforcement, speeding, safety, red light running, Empirical Bayes', before-after study, travel time savings, motor vehicle crashes	Document is available to the U.S. public through the National Technical Information Service, Springfield, Virginia 22161	

19. Security Classification	20. Security Classification	21. No. of Pages	22. Price
Unclassified	Unclassified	154	

SI (MODERN METRIC) CONVERSION FACTORS*

APPROXIMATE CONVERSIONS TO SI UNITS

Symbol	When You Know	Multiply By	To Find	Symbol
	LENGTH			
in	inches	25.4	millimeters	mm
ft	feet	0.305	meters	m
yd	yards	0.914	meters	m
mi	miles	1.61	kilometers	km
	AREA			
in^2	square inches	645.2	square millimeters	mm^2
ft^2	square feet	0.093	square meters	m^2
yd^2	square yards	0.836	square meters	m^2
ac	acres	0.405	hectares	ha
mi^2	square miles	2.59	square kilometers	km^2
	VOLUME			
fl oz	fluid ounces	29.57	milliliters	mL
gal	gallons	3.785	liters	L
ft^3	cubic feet	0.028	cubic meters	m^3
yd^3	cubic yards	0.765	cubic meters	m^3
	NOTE: Volumes greater than 1000L shall be shown in m^3.			
	MASS			
oz	ounces	28.35	grams	g
lb	pounds	0.454	kilograms	kg
T	short tons (2000lb)	0.907	megagrams (or "metric ton")	mg (or "t")
	TEMPERATURE (exact)			
°F	Fahrenheit temperature	5(F-32)/9 or (F-32)/1.8	Celsius temperature	°C
	ILLUMINATION			
fc	foot candles	10.76	lux	lx
fl	foot-Lamberts	3.426	candela/m^2	cd/m^2
	FORCE AND PRESSURE OR STRESS			
lbf	poundforce	4.45	newtons	N
lbf/in^2	poundforce per square inch	6.89	kilopascals	kPa

APPROXIMATE CONVERSIONS FROM SI UNITS

Symbol	When You Know	Multiply By	To Find	Symbol
	LENGTH			
mm	millimeters	0.039	inches	in
m	meters	3.28	feet	ft
m	meters	1.09	yards	yd
km	kilometers	0.621	miles	mi
	AREA			
mm^2	Square millimeters	0.0016	square inches	in^2
m^2	Square meters	10.764	square feet	ft^2
m^2	Square meters	1.195	square yards	yd^2
ha	hectares	2.47	acres	ac
km^2	Square kilometers	0.386	square miles	mi^2
	VOLUME			
mL	milliliters	0.034	fluid ounces	fl oz
L	liters	0.264	gallons	gal
m^3	Cubic meters	35.315	cubic feet	ft^3
m^3	Cubic meters	1.308	cubic yards	yd^3
	MASS			
g	grams	0.035	ounces	oz
kg	kilograms	2.205	pounds	lb
mg	megagrams (or "metric ton")	1.102	short tons (2000lb)	T
	TEMPERATURE (exact)			
°C	Celsius temperature	1.8C + 32	Fahrenheit temperature	°F
	ILLUMINATION			
lx	lux	0.0929	foot-candles	fc
cd/m^2	candela/m^2	0.2919	foot-Lamberts	fl
	FORCE AND PRESSURE OR STRESS			
N	newtons	0.225	poundforce	lbf
kPa	kilopascals	0.145	poundforce per square inch	lbf/in^2

SI is the symbol for the International System of Units. Appropriate rounding should be made to comply with Section 4 of ASTM E380

Table of Contents

List of Tables

List of Figures

List of Acronyms

AADT	Annual Average Daily Traffic
ADOT	Arizona Department of Transportation
AZDPS	Arizona Department of Public Safety
BA	Before-and-After
BF	Brown-Forsythe
CBD	Central Business District
CDF	Cumulative Distribution Function
CI	Confidence Interval
DPS	Department of Public Safety
EB	Empirical Bayes'
FARS	Fatality Analysis Reporting System
FF	Free Flow
FHWA	Federal Highway Administration
FMS	Freeway Management System
GIS	Geographic Information Systems
GLS	Generalized Least Square
HOV	High Occupancy Vehicle
HCM	Highway Capacity Manual
ITS	Intelligent Transportation Systems
KW	Kruskal-Wallis
LOS	Level of Service
MAG	Maricopa Association of Governments
MP	Milepost
MVD	Motor Vehicle Division
NBRM	Negative Binomial Regression Model
NHTSA	National Highway Traffic Safety Administration
NR	Non-Recurrent Congestion
OD	Origin-Destination
PCE	Passenger Car Equivalent
PDO	Property Damage Only

RTM	Regression to the Mean
SEP	Speed Enforcement Camera Demonstration Program
TLD	Trip Length Distribution
TTS	Total Time Savings
TRB	Transportation Review Board
VHT	Vehicle Hours Traveled
VMT	Vehicle Miles Traveled
VPD	Vehicles Per Day
WLS	Weighted Least Square

Executive Summary

This executive summary presents brief results of a comprehensive analysis of the fixed speed-enforcement camera demonstration program (SEP) that was implemented on Arizona State Route 101 (Loop 101) from January 2006 through October 2006. The results reflected in this report are updated and are based on more complete crash and speed data obtained since the *Draft Summary Report* was released in January of 2007. Specifically, additional speed detection data are used, and all crash data from 2006 on the Loop 101 are used (allowing for a larger comparison site and increasing the sample size of crashes during the *program* period). The analysis is focused on estimating the impact of the SEP regarding:

- Citable speeding behavior (i.e., speeds > 75 mph);
- Average speeds;
- Traffic safety (motor vehicle crashes) within the enforcement zone;
- Total travel time;
- Expected economic factors.

This evaluation, sponsored by the City of Scottsdale, utilizes data from the Arizona Department of Public Safety (crash reports), Arizona Department of Transportation (motor vehicle crashes, traffic volumes, traffic speeds), the City of Scottsdale (traffic volumes and speeds), RedFlex (detections, traffic speeds), the Arizona Crash Outcome Data Evaluation System (crashes and crash costs), the Maricopa Association Government (transportation planning data), and the National Highway Safety Administration (crash costs).

Five time periods are referenced in the analysis.

- Before (2001 – 2005: various period)
- Warning (01/22/06 – 02/21/06)
- Program (02/22/06 – 10/23/06)
- After (10/24/06 – 12/03/06)
- Reactivation (02/22/07 – 06/29/07)

The Scottsdale 101 automated enforcement program consists of six speed detection stations within a 6.5 mile segment of Loop 101 within the city limits of Scottsdale, Arizona (see Figure 1). Three cameras are positioned to enforce speeds in each direction of travel (clockwise and counter-clockwise) on the Scottsdale portion of the Loop 101 freeway. The speed limit on this stretch of the Loop 101 freeway is 65 mph, and the enforcement equipment is set to photograph and cite drivers when they are traveling 76 mph or faster.

Effect on Speeding Detections

The average number of daily speeding detections per camera (speeds ≥ 76 mph) was 162.2 during the *warning* period, 129.7 during the *program* period, 1482.4 during the *after* period, and 134.68 during the *reactivation* period, as shown in Figure 2. Frequencies were higher on weekends than on weekdays. The average detection frequency for weekdays significantly increased by about 1047% (1006% for weekends and holidays) from the *program* to *after* period.

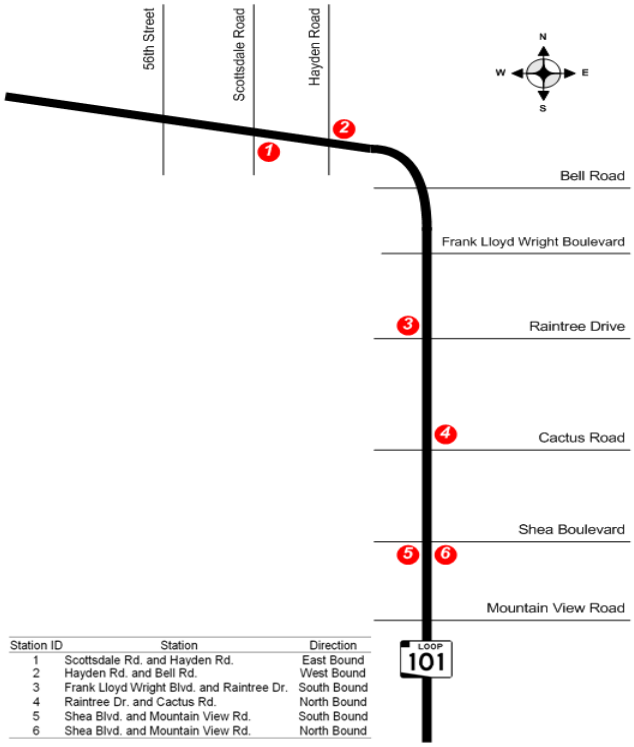

Station ID	Station	Direction
1	Scottsdale Rd. and Hayden Rd.	East Bound
2	Hayden Rd. and Bell Rd.	West Bound
3	Frank Lloyd Wright Blvd. and Raintree Dr.	South Bound
4	Raintree Dr. and Cactus Rd.	North Bound
5	Shea Blvd. and Mountain View Rd.	South Bound
6	Shea Blvd. and Mountain View Rd.	North Bound

Figure 1: Six photo enforcement sites on Loop 101

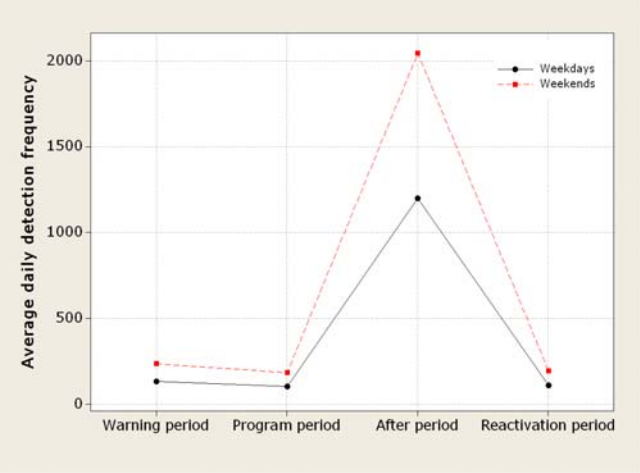

Figure 2: Average daily detection frequency (vehicles ≥ 76 mph) by period

Effect on Mean Speeds

The analysis results reveal that mean traffic speeds were reduced by about 9 mph, indicating that the SEP was an effective deterrent to speeding (see Figure 3). The impact of the SEP on speed increases as traffic flow decreases due to the well-known relationship between speed and traffic flow. Reduced speeds lead to decreases in speed variation, reduced crash impact speeds, and reduced demands on vehicular control systems (braking, steering, and suspension).

Because peak-hour traffic speeds are constrained by congestion, it is highly unlikely that speeds in excess of 76-mph are possible during peak-periods. As a result, it is assumed that the SEP will only affect unconstrained period travel speeds (and associated crashes).

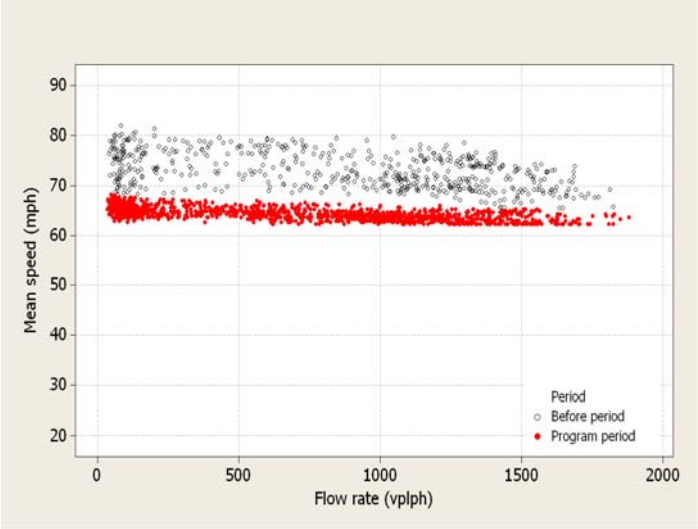

Figure 3: Observed mean speeds by flow rate by period.

Impact on Traffic Safety

The safety effects of the SEP are estimated by comparing the observed number of crashes during the SEP to the *expected number of crashes had the SEP not been implemented*. Thus, the analysis results hinge upon the ability to predict what crash counts would have been—a state that is unobserved. In the analyses described herein, three general and substantively independent procedures were applied to predict crashes in the after period in the absence of the SEP. By applying three different procedures the results are compared and contrasted, with the intent to check for consistency among the analysis results.

Only crashes that occurred during the non-peak periods are analyzed because of the uncertain and questionable expected influence of the SEP on slow moving, peak-period

traffic. Crash types affected by the SEP are categorized into four categories: single-vehicle, side-swipe (same direction), rear-end crashes, and other. These crashes constitute about 54%, 17%, 17%, and 12% of all crashes respectively.

The safety analysis consists of three different evaluation methodologies: a before-and-after (BA) analysis with a comparison group (the comparison site is used to estimate changes in safety from the before to after periods), a BA analysis with a traffic flow correction (crashes are assumed to be proportional to traffic volumes), and a state-of-the-practice empirical Bayes' BA analysis that corrects for traffic volumes, time trends, and regression-to-the-mean. The details of the three analysis methods and their varying assumptions are provided in detail in the body of the report. To avoid confusion, it is important to note that a "Before-After (BA)" analysis is conventional terminology used in the professional literature; however, in the context of the analysis periods described previously, the BA analysis in this study actually refers to a comparison of the before period to the program period (the *program period* corresponds with the period after the countermeasure was installed, the convention used in the professional literature).

BA Study with a Comparison Group

The comparison zone consists of 48 miles outside of the SEP enforcement zone on Loop 101. This comparison zone was chosen because its past crash trends are statistically similar to those within the enforcement zone. Using the BA study with the comparison zone to account for crash trends on Loop 101, the estimated change in crashes resulting from the SEP ranges from an increase of 14% (rear-end injury crashes) to a reduction of 64% (single-vehicle property damage only crashes), as shown in Figure 4. The results reflect the assumption that the prediction is modified using only trend effects (i.e., comparison ratios) in the comparison zone. Although the comparison zone resembles the enforcement zone as a whole, some zone-specific effects—if present—are not captured in the comparison zone.

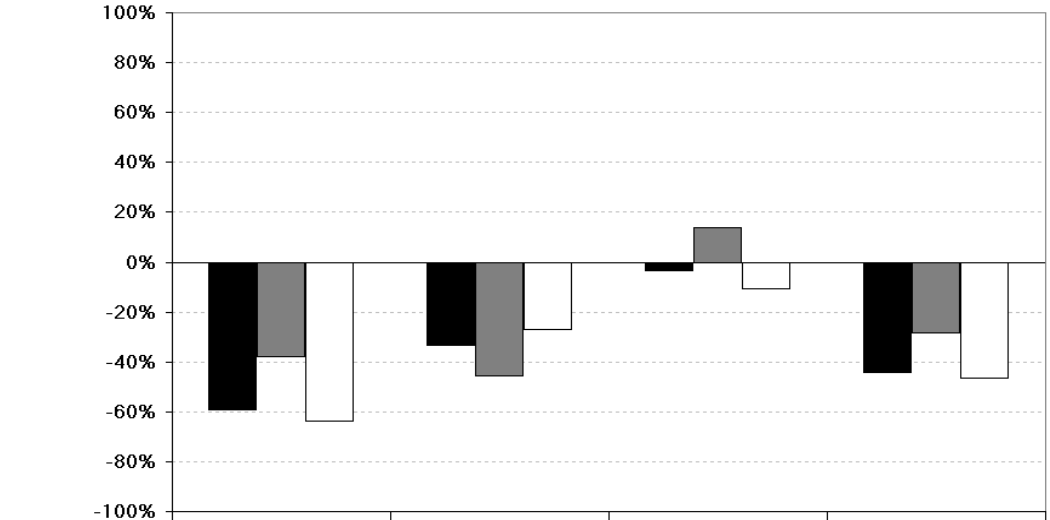

	Single-vehicle	Side-swipe (same direction)	Rear-end	Total
■ Total crashes	-59%	-33%	-4%	-44%
■ Injury crashes	-38%	-45%	14%	-28%
□ PDO crashes	-64%	-27%	-10%	-46%

Figure 4: Estimated impact of SEP on crashes by crash type and crash severity: BA method using comparison zone.

BA Study with Traffic Flow Correction

The increase in traffic volumes in the enforcement zone from the *before* to *program* periods was not only significant (42% increase on average) but also separate from the observed time trend safety effects (i.e., safety changed beyond that explained by traffic volume increases alone). This analysis procedure accounted simultaneously for the change in traffic flow in the enforcement zone and the time trend safety effects. Ignoring the significant traffic flow increase from the *before* to *program* periods would significantly underestimate the effectiveness of the SEP, and underscores the importance of this analysis approach. Using the BA study with traffic flow correction, the estimated change in crashes resulting from the SEP ranges from a reduction of 18% (rear-end injury crashes) to a reduction of 67% (single-vehicle, property damage only crashes). All types of crashes were reduced, but the decrease in the rear-end injury crashes (18%) is not statistically significant (p-value=0.377).

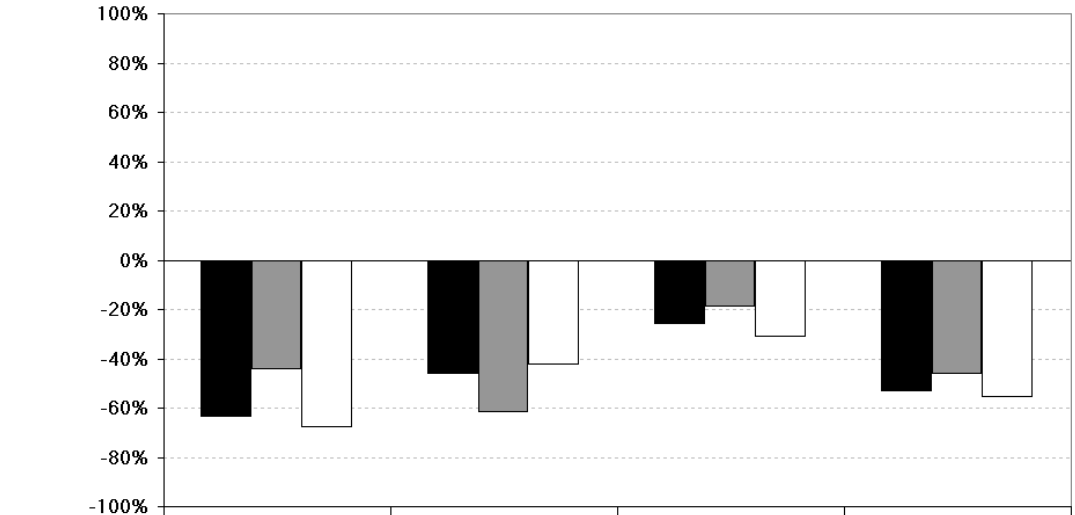

	Single-vehicle	Side-swipe (same direction)	Rear-end	Total
■ Total crashes	-63%	-46%	-26%	-53%
▩ Injury crashes	-44%	-61%	-18%	-46%
□ PDO crashes	-67%	-42%	-31%	-55%

Figure 5: Estimated impact of SEP on crashes by crash type and crash severity: BA method using correction for traffic flow.

Empirical Bayes' BA Study

The Empirical Bayes' (EB) BA analysis accounts for the change in traffic flow over time, time trends (not captured by traffic flow), and regression to the mean effects. This analysis approach reflects the current state of the practice for estimating the safety effects of the SEP. The advantage of the EB BA approach stems from the fact that countermeasures are often applied at locations with perceived safety problems, and thus the expected number of crashes in a subsequent observation period regresses toward the mean. Specifically, a location with a higher than expected crash count in a before period should reveal a reduction in crash counts in the after period (statistically speaking). This expected reduction must be taken into account when correctly evaluating the effectiveness of the countermeasure. This undesirable statistical effect is diminished by applying the EB BA study.

Applying the EB BA approach yields an estimated reduction in crashes ranging from 23% (rear-end injury crashes) to 67% (single-vehicle, property damage only (PDO) crashes), as shown in Figure 6. The results from the EB BA study reveal slightly greater effects than those obtained from the BA study with traffic flow correction, indicating that the enforcement zone was in fact slightly 'safer' than average compared to similar sections of Loop 101. This finding is important, and suggests that: 1) an increase in crashes is predicted (in the absence of the SEP) in the after period; and 2) since the SEP section was safer than similar 101 sections during the before period, applying the SEP to

a freeway section that is 'worse than average' with respect to safety may reveal greater safety benefits than observed in this study.

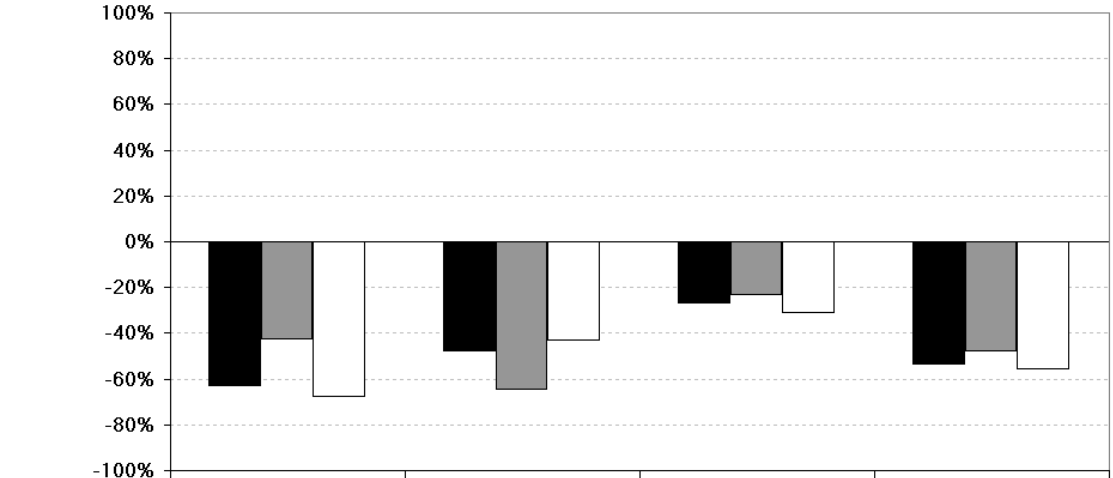

	Single-vehicle	Side-swipe (same direction)	Rear-end	Total
■ Total crashes	-63%	-48%	-26%	-54%
■ Injury crashes	-43%	-64%	-23%	-48%
□ PDO crashes	-67%	-43%	-31%	-56%

Figure 6: Estimated impact of SEP on crashes by crash type and crash severity: Empirical Bayes' BA method.

Economic Benefits

To estimate the economic impact of the safety effects of the SEP, the results from both the BA study with traffic flow correction and the EB BA study (the two extremes) are used with Arizona-specific crash cost estimates. Annual estimated benefits of the SEP program range from $16.5 million (BA study with traffic flow correction) to $17.1 million (EB BA study). These benefits include medical costs, other costs (lost productivity, wages, long-term care, etc.), and quality of life costs. The overall benefits appear to be similar in magnitude across categories.

Analysis method and crash severity	Fatal crashes	Disabling injury	Evident injury	Possible injury	Property damage	Total
BA study with traffic flow correction	$4,902	-$358	$3,234	$521	$8,204	$16,503
Empirical Bayes' BA study	$5,036	-$364	$3,379	$669	$8,328	$17,048

Table 1: Crash benefits in $1,000/year from BA with traffic flow correction and Empirical Bayes' BA

Impact on Travel Time

The SEP slows drivers down (increases travel times) but reduces incidents (reduces travel times via non-recurrent congestion effects). The impact of the SEP on travel times and travel time uncertainty was evaluated by simulating network traffic conditions with and without the SEP. A microscopic traffic simulation tool, which models the acceleration and speed choice behavior of individual vehicles in detail, was calibrated for the Loop 101 section and used to capture the effects under numerous traffic conditions (see Figure 7).

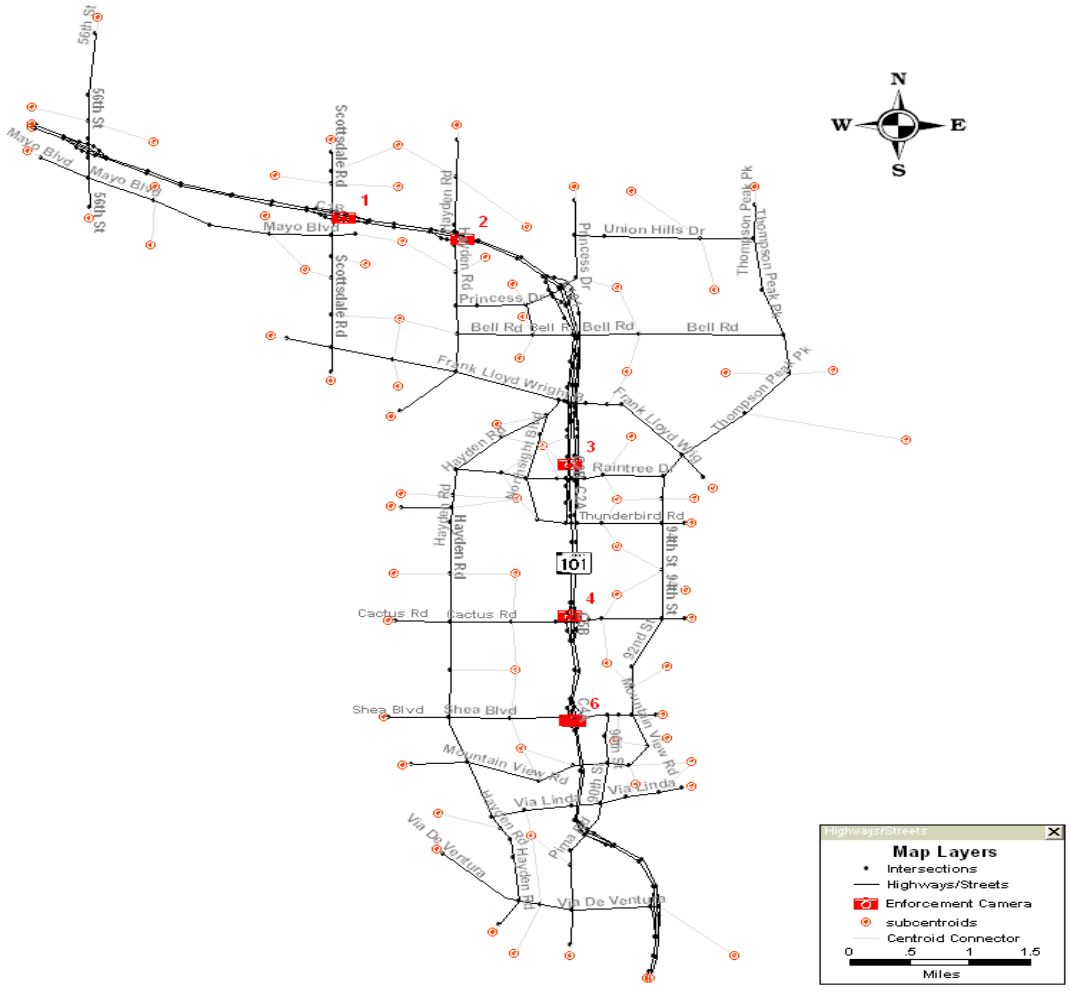

Figure 7: Loop 101 sub-area simulated network for travel time impact analysis

The selected sub-area used in the simulation model encompasses the 13-mile stretch on the Loop 101 segment including the enforcement zone as well as adjacent arterials that are used as alternative routes for the Loop 101 in Scottsdale. The average results from a total of 180 simulation runs suggest that total travel time savings from the SEP is statistically significant, with an estimated average of 1,336 vehicle-hours/year saved assuming one-lane blockage crashes and an average of 45,060 vehicle-hours/year assuming two-

lane blockage crashes. Mean estimates (using EB BA study results) of the value of travel time savings as a result of the SEP range from a low of $20,040 to a high of $26,720 for a one-lane blockage crash. For a two-lane blockage crash, mean estimates of the value of travel time savings range from $675,900 to $901,200 per year. The complete details of the simulation, assumptions, and results are described in detail in the body of the report.

Conclusions and Recommendations

The following conclusions were drawn from a variety of detailed statistical analyses, site visits, logical reasoning, and simulation analyses:

Impact of the SEP on Speeding Behavior and Speed

1. Speeding detection frequency (speeds ≥ 76 mph) increased by a factor of 10.5 times after the SEP was temporarily terminated. During this termination the cameras were "bagged" and advertising and news media advertised the end of the program. The SEP seems to be an effective deterrent to speeding within the enforcement zone, since removing the deterrent resulted in increased speeding.
2. The detection frequency for the *reactivation* period in 2007 is not statistically different than that for the *program* period in 2006, indicating that the activation of the SEP contributed to reducing drivers' speeding behavior. The SEP seems to be an effective deterrent to speeding within the enforcement zone, since reactivating the potential deterrent resulted in decreased speeding.
3. The SEP reduced the average speed at the enforcement camera sites by about 9 mph and also contributed to reducing the speed dispersion at the enforcement camera sites. In agreement with a substantial body of prior national and international research, reduced speeds and speed dispersion improve safety.
4. The reduction in the mean and variance of speed resulting from the SEP depends on traffic flow: the reductions increased as traffic flow decreased due to the well-known relationship between speed and traffic flow. Thus, the magnitude of speed effects of the SEP is inversely related to traffic flow.

Impact of the SEP on Safety

1. As a result of the SEP, the total number of target crashes decreased by 44% to 54%, depending on the analysis. In addition, the total number of injury crashes decreased by 28% to 48%, while the total number of PDO crashes decreased by 46% to 56%. The state-of-the-practice analysis method resulted in the highest estimates of reductions. The SEP appears to be effective in improving the overall crash risk within the selected area.

2. All but rear-end crashes types appear to have been reduced. Although the changes in safety for rear-end crashes were inconsistent among evaluation methods (and their assumptions), the decrease in rear-end crashes was not statistically significant. Moreover, the state-of-the-practice analysis method revealed a non-statistically significant decrease in rear-end crashes. It is concluded that the effect of the SEP on rear-end crashes is uncertain, and slight increases or decrease are possible depending on site-specific conditions.
3. Swapping of crash types is common for safety countermeasures—many countermeasures exhibit the 'crash swapping' phenomenon observed in this study (left-turn channelization, red-light cameras, conversion of stop signs to signals, etc.) Thus, it is quite expected to see varying magnitudes of reductions across crash categories, and even some increases are possible.
4. The total estimated SEP benefits (looking at the costs of crashes only) range from an estimated $16.5 million to $17.1 million per year, depending on the analysis type and associated assumptions. This estimate does not reflect a cost-benefit analysis, merely an estimate of the annual safety benefit of the program.
5. This study revealed that the SEP, in terms of safety impacts, is a promising countermeasure to reduce crashes in Arizona. This finding is consistent with findings in other countries and reported in the professional literature.

Impact of the SEP on Travel Time

1. The SEP shifted the distribution of the travel time by significantly reducing the number of speeding drivers (by at least a 67.5% decrease in the proportion of the number of faster drivers), while travel time reliability remains the same regardless of the existence of the SEP.
2. The significant change in the travel time distribution by the reduction in speeding vehicles was a primary factor in reducing the speed variance and mean speeds. As is known from prior research and from physics principles, reduced speeds and speed variance generally translates to improved safety.
3. There is not a statistically significant difference in the total free-flow travel time with and without the SEP, suggesting that drivers travel in the enforcement zone in the same amount of travel time regardless of the existence of the SEP. If a larger enforcement zone was used, the difference in free-flow travel time may become significant.
4. The insignificant difference in total free-flow travel time with and without the SEP conditions led to total travel time savings, which resulted from the reduction in crash frequency. The reduction is estimated to be at least (95% lower bound)

569 vehicle-hours/year assuming a *one-lane block crash* state (as a result of a crash) and at least (95% lower bound) 37,981 vehicle-hours/year assuming the *two-lane block crash*.

5. Speed enforcement on the Scottsdale section of Loop 101 not only improved safety but also improved mobility through travel time savings, improved travel time reliability, and reduced travel time uncertainty. The annual benefit of travel time savings ranges from a low of $20,040 (one-lane-blockage crash assuming $15/hr value of travel time savings) to a high of $901,200 (two-lane-blockage crash assuming $20.00/hr of travel time savings).

Recommendations

The following actions are recommended to maximize the impacts of speed enforcement cameras and to improve the results of this study. These recommendations should be considered in the implementation and/or consideration of an expanded SEP in Arizona. Although the SEP is not a panacea for reducing speeding-related crashes and other non-speeding offenses within the enforcement zone, the SEP may be a promising countermeasure given the following considerations:

1. An "ideal" site for SEP will reveal relatively high rates of speed and corresponding severity of crashes prior to implementation. The crash history of a site should be used to aid in selection, and sites that reveal a 'worse than average' safety record should be identified as candidate sites. A statistical model that predicts the expected safety performance of sites should be developed to help identify candidate sites, and predictors should include exposure and some important geometric features.
2. Design of SEP sites should consider the element of surprise to drivers and should aim to minimize it. For example, the placement of cameras in close proximity to high information load locations (e.g., on- and off-ramps, under-passes, billboards, weaving sections, directional signs, etc.) should be avoided. Placement of cameras in sight restricted locations should be avoided. Efforts should be made to increase driver expectation of speed enforcement camera locations.
3. Photo enforcement technology that measures average speeds (instead of instantaneous speeds) over a long section of freeway (e.g., five miles) may offer some operational advantages over the currently used technology, including reduced sudden braking (and subsequent rear-end accidents).
4. Spillover effects are more likely in a dispersed system of enforcement zones compared to a concentrated location.

5. Further evaluation (of future programs) is needed to enable the continued knowledge and improvement of safety performance of SEPs.
6. In future evaluations, additional speed data may enable the assessment of spillover effects. Currently, the extent and magnitude of spillover effects of the SEP are uncertain.

Chapter 1 Introduction

1.1 Background and Objectives

Speeding is recognized as one of the most important factors causing traffic crashes. In 2005, 30% of all fatal crashes were speeding-related (National Highway Traffic Safety Administration 2005). According to the National Highway Traffic Safety Administration (NHTSA), the cost of speeding-related crashes is estimated to be $40.4 billion per year (National Highway Traffic Safety Administration 2005). Intelligent Transportation Systems (ITS) now exist to reduce speeding-related crashes by enforcing speed limits with camera-based technologies. These enforcement technologies are generically called "speed cameras" and have been effective on municipal streets and arterials in Arizona (Roberts and Brown-Esplain 2005).

The City of Scottsdale began automated enforcement efforts in December of 1996. Between 1996 and 1998, four wet-film mobile speed units and six wet-film red-light cameras were deployed for a total of nine intersections on enforcement rotation, depending on the needs of the city. The cameras on city streets have helped Scottsdale improve safety (Washington and Shin 2005). Scottsdale expanded these efforts in August of 2004 with a dual-direction fixed-speed enforcement system at 7700 Frank Lloyd Wright Blvd. This system covers three lanes of traffic eastbound and three lanes of traffic westbound on Frank Lloyd Wright Boulevard. The city's recent experience on Frank Lloyd Wright Boulevard is that speed violations significantly decreased in a one-year period after installation of cameras.

With these experiences, the City Council on October 25, 2005, approved the nine-month *speed enforcement camera demonstration program* (hereafter SEP) on a 7.8-mile stretch of the Loop 101 segment within Scottsdale. The SEP began on January 22, 2006, and ended on October 23, 2006. The demonstration program on the Loop 101 freeway segment in Scottsdale is the first use of the fixed-site photo-enforcement equipment on a freeway in Arizona and is believed to be the first in the nation.

Accurately estimating the impacts of the traffic safety countermeasures such as the speed-enforcement cameras is challenging for several reasons. First, many safety-related factors such as traffic volume, the crash-reporting threshold (legal requirement to report a crash), the probability of reporting, and the driving population are uncontrolled during the periods of observation. Second, 'spillover' effects can make the selection of comparison sites difficult. Third, the sites selected for the treatment may not be selected randomly,

and as a result may suffer from the regression-to-the-mean effect. Fourth, a speed-enforcement program may influence specific types of crashes—called target crashes—which often may be difficult to define and identify. Fifth, crash severity needs to be considered to fully understand the safety impact of the treatment. Finally, the cause-and-effect relationship should be investigated before evaluating the impact of the traffic safety countermeasure because traffic safety is often indirectly influenced by the treatment.

With these challenges in mind, this study was conducted to estimate the impact of the SEP on traffic safety, speed, speeding behavior, and daily travel time uncertainty. More specifically, the objective of the research was to:

- Estimate the impact of the SEP on speeding behavior, which is represented as the detection frequency;
- Estimate the changes in mean speed due to the SEP;
- Estimate the impact of the SEP on traffic safety in the enforcement zone;
- Estimate total travel time savings as a potential byproduct of the SEP;
- Translate the impacts on crashes into estimated economic costs and/or benefits.

1.2 Description of the Demonstration Program

The photo radar technologies have been used in 75 countries throughout the world to enforce speed. Until 2006, the United States had not seen an application of photo enforcement on limited-access freeways. In order to reduce speed-related crashes, the City of Scottsdale in Arizona implemented the first fixed-photo speed-enforcement camera demonstration program on a freeway in the United States. The nine-month demonstration program spanning the period January 2006 to October 2006 was implemented on a 6.5-mile urban freeway segment of Loop 101 running through Scottsdale, Arizona.

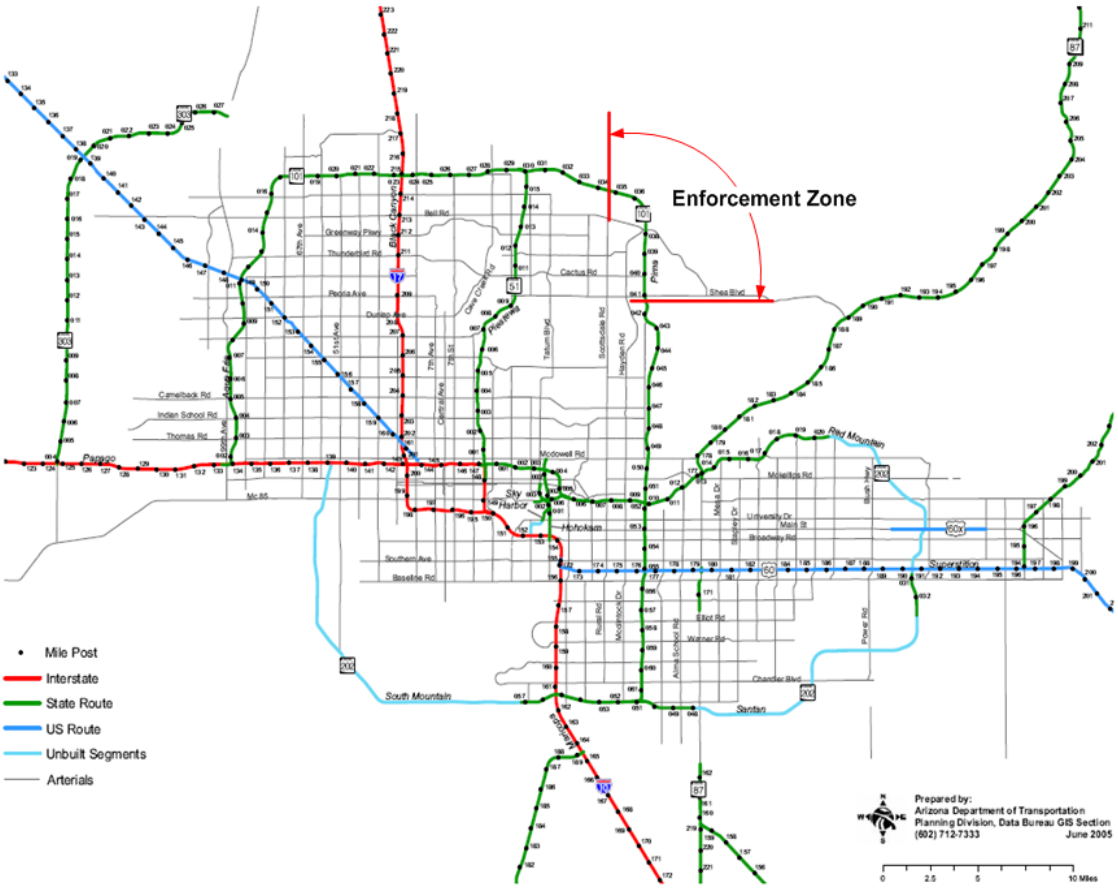

Figure 8: Location of the speed enforcement zone

The speed enforcement zone is located on the northeast side of the Phoenix metropolitan area as shown in Figure 8. The cameras within the enforcement zone are at six fixed locations (in contrast to mobile photo enforcement vans) along the Loop 101 freeway from the Shea Boulevard exit to the Scottsdale Road exit as shown in Figure 9.

Three cameras were positioned to enforce speed for each direction of travel. The speed limit on this stretch of the Loop 101 freeway is 65 mph, and the enforcement equipment is set to photograph drivers when they are traveling at 76 mph or faster. Vehicle speed is determined by measuring the time it takes a vehicle to travel from the first sensor to the last sensor on the detection zone installed at each enforcement site. The enforcement system uses the known distance between the sensors and the measured time to calculate speed. Of course time is measured precisely in order to estimate speeds precisely.

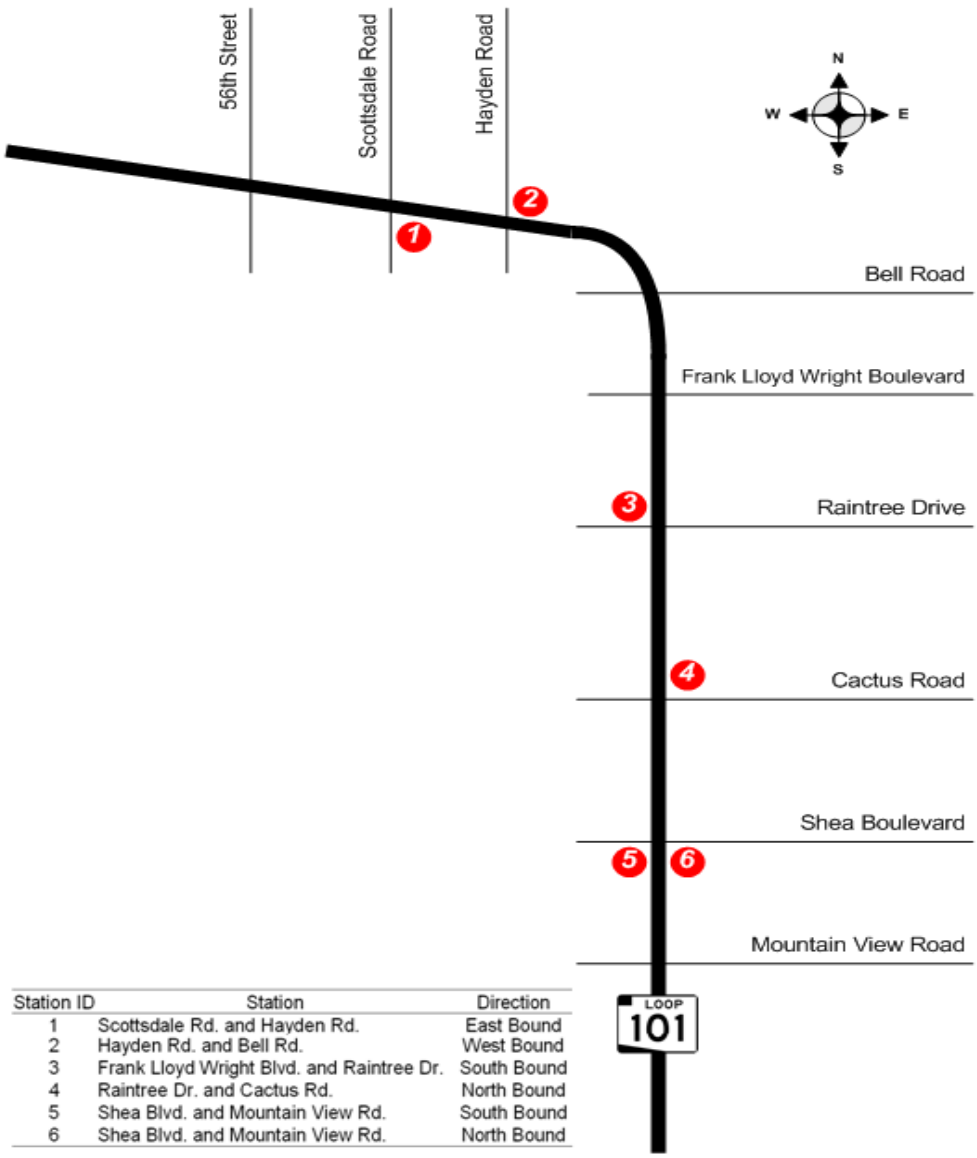

Station ID	Station	Direction
1	Scottsdale Rd. and Hayden Rd.	East Bound
2	Hayden Rd. and Bell Rd.	West Bound
3	Frank Lloyd Wright Blvd. and Raintree Dr.	South Bound
4	Raintree Dr. and Cactus Rd.	North Bound
5	Shea Blvd. and Mountain View Rd.	South Bound
6	Shea Blvd. and Mountain View Rd.	North Bound

Figure 9: Location of six enforcement sites

As discussed, the SEP began on January 22, 2006, and ended on October 23, 2006. For the first 30 days of the program, the city sent warning notices to drivers who exceeded the 76-mph threshold. The cameras were operated for a total of 275 days:

- Warning period: 1/22/2006 – 2/21/2006 (31 days)
- Program period: 2/22/2006 –10/23/2006 (244 days)

After the SEP ended in October, the City of Scottsdale continued to collect speed and traffic flow data at the stations. The cameras were reactivated on February 22, 2007, at the request of Governor Janet Napolitano, and Scottsdale has been operating the cameras since that date.

Chapter 2 Literature Review

In this chapter, numerous studies that analyzed the relationship between speed and safety as well as the effect of speed-enforcement cameras are summarized, and the lessons and issues raised by literature that could affect study consideration are discussed. As of 2005, at least 75 countries rely on such cameras to enforce speed limits, especially on high-risk roads, including Australia, Austria, Canada, Germany, Greece, Italy, the Netherlands, Norway, Singapore, South Africa, South Korea, Spain, Switzerland, and Taiwan. Although speed enforcement cameras have frequently been used in the United States, their use has been limited (i.e., not at fixed-site) compared to other countries. Cameras currently are being used in several states, including Arizona, California, Colorado, North Carolina, Ohio, Oregon, and the District of Columbia (Roberts and Brown-Esplain 2005). Out of numerous studies conducted in these countries and the nation, all possible studies of relevance were initially identified on the basis of internet journal database searches. Then, a number of "critical studies,"—appropriate in terms of methodological rigor and frequently cited by other researchers or in discussions of speed enforcement effectiveness, are examined. Extracted from the critical studies is general information on the effects of speed enforcement cameras and issues that need to be considered in this study.

2.1 Relationship between Speed and Safety

Numerous studies have been conducted to elucidate the relationship between speed and safety: a detailed review of which is provided in elsewhere (Kweon and Kockelman 2005; Lave and Lave 1998; Skszek 2004; Stuster et al. 1998). In the 1960s, many studies found that the variance of speed is one of the most important factors affecting safety, suggesting a U–shaped relationship between crash rate and variance in speed. The relationship illustrates that the more the speed of driver deviates from the mean speed of traffic, the greater the likelihood of a crash (Solomon 1964).

In 1985, Lave revitalized the U–shaped relationship by estimating regression models to test the relationship between the fatality rate, average speed, and the difference between the 85th percentile and average speed (as a proxy for speed variance) with cross-sectional data from 1981 and 1982. Lave concluded that there was no statistical evidence indicating that average speed affects the fatality rate. Consequently, Lave suggested that the focus of speed laws should be changed so that they coordinate speed rather than limit it. Other studies also agreed that crash rates increase with increasing speed variance, but not with average speed (Garber and Ehrhart 2000; Garber and Gadiraju 1989).

Snyder (1989) re-estimated Lave's model using a fixed effect linear model with two measures for speed variability: the difference between the 85th percentile and median speed (for faster drivers) and the difference between the 15th percentile and median speed (for slower drivers). He concluded that both average speed and speed dispersion are important factors in highway fatalities, but the speed dispersion for faster drivers is only significant in explaining fatality rate. Levy and Asch (1989) also concluded that lack of coordination implies greater risk, but average speed also contributes to increasing the fatality risk depending on speed variance. The authors suggested that enforcement efforts would be better directed toward slowing down high speed drivers rather than speeding up low speed drivers. In addition, it is evident that a driver's speed is one of the most important factors affecting crash severity, owing to the relationship between vehicle velocity and kinetic energy (Joksch 1993; Kloeden et al. 2001; Moore et al. 1995; Solomon 1964). In summary, the results of previous studies that analyzed the relationship between speed and safety show that traffic safety can be improved by reducing the average speed and speed dispersion.

2.2 Impact of Speed Enforcement Cameras

The studies summarized in the previous section imply that speed enforcement—through reduction of high speeds and resulting speed variance—is a promising countermeasure for reducing crash frequency and severity. The results of numerous studies that evaluated the effect of speed enforcement programs on safety and speed have confirmed the validity of the paradigms discussed above (Champness and Folkman 2005; Chen et al. 2002; Cunningham et al. 2005; Elvik 1997; Goldenbeld and van Schagen 2005; Ha et al. 2003; Hauer et al. 1982; Hess 2004; Hess and Polak 2003; Lamm and Kloeckner 1984; Retting and Farmer 2003; Sisiopiku and Patel 1999; Vaa 1997).

The studies in general show that speed enforcement programs lead to a significant reduction in speed and crash frequency. Several studies solely evaluated the effect of speed enforcement on speed (Champness and Folkman 2005; Hauer et al. 1982; Retting and Farmer 2003; Sisiopiku and Patel 1999; Vaa 1997) or on traffic safety (Elvik 1997; Hess 2004), while others evaluated both speed and safety (Chen et al. 2002; Cunningham et al. 2005; Goldenbeld and van Schagen 2005; Ha et al. 2003; Hess and Polak 2003; Lamm and Kloeckner 1984). Two studies (Ha et al. 2003; Lamm and Kloeckner 1984) have an enforcement condition similar to that of Scottsdale (i.e., fixed cameras on freeway), but differed with respect to traffic conditions, road users (skills and 'safety culture'), geometric design standards, and weather compared to the Loop 101 in Scottsdale. Although all studies suggest that photo enforcement cameras are effective in

reducing speed and crash frequency at photo enforcement camera deployment sites, the estimates of the impact of speed cameras on safety varied considerably.

Elvik and Vaa (2004) conducted a meta analysis that combined the effects of automated enforcement on safety reported in Australia, England, Germany, the Netherlands, Norway, Sweden, and the United States (Elvik and Vaa 2004). The results yield a 19% reduction in total crash frequency and a 17% reduction in injury crash frequency. The reduction in total crash frequency was greater in urban areas (28%) than in rural areas (4%). A recent meta analysis also combined the effect of speed enforcement cameras on safety using the evaluation results from 14 observational studies, which were selected from 92 studies (Pilkington and Kinra 2005). The results show that the effects varied across studies: reductions from 5% to 69% in crash frequencies, 12% to 65% in injuries, and 17% to 71% in fatalities. In the following subsections, the results of each study are summarized in detail.

2.2.1 Speed Enforcement Cameras on Freeways

Several studies have evaluated the impacts of speed enforcement cameras on speed and safety on freeways. Lamm and Kloeckner (1984) assessed the effects of fixed automated cameras at the Autobahn in Germany. In addition to a reduction of about 12.4 mph in speed, the accident frequency decreases from 200 accidents/year to 84 accidents/year, and the number of fatal and injury accidents is reduced from 80 accidents/year to 30 accidents/year.

Chen et al. (2002) evaluated the effects of mobile cameras on Highway 17 in British Columbia in Canada. By using the simple before and after study, they reveal that the mean speed at the deployment locations is reduced to below the posted speed limit. Overall, the mean speed decreased by approximately 1.74 mph, representing a 3% reduction, and the standard deviation of speed declined by 0.3 mph (6% reduction).

Some studies on freeways focused on the spillover effects—time or distance halo effects— rather than the direct effects. The time halo effect is defined as the length of time during which the effect of enforcement is still present after enforcement activity has been withdrawn. The distance halo effect is the number of kilometers from the enforcement site, in which the effect is maintained (Hauer et al. 1982; Vaa 1997). Sisiopiku and Patel (1999) analyzed both time and distance halo effects of mobile speed cameras on Interstate 96 in Ionia County, Michigan. The average speed just upstream of the police car's location was reduced, but as soon as vehicles passed the patrol car, drivers accelerate to their normal speeds or more, but no "time halo" effects on the vehicles at the increased speed zone were observed.

Ha et al. (2003) investigated the distance halo effects using speed data collected from seven measurement sites on urban highway in South Korea. Drivers tended to reduce their speeds when approaching the speed enforcement camera, but drivers accelerated back to their original speeds on passing the enforcement camera—thus no evidence of distance spill-over effects were observed.

Champness and Folkman (2005) also examined the time and distance halo effects of mobile overt speed cameras in Australia. Time and distance halo effects were analyzed using numerous measurements: mean speeds, 85th, 90th, and 95th percentile speeds, etc. Distance halo effects were clearly identifiable, with an observed reduction in speeds one kilometer downstream, but the magnitude of the reduction diminishes at 500 meters downstream of the camera site. The effect of the speed camera was completely dissipated at 1.5 kilometers downstream.

Another study attempted to compare the reduction in speed in terms of enforcement type and time delay in the case of mailed fines on a 75 mph motorway in the Netherlands (Waard and Rooijers 1994). Two field experiments were conducted to establish the most effective method of enforcement in reducing driving speeds. The enforcement intensity study showed a clear relationship between intensity level of enforcement and the proportion of speeding drivers. The highest intensity levels led to the largest and longest lasting reduction in driving speeds, but effects on average driving speeds of the methods on-view stopping versus photographing of offenders were similar.

Table 2: Summary of studies on freeways

Reference	Country	Camera type	Enforcement sites	Posted speed limits
Lamm and Kloeckner (1984)	Germany	Fixed	2 sites on Autobahn	62 mph (100kph)
Waard and Rooijers (1994)	Netherlands	Mobile	6 sites on motorways	75 mph (120kph)
Sisiopiku and Patel (1999)	US	Mobile	29-mile segment on I 96, Michigan.	70mph (113kph)
Chen et al. (2002)	Canada	Mobile	12 sites on Highway 17	56mph (90kph)
Ha et al. (2003)	South Korea	Fixed	1 site on urban highway	50mph (80kph)
Champness and Folkman (2005)	Australia	Mobile	1 site Highway section, Queensland	62 mph (100kph)

Table 2 summarized the experimental details of these studies. Only two studies (Ha et al. 2003; Lamm and Kloeckner 1984) are similar to the Scottsdale's enforcement environment (i.e., fixed camera). However, highways in Germany and South Korea are likely to have different traffic conditions, road users (skills and 'safety culture'),

geometric design standards, and weather compared to the Scottsdale Loop 101. In fact, the cameras on the Autobahn were deployed at steep downgrade sections (5% grade).

2.2.2 Speed Enforcement Cameras on non-Freeways

While there were relatively few studies for the speed enforcement cameras on freeways, a number of studies analyzed the effects of speed cameras on non-freeway roads. Table 3 shows the summary of outline of these studies.

Table 3: Summary of outline of studies on non-freeways

Reference	Country	Camera type	Enforcement sites	Posted speed limits
Hauer et al. (1982)	Canada	Fixed	4 sites on suburban two-lane road	37 mph (60kph) or 50mph (80kph)
Vaa (1997)	Norway	Fixed and Mobile	Roadway 22 and 170 in Norway (suburban two-lane road)	37 mph (60kph) or 50mph (80kph)
Elvik (1997)	Norway	Fixed	64 sites	31 mph (50kph) to 56mph (90kph)
Retting and Farmer (2003)	US	Mobile	7 sites on surface streets in Washington, D.C.	25 mph or 30 mph
Hess (2004; 2003)	UK	Fixed	43 sites on rural road	Speed limits vary from sites
Goldenbeld and van Schagen (2005)	Netherlands	Mobile	28 sites on rural road	50 mph (80kph) or 62 mph (100kph)
Cunningham et al. (2005)	US	Mobile	14 sites in Charlotte, North Carolina	25 mph to 55mph

Elvik (1997) assessed the effects of 64 fixed speed enforcement cameras in Norway on safety. The study controlled for general trends in the number of accidents and regression to the mean bias by using comparison groups and empirical Bayesian estimation respectively. The injury accidents were significantly reduced by 20%, and the property damage-only accidents were reduced by 12%. However, the reduction in the PDO accidents was not statistically significant.

Retting and Farmer (2003) evaluated the effects of mobile speed enforcements on speed at seven sites in Washington, D.C. With eight comparison sites in Baltimore, Maryland, speed data collected one year before enforcement and approximately six months after enforcement began were analyzed. Mean speeds at seven sites declined by 14%, and the proportion of vehicles exceeding the speed limit by more than 10 mph declined by 82%.

Goldenbeld and Schagen (2005) assessed the impacts of mobile inconspicuous speed cameras on the speed and safety at 28 enforcement sites in the Netherlands. With 15 sites

on 80kph rural roads and all other non-enforced roads outside urban areas as comparison sites, the evaluation was performed. The results show that the mean speed decreased by 4kph on the enforced roads and by 0.5kph on the non-enforced comparison roads during the enforcement period. With regard to reduction in safety, the number of road accidents and casualties decreased by 21%.

Again, there are several studies focusing on the spillover effects. Hauer et al. (1982) attempted to investigate both spillover effects (i.e., time halo and distance halo effects) comprehensively. The distance halo effects were measured at four enforcement sites with upstream and downstream measurement sites, which are located on semi-rural two-lane roads in Halton and Peel counties west of the Toronto metropolitan area. To investigate time halo effects, speeds were monitored prior to, during, and after exposure to enforcement. The investigation on aggregate speed distributions suggested that the average speed of the free flowing vehicles was remarkably reduced at the enforcement site. When enforcement was in place, the average speed at the site was close to the posted speed limit. The downstream distance halo effect follows the general form of exponential decay, representing that the effect of enforcement is reduced by half for approximately every 900 meters. The time halo appeared to be the only phenomenon to be affected by the intensity of enforcement: the effect of enforcement at single day has disappeared after three days, while enforcement on several consecutive days had a longer term effect. Vaa (1997) also investigated the impacts of the intensity level of speed enforcement on speeds. Speed was measured at 12 sites in Norway consecutively for 16 weeks: two before weeks, six enforcement weeks, and eight after weeks. Vaa concluded that the average speeds during the enforcement period were reduced, but durations for time halo effects were influenced by the intensity of the enforcement, which were consistent with other results (Hauer et al. 1982; Waard and Rooijers 1994).

Hess (2004) assessed the effects of 49 fixed speed enforcement cameras in Cambridgeshire, U.K. Two consecutive studies (Hess 2004; Hess and Polak 2003) were conducted in order to quantify the performance of the cameras in terms of their catchment area (the effects of cameras for various ranges around the cameras). In the 250-meter range, injury accident numbers were reduced by 45.74%. However, the reductions in the 500-meter, 1,000-meter, and 2,000-meter ranges decreased by 41.30%, 31.62%, and 20.86% respectively.

Cunningham et al. (2005) analyzed the impact of mobile automated speed enforcement on speed and safety, which was implemented on 14 key corridors in North Carolina. They found that median and 85th percentile speeds respectively decreased by 0.88 mph and 0.99 mph from the before period to the after period. In addition, a reduction of 11% to

14% in total crashes resulting from the speed enforcement cameras was estimated, which was obtained by using the comparison group methodology. However, the authors concluded that the results should be interpreted with limitations, such as the brief duration of the after period.

2.3 Summary of Findings

A number of studies have evaluated the effects of speed enforcement cameras on safety and speed. Some studies evaluated the effects on speed or traffic safety solely, while others evaluated both. In addition, several studies focused on the spillover effects in terms of time and space. Not surprisingly, the estimates of the safety effect of speed cameras vary considerably, even though all studies suggest that photo enforcement cameras are effective in reducing speed and crash frequency at photo enforcement camera deployment sites.

However, many studies suffer from one or more non-ideal conditions. For example, the results of some studies may underestimate or overestimate the effects of the speed enforcement cameras on traffic safety, since total crashes instead of target crashes (crashes that are materially affected by the photo enforcement speed cameras) were analyzed. In addition, failure to account for regression to the mean can overestimate the effects, while benefits can be underestimated if spillover effects are ignored. From the literature review several noteworthy observations are relevant:

- *Change in violation frequency due to the SEP*: Since the direct effect of speed enforcement cameras is a reduction in speeding, it is expected that the number of violations will decrease, thereby reducing relevant crashes. However, if this assumption does not hold, the speed enforcement countermeasure could be invalid.
- *Reduction in mean speed and speed dispersion due to the SEP*: In addition to the reduction in violation frequency, it is also expected that the mean speed and speed dispersion will be reduced, which should be carefully investigated.
- *Target crashes*: The lack of precise definition for target crashes in past studies could have led to the under-estimation of the safety effects.
- *Comparison group not affected by SEP*: If crashes at comparison sites (zone) are affected by the demonstration program, estimating the program effect at the treated enforcement zone becomes more difficult.
- *Exposure changes between the before and program periods*: It is important to account for changes in traffic exposure between the before and program periods.

- *Regression to the mean effects*: In many studies, speed enforcement cameras were installed at high-crash sites—which could lead to significant regression to the mean bias that needs to be accounted for—often leading to over-estimation of safety impacts.

Chapter 3 Effects of the SEP on Speeding Behavior and Speed

In this chapter, the effects of the SEP on speeding behavior and speed are examined. The speeding behavior is analyzed by comparing the detection frequencies during the *warning*, *program*, *after*, and *reactivation* periods, collected at the six enforcement camera locations, and the impact on speed was compared by analyzing the mean speeds during the *before* and *program* periods. The detection frequency data were obtained from Redflex, the vendor of Scottsdale's enforcement cameras during the program, and the average speed data were obtained from ADOT and Redflex. In the following sections, all relevant analysis results are discussed in detail.

3.1 Changes in the Detection Frequency

3.1.1 Data Description

The detection frequency data used in this analysis are the number of vehicles detected by the six enforcement cameras, which were collected from the 4 periods of observation:

- *warning* period: 1/22/2006 – 2/21/2006 (31 days)
- *program* period: 2/22/2006 –10/23/2006 (244 days)
- *after* period: 10/24/2006 – 12/31/2006 (69 days)
- *reactivation* period: 2/22/2007– 6/29/2007 (128 days)

Note that no detection data were collected prior to the *warning* period.

Table 4: Summary statistics for daily detection frequency by site and period

	Warning period (N=31 days)		Program period (N=244 days)		After period (N=69 days)		Reactivation period (N=128 days)	
Site*	Mean	Std.Dev.	Mean	Std.Dev.	Mean	Std.Dev.	Mean	Std.Dev.
1	203.52	84.08	158.41	62.08	1624.26	615.77	134.21	47.73
2	117.16	47.1	87.20	34.96	1163.45	453.52	108.54	55.43
3	245.42	80.47	254.76	78.93	2742.71	966.66	227.16	78.30
4	38.84	19.53	31.09	18.30	431.23	241.57	52.32	28.61
5	186.32	71.68	132.39	58.03	1904.48	867.41	127.44	56.27
6	181.94	78.27	114.35	57.66	1028.07	520.22	160.34	69.00
Total	973.19	339.15	778.20	273.24	8894.20	3455.26	808.06	276.08
Mean	162.20	94.57	129.70	88.06	1482.37	981.21	134.68	78.41

Table 4 shows the summary statistics for daily detection frequency by period as well as site, and the interval plot for the mean detection frequency by period (with 95% Confidence Interval) is shown in Figure 10.

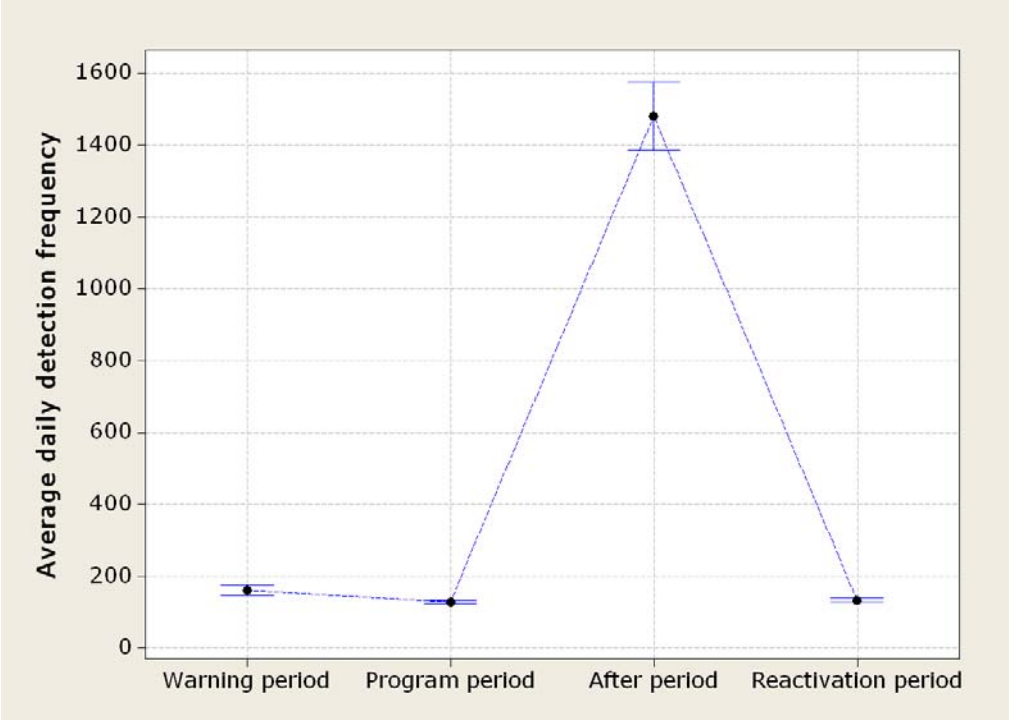

Figure 10: Average daily detection frequency by period

The detection frequencies vary over the enforcement sites—the detection frequencies at site 3 (see Figure 9: site 3 is located on Frank Lloyd Wright Blvd. and Raintree Dr.) are greater than those at other sites (see Figure 11).

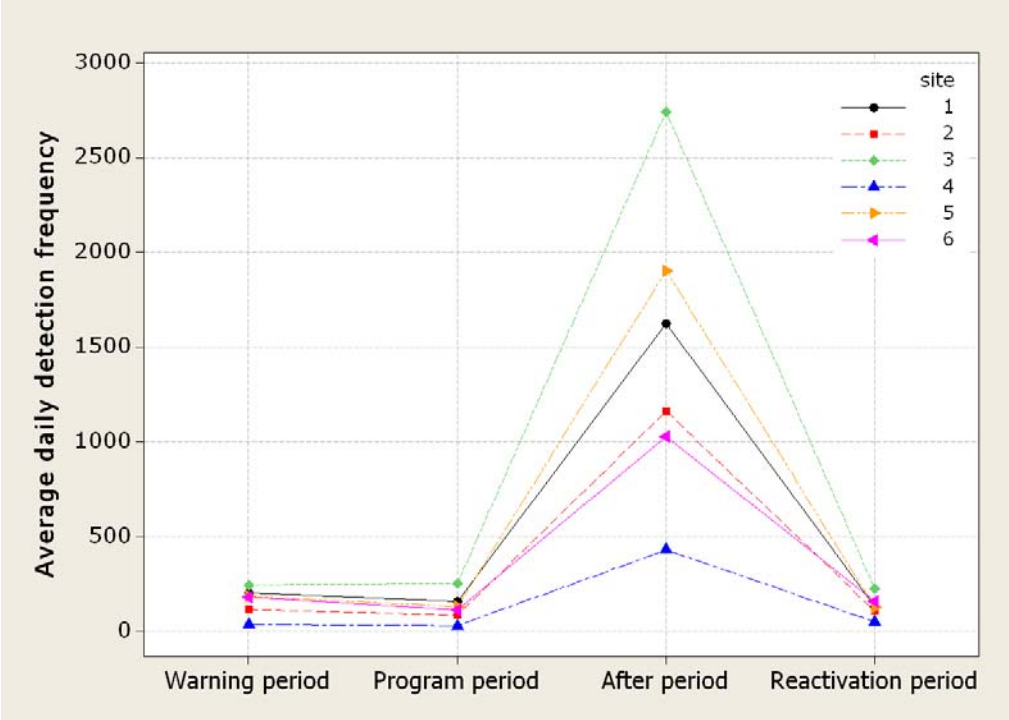

Figure 11: Average daily detection frequency by period and site

Table 5: Summary statistics for the daily detection frequency per camera by day of week and period

	Warning period		Program period		After period		Reactivation period	
	Mean	Std.Dev.	Mean	Std.Dev.	Mean	Std.Dev.	Mean	Std.Dev.
Monday	138	69	110	69	1154	681	111	55
Tuesday	131	61	98	63	1203	876	105	52
Wednesday	126	58	99	66	1231	911	110	54
Thursday	124	71	102	66	1157	795	109	56
Friday	140	78	114	76	1250	862	118	63
Saturday	230	104	190	104	1905	1109	193	94
Sunday	241	119	190	100	1854	899	198	93
Holiday	.	.	153	86	2304	1001	176	82
Total	162	95	130	88	1482	981	135	78

Since our interest is in comparing the change in the detection frequency resulting from the SEP, the change in the average daily detection frequency per camera (i.e., site) by period was analyzed. The time series plot illustrated in Figure 13 shows that the average daily detection frequency per camera has periodic patterns–spikes for weekends and holidays. Table 5 shows the summary statistics for the average daily detection frequency per camera during the four periods by the day of the week. The list of holidays used in this analysis is summarized in Table 6, which is equivalent to the list of holidays used in the annual Arizona Crash Fact Summary Report (ADOT 2006). The daily detection frequencies during weekends and holidays are relatively greater than those during weekdays, while the detection frequencies during weekdays appear to be similar to each other (see Table 5).

Table 6: A list of holidays in 2006 and 2007

Description	Official observed date	Holiday	
		Start	End
New Year's Day	Monday, January 2	December 31, 2005	January 2, 2006
Memorial Day	Monday, May 29	May 27, 2006	May 29, 2006
Independence Day	Tuesday, July 4	July 1, 2006	July 4, 2006
Labor Day	Monday, September 4	September 2, 2006	September 4, 2006
Thanksgiving Day	Thursday, November 23	November 23, 2006	November 26, 2006
Christmas Day	Monday, December 25	December 23, 2006	December 25, 2006
New Year's Day	Monday, January 1	December 30, 2006	January 1, 2007
Memorial Day	Monday, May 28	May 26, 2007	May 28, 2007

Table 7 shows the summary statistics for the average daily detection frequency per camera during the four periods, in which each day is aggregated by two categories: "weekdays" and "weekends and holidays." Regardless of the periods, detection frequencies during weekends and holidays are greater than those during weekdays as shown in Figure 12, which indicates that the likelihood of speeding on weekends and

holidays is relatively high due to the low traffic demand on those days. This finding suggests that the detection frequency needs to be analyzed by controlling for the day of week effect.

Table 7: Summary statistics for the daily detection frequency during the 4 periods by the 2 categories

	Weekdays		Weekends and holidays		Total	
	Mean	Std. Dev.	Mean	Std. Dev.	Mean	Std. Dev.
Warning period	132.02	66.75	235.98	111.31	162.20	94.57
Program period	104.68	68.61	185.00	100.32	129.70	88.06
After period	1200.72	829.60	2045.66	1020.53	1482.37	981.21
Reactivation period	110.50	56.22	194.13	92.45	134.68	78.41

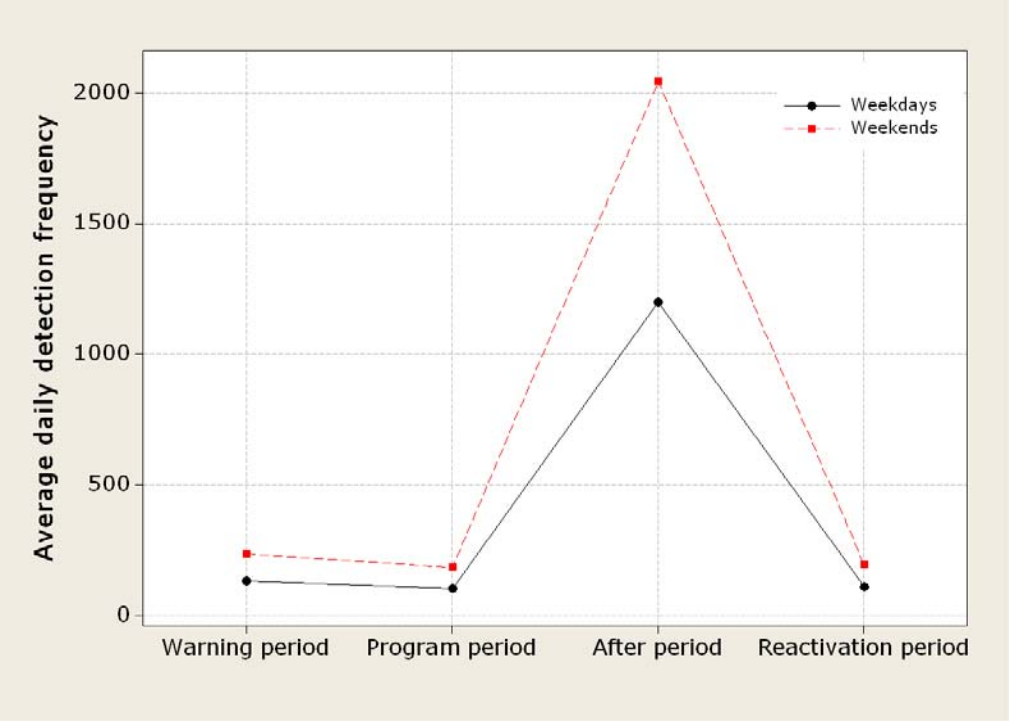

Figure 12: Average daily detection frequency by periods and day of week

The time series plots also suggest that the day of week is one of several important factors that affect the detection frequency. As previously discussed, the time series plots have periodical spikes when weekends and holidays are not excluded (see Figure 13). However, more stable time series plots can be obtained when the day of week effects are eliminated from the time series plots (see Figure 14 and Figure 15).

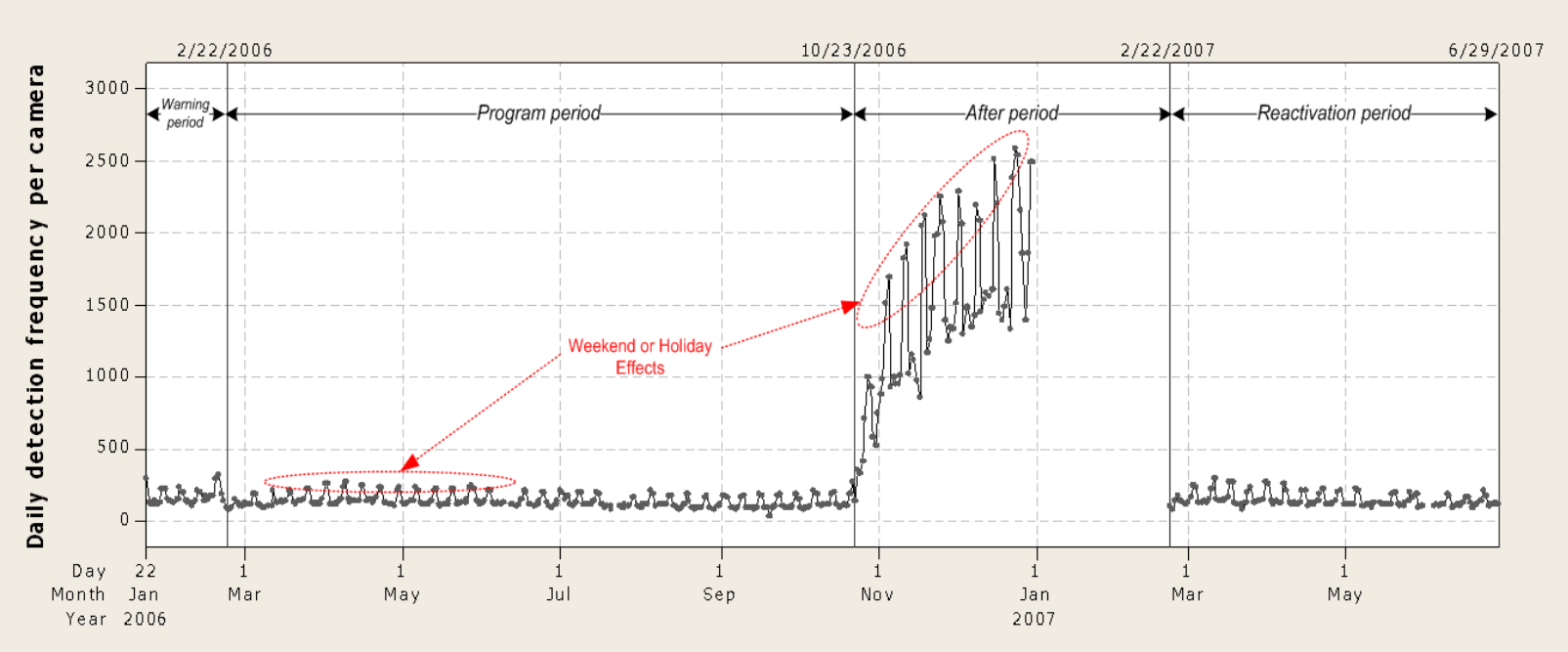

Figure 13: Average daily detection frequency per camera during the four periods

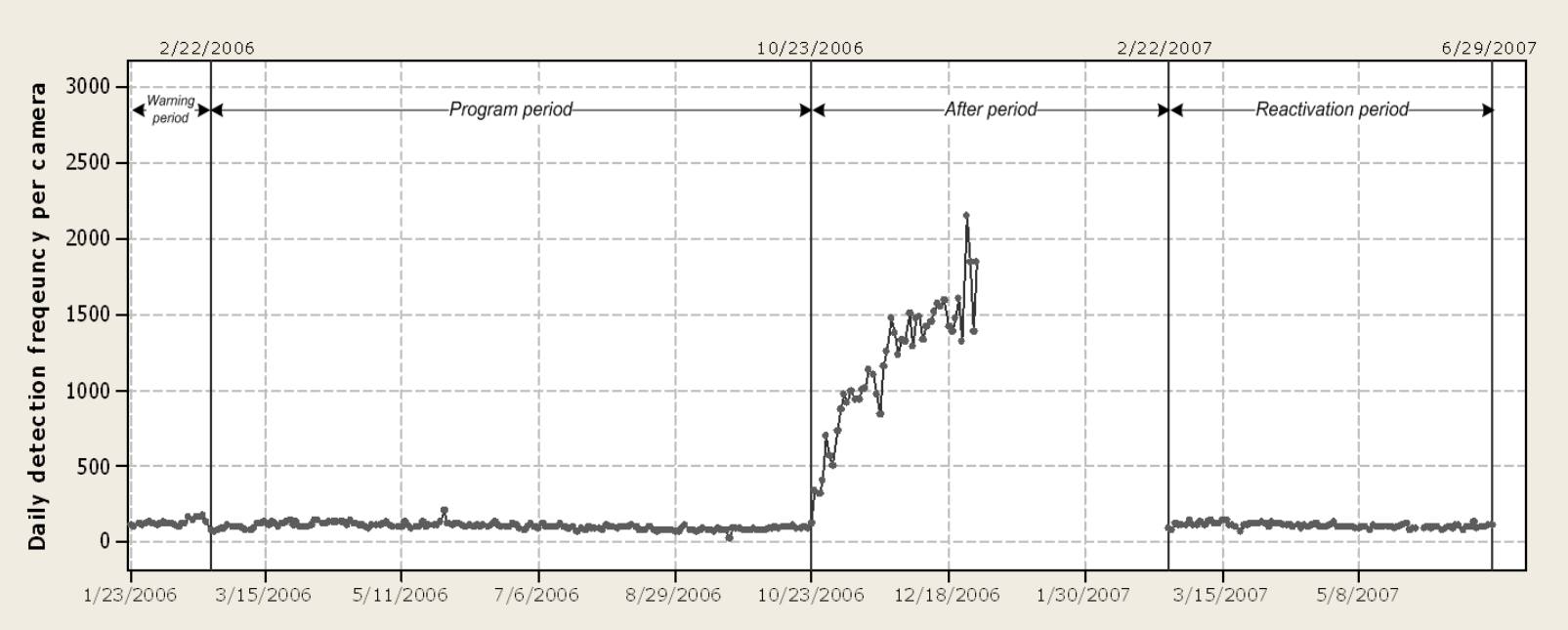

Figure 14: Average daily detection frequency per camera during the four periods (weekdays)

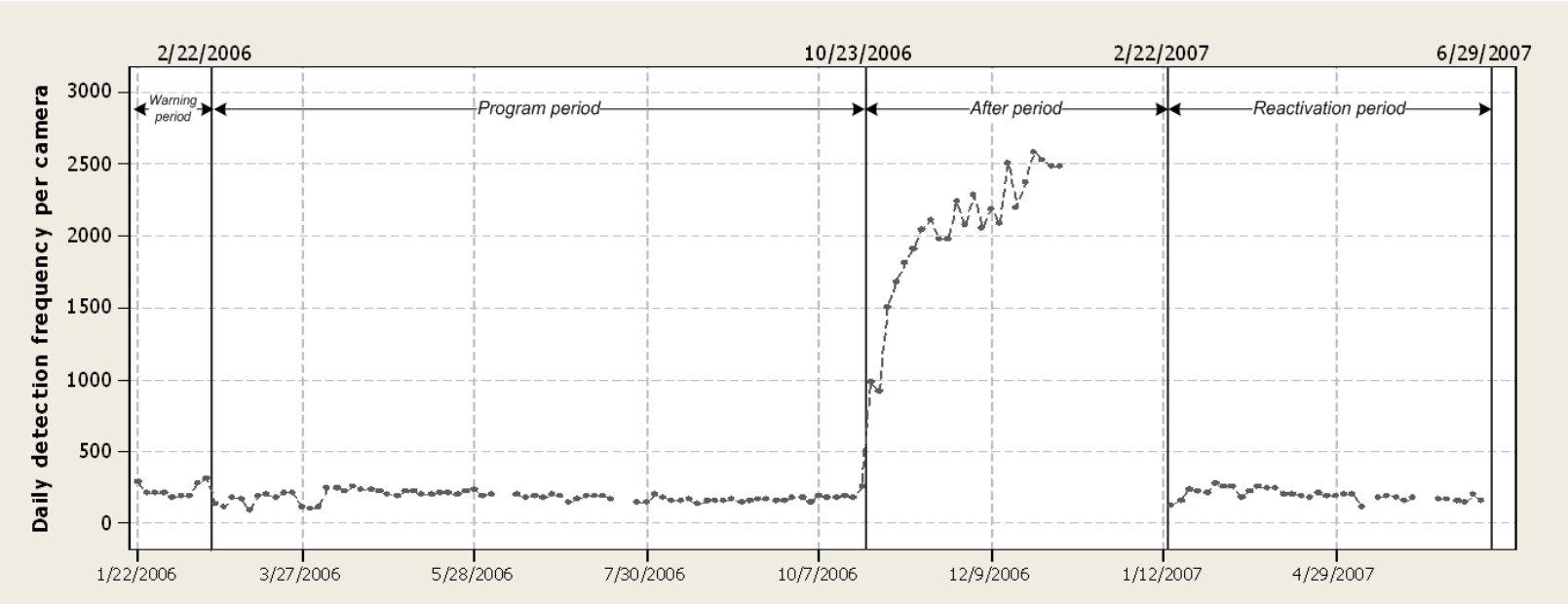

Figure 15: Average daily detection frequency per camera during the four periods (weekends and holidays)

3.1.2 Effect of SEP on the Detection Frequency

The preliminary explanatory analyses suggest that the change in speeding detection frequency needs to be analyzed by accounting for the day of the week effects as well as the presence (or operation) of the SEP. Therefore, the impact of the SEP on the speeding detection frequency is analyzed by using the two sub-samples (weekdays vs. weekends and holidays) in order to develop parsimonious models with the one factor (i.e., the presence of the SEP). The one factor analyses are consistently used in this analysis because the interactions between the day of the week effect and the presence of the SEP are not quite meaningful.

We observed the variances of speeding detection frequency are significantly different according to the presence of the SEP as shown in Table 7. Regardless of the day of week, the standard deviations of the speeding detection frequency during the after period are remarkably larger than those during the remaining periods. The Brown-Forsythe (BF) test, which is an extension of the Levene's test, was conducted to investigate as to whether or not the variance of speeding detection frequency in each period of observation is different. Equation (1) shows the BF test statistic, which is insensitive to departures from normality (Kutner et al. 2005):

$$F_{BF} = \frac{(n_T - s)\sum_i n_i(\overline{d}_{i\cdot} - \overline{d}_{\cdot\cdot})^2}{(s-1)\sum_i \sum_j (d_{ij} - \overline{d}_{i\cdot})^2}, \quad (1)$$

where d_{ij} is the absolute deviations of the y_{ij} (the detection frequency for the *j*th day during the *i*th period of observation) about their respective medians $\tilde{y}_{i\cdot}$, $\overline{d}_{i\cdot}$ ($\overline{d}_{\cdot\cdot}$) indicates an aggregation of the absolute deviations over the *j* index (over the *j* and *i* indexes), n_T is total number of days during the 4 periods, n_i is the number of days for the *i*th period of observation, s is the number of observation periods (i.e., $s = 4$). Under the null hypothesis (H_0: $\sigma_i^2 = \sigma^2 \ \forall i$), the F_{BF} follows approximately an *F* distribution with $s-1$ and $n_T - s$ degree of freedom. In all tests, the *program* period was considered consistently as a reference group.

Table 8: Brown-Forsythe test results for the homogeneity of variance

Period Pair	Weekdays		Weekends and holidays	
	Test statistic (F_{BF})	p-value	Test statistic (F_{BF})	p-value
Warning–Program	0.0715	0.7893	0.7451	0.3884
After– Program	1099.8168	<0.001	738.2187	<0.001
Reactivation– Program	18.1769	<0.001	3.4350	0.0643
All periods	612.5597	<0.001	389.1279	<0.001

The test results summarized in Table 8 show that the variance of speeding detection frequency for each period of observation is significantly different at α=0.05. Therefore, the impact of the SEP on the speeding detection frequency is analyzed by using weighted least square (WLS) estimation, which is a standard modification of the general linear models with the unequal variances (Greene 2003; Kutner et al. 2005; Washington et al. 2003).

Since the variances for each period of observation are often unknown, the sample variances s_i^2 (see Table 7) are used as the estimate. The weight w_{ij} for the *j*th day of the *i*th period of observation is:

$$w_{ij} = \frac{1}{s_i^2}, \tag{2}$$

where the weight is the inverse of the variance in each group by the period and the day the week. Table 9 shows the estimates for the difference in the daily speeding detections per camera by period and the day of the week. The difference in the mean number of speeding detections between the *after* (or warning) period and the *program* period is significant at α=0.05. However, the mean speeding detection frequency between the *program* period and the *reactivation* period is not significant at α=0.05, suggesting that the activation of the SEP contributed to reducing the number of motorists exceeding 75mph. The WLS estimates summarized in Table 9 are used to calculate the relative change in daily speeding detection frequency per camera, which is summarized in Table 10.

Table 9: WLS estimates for the difference in daily speeding detection frequency per camera

Day of Week	Period Pair	Difference in Daily Speeding Detection (p-value)	95% C.I.s	
			Lower	Upper
Weekdays	Warning–Program	27.33 (<0.001)	15.17	39.49
	After– Program	1096.04 (<0.001)	998.01	1194.06
	Reactivation– Program	5.81 (0.072)	–0.53	12.16
Weekends and Holidays	Warning–Program	50.98 (<0.001)	19.86	82.11
	After– Program	1860.66 (<0.001)	1689.91	2031.42
	Reactivation– Program	9.13 (0.241)	–6.14	24.41

Table 10: Relative changes in daily speeding detection frequency per camera

Day of Week	Period Pair	Relative difference in daily Speeding detection	95% C.I.s	
			Lower	Upper
Weekdays	Warning–Program	0.261	0.145	0.377
	After– Program	10.470	9.534	11.406
	Reactivation– Program	0.056	-0.005	0.116
Weekends and Holidays	Warning–Program	0.276	0.107	0.444
	After– Program	10.058	9.135	10.981
	Reactivation– Program	0.049	-0.033	0.132

The estimated results show that:

- After the SEP was implemented, the detection frequency decreased by 26% (or 27%) from the *warning* to *program* period. The decrease in the speeding detection frequency is statistically significant.
- After the SEP ended, the detection frequency increased by 1047 % (or 1006%) from the *program* to *after* period.
- The detection frequency for the *reactivation* period is not statistically different than that for the *program* period, indicating that the activation of the SEP contributed to reducing drivers' speeding behavior.
- The pairwise comparisons suggest that the activation of the SEP is an effective countermeasure for reducing speeding behavior, resulting in significant reductions in the number of motorists exceeding 75mph.

3.2 Changes in the Mean Speed

In this section, the effects of the SEP on the mean speed are analyzed by comparing the mean speeds that were collected from the enforcement zone during the *before* and *program* period. Unlike the analysis for the changes in the speeding detection frequency, the mean speeds during the *after* and *reactivation* period are not compared in this analysis due to insufficient data. The analysis was conducted using mean speeds during unconstrained traffic conditions, since the SEP will not significantly affect peak-period travel.

3.2.1 Data Description

In this subsection, the speed data obtained from the enforcement zone during the *before* period (see Table 11) are summarized, and the speed data during the *program* period are described in the analysis subsection.

Table 11: Description of the 6 measurement sites for the *before* period

ID	Direction	Location	Measurement date		
1	NB	CACTUS RD & SHEA BLVD	4/13/2005	4/14/2005	4/15/2005
2	SB	CACTUS RD & SHEA BLVD	4/13/2005	4/14/2005	4/15/2005
3	NB	RAINTREE DR & CACTUS RD	4/19/2005	4/20/2005	4/21/2005
4	SB	RAINTREE DR & CACTUS RD	4/19/2005	4/20/2005	4/21/2005
5	NB	SCOTTSDALE RD & PIMA/PRINCESS DR	6/27/2005	6/28/2005	6/29/2005
6	SB	SCOTTSDALE RD & PIMA/PRINCESS DR	6/27/2005	6/28/2005	6/29/2005

In order to reduce the variance from the different measurement dates, the middle of the day (24 hours) was consistently used in this analysis (i.e., 4/14/2005; 4/20/2005; 6/28/2005). The descriptive statistics for the speed data are summarized in Table 12, in which an individual speed data observation is the aggregated mean speed in each lane during 15-minute intervals. For instance, the mean speed at site *i* ($\overline{S_{i\bullet}}$) is estimated by the aggregated mean speed at site *i* during the *j*th interval (S_{ij}).

$$\overline{S_{i\bullet}} = \frac{\sum_{j=1}^{n_i} S_{ij}}{n_i}$$

where $i = 1, 2, \cdots, 6$ and $j = 1, 2, \cdots, n_i$.

Table 12: Summary of statistics for speed by site

Site ID	Mean	Std. Dev.	Min.	Median	Max.	N (n_i)
1	70.40	6.46	46	71	83	288
2	75.17	5.35	43	75	90	288
3	70.83	4.90	62	70	87	384
4	77.27	4.51	52	78	91	384
5	70.67	6.14	40	72	83	288
6	73.22	7.70	31	74	87	288

3.2.2 The Speed-Flow Relationship and Level of Service

Before comparing the speed data of the *before* period to those of the *program* period, the relationship between speed and traffic flow is examined because the former is sensitive to the latter. There are three commonly referenced macroscopic parameters to describe a traffic stream: speed, density, and rate of flow. They are related as follows:

$$V = S \times D$$

- V= Rate of flow (vehicle/hour/lane)
- S= Space mean speed (mph)
- D= Density (vehicles/mile/lane)

Density and speed are parameters for a specific section, while rate of flow is a parameter for a point. There have been a number of studies to reveal the shape of these relationships, but the relationship depends upon prevailing conditions. Figure 16 shows a recently depicted speed-flow relationship (Transportation Research Board 2000), which is typical of traffic patterns on uninterrupted flow facilities.

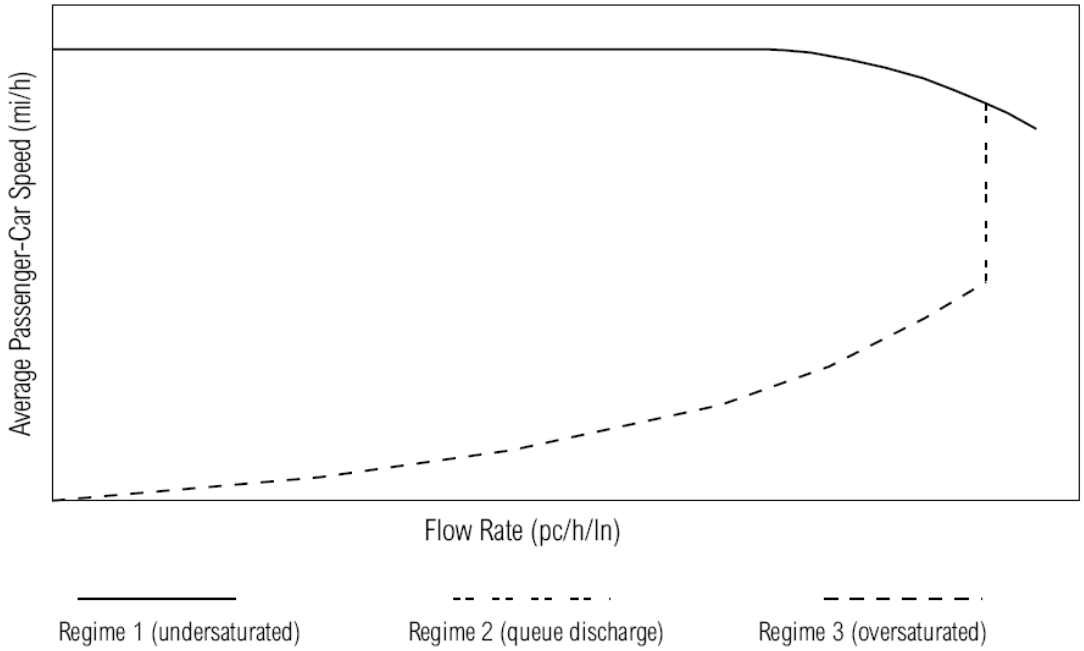

Figure 16: Speed-flow curve [Source: HCM 2000]

The modern speed-flow curve show in Figure 16 implies that the effects of traffic flow on speed are different across regimes. Since focus in this study is on the speed distribution in regime 1 rather than that in regimes 2 or 3, it is necessary to determine and classify regime 1.

In order to extract the speed in the stable flow (i.e., regime 1), the concept of the level of service (LOS) is used. In general, LOS is characterized using three performance measures: density in terms of passenger cars per mile per lane, speed in terms of mean passenger-car speed, and the volume-to-capacity (v/c) ratio. Each of these measures is an indication of how well traffic flow is being accommodated by the freeway. For a basic freeway section, the LOS is defined by reasonable ranges using the three critical flow variables: speed, density, and flow rate.

The three identified regimes of the speed-flow curve in Figure 16 can be described as follows (Roess et al. 2004):

- Regime 1: This regime is in the stable (or undersaturated) condition where drivers can maintain a high speed that is unaffected by upstream or downstream conditions. The flat portion of the curves usually defines free-flow speed. Speed begins to decline in response to increasing flow rates. However, the total decline in speed from free-flow speed to the speed at capacity is often 5 mph or less.
    - The inflection point, which indicates the flow rate at which speed begins to decline, is often in the range of 1,500–1,700 pc/h/ln (passenger cars per hour per lane).
    - Note that the path from free-flow speed to capacity is often associated with a relatively small increase in the flow rate.
- Regime 2: This portion of the curve is called "queue discharge." Once demand exceeds capacity, a breakdown occurs and a queue propagates upstream of the point of breakdown. Once the queue forms, flow is restricted to what is discharged from the front of the queue. The variable speed for Regime 3 reflects the fact that vehicles discharge from a queue into an uncongested downstream segment.
- Regime 3: This portion of the curve reflects the unstable operating conditions within the queue, upstream of the breakdown, in which traffic flow is influenced by the effects of a downstream condition. Traffic flow in the regime can vary over a broad range of flows and speeds depending on the congestion severity.

Figure 17 shows the speed-flow curves that depend on free-flow speeds. All curves have the same speed-flow relationship for regime 1 as illustrated in Figure 16, but each curve has a different intercept that depends on free-flow speed. In addition, each LOS has the minimum or maximum values for the three parameters. The minimum or maximum values for the parameters are summarized in Table 13, which can be used to determine LOS. In this study, a speed of 62.2 mph was used as the threshold average speed for delineating congested and uncongested conditions, which is equivalent to the threshold speed for 'LOS E' when free-flow speed is assumed as 75 mph.

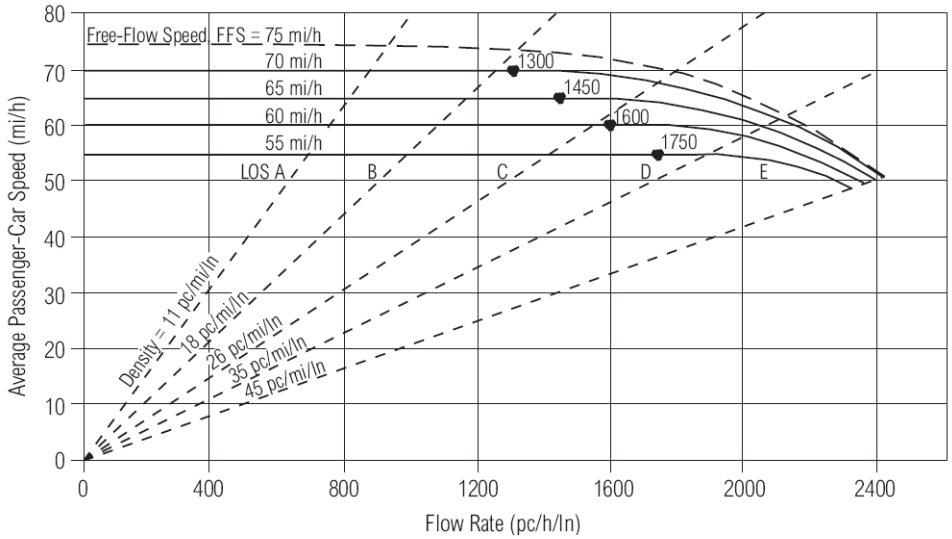

Figure 17: Speed-flow curves and LOS on a basic freeway segment [Source: HCM 2000]

Table 13: LOS criteria for basic freeway sections

Criteria	LOS				
	A	B	C	D	E
FFS = 75 mi/h					
Maximum density (pc/mi/ln)	11	18	26	35	45
Minimum speed (mi/h)	75.0	74.8	70.6	62.2	53.3
Maximum v/c	0.34	0.56	0.76	0.90	1.00
Maximum service flow rate (pc/h/ln)	820	1350	1830	2170	2400
FFS = 70 mi/h					
Maximum density (pc/mi/ln)	11	18	26	35	45
Minimum speed (mi/h)	70.0	70.0	68.2	61.5	53.3
Maximum v/c	0.32	0.53	0.74	0.90	1.00
Maximum service flow rate (pc/h/ln)	770	1260	1770	2150	2400
FFS = 65 mi/h					
Maximum density (pc/mi/ln)	11	18	26	35	45
Minimum speed (mi/h)	65.0	65.0	64.6	59.7	52.2
Maximum v/c	0.30	0.50	0.71	0.89	1.00
Maximum service flow rate (pc/h/ln)	710	1170	1680	2090	2350
FFS = 60 mi/h					
Maximum density (pc/mi/ln)	11	18	26	35	45
Minimum speed (mi/h)	60.0	60.0	60.0	57.6	51.1
Maximum v/c	0.29	0.47	0.68	0.88	1.00
Maximum service flow rate (pc/h/ln)	660	1080	1560	2020	2300
FFS = 55 mi/h					
Maximum density (pc/mi/ln)	11	18	26	35	45
Minimum speed (mi/h)	55.0	55.0	55.0	54.7	50.0
Maximum v/c	0.27	0.44	0.64	0.85	1.00
Maximum service flow rate (pc/h/ln)	600	990	1430	1910	2250

The general definitions of LOS are as follows (Transportation Research Board 2000):

- LOS A describes free-flow operations. Free-flow speeds prevail. Vehicles are almost completely unimpeded in their ability to maneuver within the traffic stream. The effects of incidents or point breakdowns are easily absorbed at this level.
- LOS B represents reasonably free flow, and free-flow speeds are maintained. The ability to maneuver within the traffic stream is only slightly restricted, and the general level of physical and psychological comfort provided to drivers is still high. The effects of minor incidents and point breakdowns are still easily absorbed.
- LOS C provides for flow with speeds at or near the free-flow speed of the freeway. Freedom to maneuver within the traffic stream is noticeably restricted, and lane changes require more care and vigilance on the part of the driver. Minor incidents may still be absorbed, but the local deterioration in service will be substantial. Queues may be expected to form behind any significant blockage.
- LOS D is the level at which speeds begin to decline slightly with increasing flows and density begins to increase somewhat more quickly. Freedom to maneuver within the traffic stream is more noticeably limited, and the driver experiences reduced physical and psychological comfort levels. Even minor incidents can be expected to create queuing, because the traffic stream has little space to absorb disruptions.
- LOS E describes operation at capacity. Operations at this level are volatile, because there are virtually no usable gaps in the traffic stream. Vehicles are closely spaced, leaving little room to maneuver within the traffic stream at speeds that still exceed 49 mph. Any disruption of the traffic stream, such as vehicles entering from a ramp or a vehicle changing lanes, can establish a disruption wave that propagates throughout the upstream traffic flow. At capacity, the traffic stream has no ability to dissipate even the most minor disruption, and any incident can be expected to produce a serious breakdown with extensive queuing. Maneuverability within the traffic stream is extremely limited, and the level of physical and psychological comfort afforded the driver is poor.
- LOS F describes breakdowns in vehicular flow. Such conditions generally exist within queues forming behind breakdown points.

3.2.3 Effect of the SEP on Mean Speeds

In order to control for the measurement date and day of week effects, the traffic volume and speed data obtained from the enforcement zone during the program period were carefully selected from the set of the speed and traffic flow data collected during the program period. Therefore, the speed and traffic flow data during the three identical times and days of the program period (Table 11) were selected: 4/13/2006 (Thursday), 4/19/2006 (Wednesday), and 6/27/2006 (Thursday). In addition, the data collected from the unstable condition were excluded by using the speed threshold (i.e., 62.2 mph), which is described in the previous subsection. The descriptive statistics for the speed data at stable condition during the *before* and *program* period are summarized in Table 14.

Table 14: Summary statistics for the speed at stable condition during the before and program period

Period	Mean	Std.Dev.	Min.	Q1	Q2	Q3	Max.
Before	73.11	3.53	64.80	70.00	72.90	76.00	82.00
Program	64.36	1.20	62.33	63.67	64.33	65.00	68.33
Total	66.90	4.51	62.33	63.67	65.00	69.20	82.00

The statistics in Table 14 show that the mean speed decreased in the *program* period from 73.1 mph to 64.4 mph, and the standard deviation of speed also reduced from 3.5 mph to 1.2 mph. Since one of the interests is also to estimate the impact of the SEP on speed, the variance-weighted least square technique was used again due to the group-wise heteroskedasticity in speed (the Brown-Forsythe test statistic=1193.78; p-value<0.001).

Unlike the WLS estimation used for analyzing the speeding detection frequency, the variable *traffic flow* was included in the model because the speed is highly sensitive to the change in traffic flow as discussed in the previous subsection (see "The Speed Flow Relationship and Level of Service" on page 35). In addition, the interaction term between the variable *traffic flow* and the *period* was added because the treatment effect is likely to interact with the covariate *traffic flow*.

Table 15: WLS estimates for the impact of the SEP on speed (n=1934)

Variable	Estimate	Std. Err.	t-value	p-value	95% CIs	
					Lower	Upper
Constant	65.297	0.047	1391.11	<0.001	65.297	65.481
Dummy variable for period (1=before; 0=program)	10.286	0.242	42.49	<0.001	9.811	10.760
Traffic flow rate (vplph)	-0.001	0.000	-26.63	<0.001	-0.002	-0.001
Interaction between the period dummy variable and traffic flow rate	-0.002	0.000	-6.41	<0.001	-0.002	-0.001
F-statistic (associated p-value)	1880.24 (<0.001)					
Adjusted R^2	0.7447					

Equation (3) shows the WLS estimation results, where s_i is the mean speed for the ith observation, D_i is the dummy variable for period (1 for the *before* period; otherwise 0), F_i is the mean flow rate for the ith observation, and $D_i \cdot F_i$ is an interaction term between D_i and F_i. The standard errors for each estimate are in parentheses (all estimates are significant at α=0.05). All estimation outputs are also summarized in detail in Table 15.

$$s_i = \underset{(0.04701)}{65.39} + \underset{(0.24206)}{10.29}\, D_i - \underset{(0.00005)}{0.0014}\, F_i - \underset{(0.00024)}{0.0016}\, D_i \cdot F_i;\ Adj\ R^2 = 0.745 \qquad (3)$$

The significant negative estimate for the traffic flow rate reflects the well-known relationship between speed and traffic flow in the stable regime: as traffic flow increases, speed decreases. The significant negative estimate for the interaction indicates that the speed of a driver for the *program* period is relatively insensitive to change in traffic flow due to the SEP as shown in Figure 18.

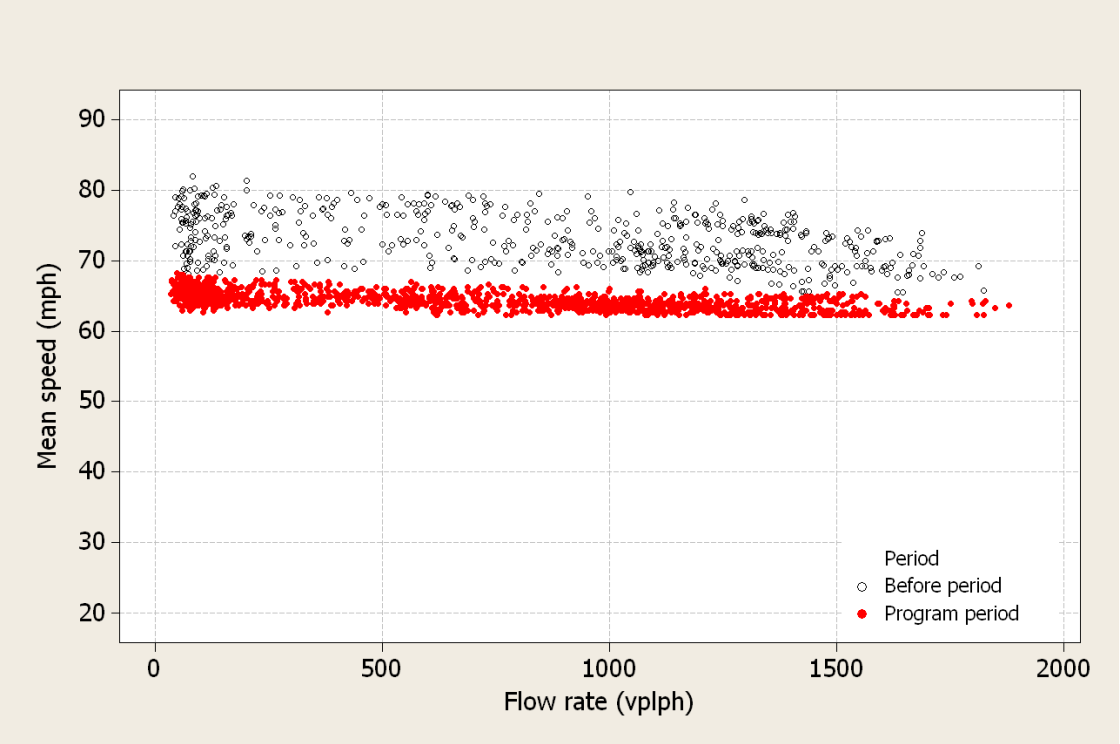

Figure 18: Impact of the SEP on speed by period

Consequently, it is evident that the impact of the SEP on speed increases as traffic flow decreases due to the well known relationship between speed and traffic flow. Thus, the impact of the SEP on speed was estimated using quartiles of the flow rate during both periods as shown in Table 16. Specifically, the mean speed decreased by 9.97 mph when traffic flow was 206 vplph (Q1), while the mean speed decreased by 8.47 mph when traffic flow was relatively high (i.e., 1,169 vplph: Q3).

Table 16: Estimated speed reduction (mph) due to the SEP

Period Pair	Speed Reduction (Std. Err.)	95% C.I.s	
		Lower	Upper
Before– Program (Flow=Q1*)	9.97 (0.201)	9.57	10.36
Before– Program (Flow=Q2)	9.04 (0.127)	8.79	9.29
Before– Program (Flow=Q3)	8.47 (0.149)	8.17	8.75

* Q1, Q2, and Q3 are quartiles for the flow rate: 206 vplph, 800 vplph, and 1,169 vplph respectively.

In summary, the estimated results reveal that:

- The SEP not only reduced the average speed at the enforcement camera sites by about 9 mph, but also contributed to reducing the speed dispersion at the enforcement camera sites. Thus, as prior research has revealed, both the prerequisites for crash reduction (safety improvement) are met with the SEP.
- The reduction in the mean and variance of speed resulting from the SEP depends on traffic flow: the reduction increased as traffic flow decreased due to the well known relationship between speed and traffic flow. Thus, the magnitude of speed effects of the SEP is inversely related to traffic flow.

Chapter 4 Effects of the SEP on Traffic Safety

In this chapter, the effects of the SEP on traffic safety are comprehensively analyzed. Target crashes are first carefully determined by using the detection trend in terms of time of day, and the evaluation methodologies used in the study are described in detail. After presenting some preliminary analysis concepts, we discuss the results of three analysis methodologies, their assumptions, and the results of the analysis.

4.1 Preliminaries: Target Crashes and Data Description

4.1.1 Determining Target Crashes

Before estimating the impact of the SEP on traffic safety, it is necessary to define which crashes are materially affected by the speed enforcement cameras—referred to as "target" crashes. Since the crashes occurring during the peak travel periods are unlikely to be affected by the photo enforcement cameras, target crashes should be defined as crashes that occurred during the off-peak-periods.

Since traffic conditions for each crash are often unknown, we investigated the speeding detection rate by time of day (TOD) in order to test whether or not the TOD can be used as a proxy to determine the off-peak-period. Figure 19 shows the detection frequency by TOD, in which the detection frequency is the average number of detections per 15-minute interval at the enforcement sites for the program period. The detection frequency by TOD indicates that detection frequency decreases during peak hours for weekdays, while they are almost proportional to traffic flow for weekends and holidays. Therefore, TOD is generally related to speeding behaviors on weekdays.

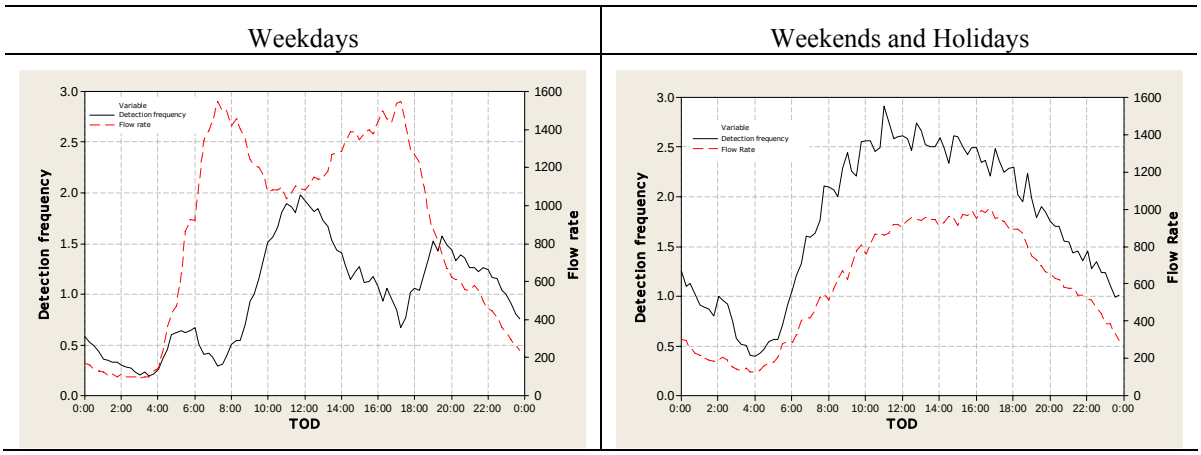

Figure 19: Detection frequency by TOD

In addition, the relationships between TOD and detection rate shown in Figure 20 indicate that the detections could occur for weekends and holidays regardless of traffic flow, while the detections are related to the changes in traffic flow, in which the detection rate is the ratio of detection frequency to the average traffic volume per 15-minute interval at the enforcement sites for the program period. For example, the detection rates during peak hours for weekdays are remarkably low—less than 0.25% between 6:00 AM and 9:00 AM.

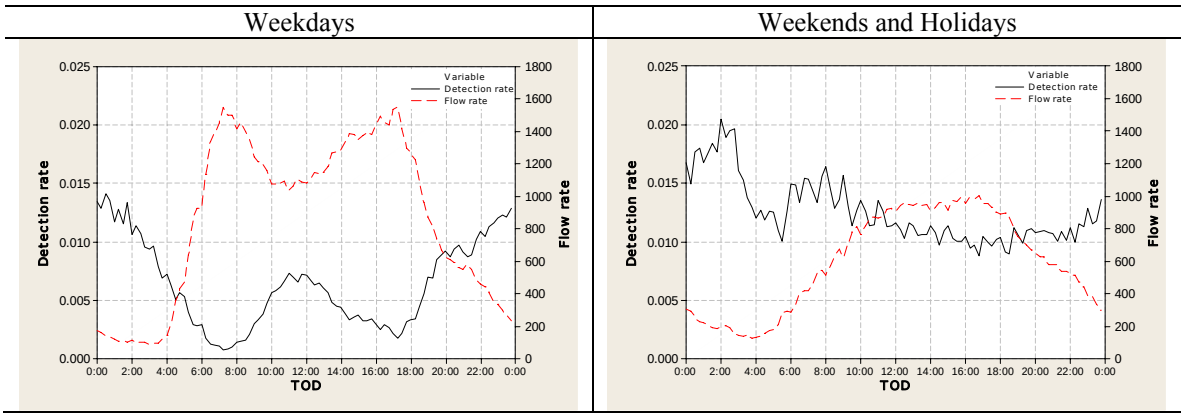

Figure 20: Detection rate by TOD

Since the detection trends by TOD suggest that TOD can be used to identify traffic flow regimes, two traffic flow regimes (peak and off-peak periods) are defined by using TOD.

- Peak periods (6 hours)
  - 06:00 AM — 09:00 AM
  - 16:00 PM — 19:00 PM
- Off–peak periods
  - The remaining 18 hours for weekdays
  - 24 hours for weekends and holidays

Consequently, the target crashes in this analysis are the crashes that occurred within the enforcement zone (milepost 34.51 – milepost 41.06: 6.5 miles) during the off-peak travel periods defined by TOD (because of the limited expected influence of the cameras on slow moving peak-period traffic). Note that the target crashes are "mainline" crashes classified by ADOT, excluding crashes that occurred on Loop 101 ramps and frontage roads. In the next subsection, the characteristics of the target crashes are discussed in detail.

4.1.2 Crash Data Description

In this subsection, the characteristics of the target crashes determined in the previous subsection are discussed. The durations of the target crash data are summarized below:

- Crash data during the *before* period
  - Duration: 2/22 – 10/23 (2001 through 2005)
- Crash data during the *program* period
  - Duration: 2/22/2006 – 10/23/2006 (244 days)

Note that the SEP was reactivated February 22, 2007, but the current analysis is based on the crash data for the *program* period. Figure 21 shows the number of crashes that occurred within the enforcement zone during the *before* period. It contains target crashes as well as the crashes that occurred during the peak periods. Although the average number of crashes during the two periods (peak and off-peak periods) cannot be compared directly, three crash types are most frequent: single-vehicle, side-swipe (same), and rear-end crashes. Therefore, the remaining crash types such as angle, left-turn, side-swipe (opposite), head-on, and other crashes are aggregated as "other" in this analysis.

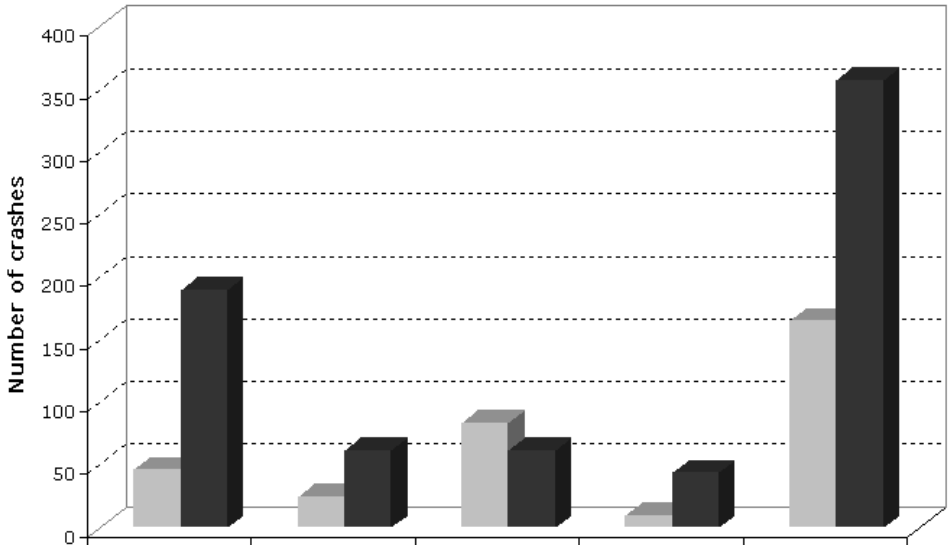

	Single vehicle	Sideswipe (same)	Rear-end	Other	Total
peak	46	25	84	10	165
off-peak	190	62	62	44	358

Figure 21: Number of crashes that occurred at the enforcement zone during the before period

Figure 22 and Figure 23 show the percentage of the peak or off-peak crashes by crash type, which occurred during the *before* period. The most frequent crash type was single-vehicle crashes (54%) for the off-peak periods, while rear-end crashes type (51%) was most frequent for the peak periods.

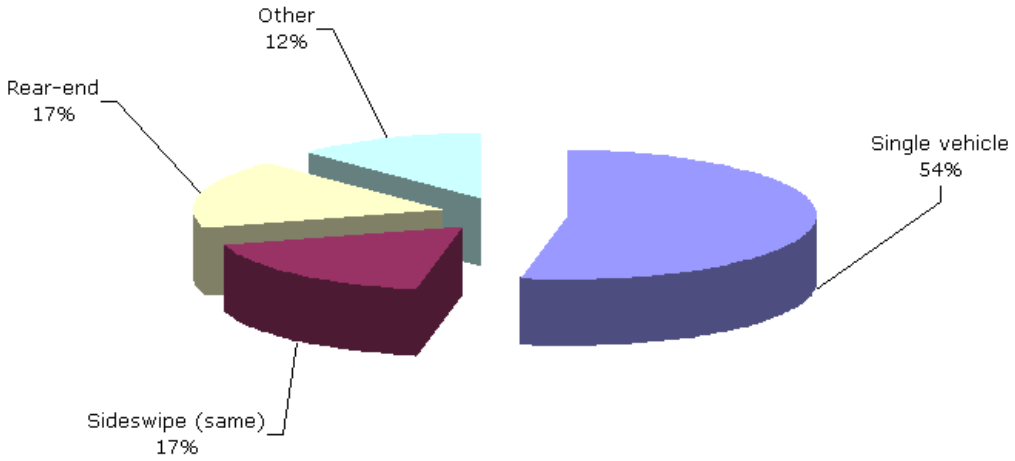

Figure 22: Percentage of off-peak crashes by crash type (before period)

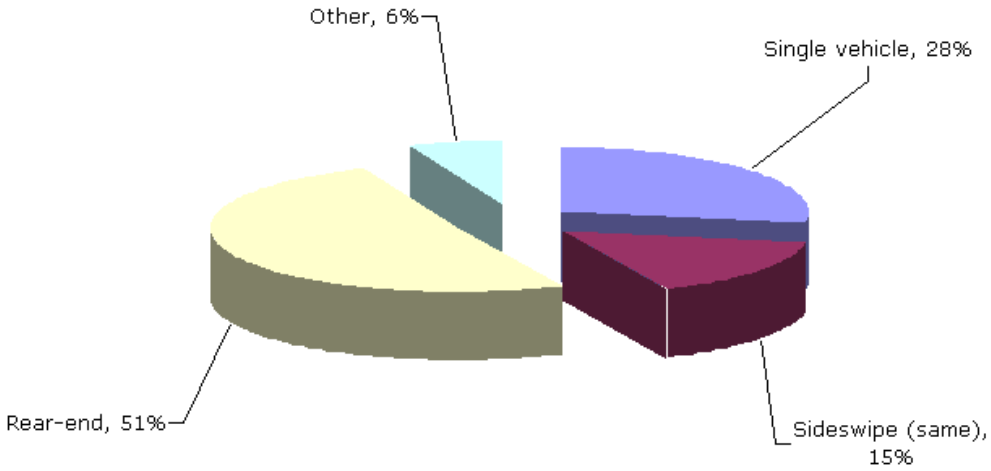

Figure 23: Percentage of peak-period crashes by crash type (before period)

Although it is evident that the characteristics of crashes are different for the two periods, the analysis using the target crashes is conservative because the peak period is likely to increase over time (the *before* to *program* period). Therefore there is increasing constraint on speed over time, or lesser constraint on speed going back in time (the *before* period), resulting in target crashes in the *before* period being eliminated from the analysis (because they occurred during the peak period). Fewer *before* crashes reduce the estimated effectiveness of a countermeasure; therefore this approach is conservative.

4.2 The Four-Step Procedures for Before-and-After Study

In this section, the basic concepts of the before-and-after (hereafter BA) study are described, and the basic four-step procedure for estimating the effects of SEP is also provided. This analysis approach used in this study is an expansion of the generally accepted and widely applied methods described by Hauer (Hauer 1997; Hauer et al. 2002).

The key objective of the BA study is to estimate the change in safety for the program period as a result of the treatment. The key notations used are:

- π: Expected number of crashes for the *program* period without the SEP;
- λ: Expected number of crashes for the *program* period with the SEP;
- κ: Expected number of crashes for the *before* period;
- $\delta = \pi - \lambda$: Change in safety resulting from the SEP;
- $\theta = \lambda/\pi$: Index of the effectiveness of the SEP;
- K: Observed number of crashes in the enforcement zone for the *before* period;
- L: Observed number of crashes in the enforcement zone for the *program* period;
- M: Observed number of crashes in the comparison site for the *before* period;
- N: Observed number of crashes in the comparison site for the *program* period.

If either δ is greater than 1 or θ is less than 1, then we conclude that the treatment is effective. The parameters π, λ, δ, and θ are unknown parameters and must be estimated using the available data. There are numerous arduous aspects of estimating these unknown parameters. Generally, the value of λ is being estimated using the observed number of crashes in the *program* period (i.e., L). It might seem that the observed number of crashes in the *before* period would be employed to predict the value of π.

Figure 24 illustrates the basic concept of the BA study. As discussed, the key objective of the analysis is to predict the expected number of crashes in the *program* period if the SEP had not been implemented. If we do not assume any change from *before* to *program* periods, the estimates of the π's are the same as the observed target crash frequency during the *before* period (i.e., K). However, it is insufficient to predict the value of π using the observed number of crashes in the *before* period. Problems arise because there are either potentially many recognizable and unrecognizable factors which may have changed from the *before* to *after* periods, or the regression to the mean bias that has resulted from sites being selected based on prior crash histories. Thus, often more

rigorous evaluation methodologies are needed to obtain accurate estimates of π, which are described in detail in the following subsection.

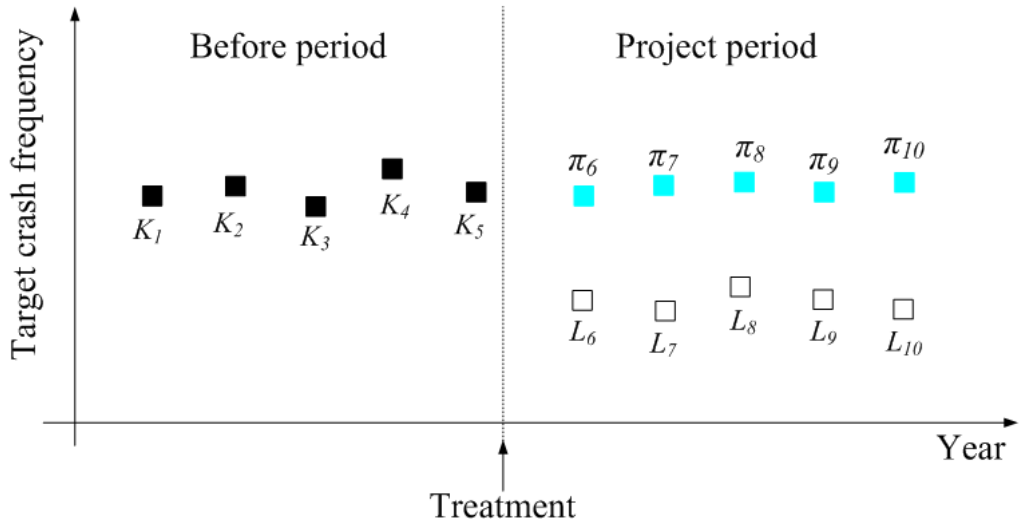

K: The observed number of target crashes during the *before* period
L: The observed number of target crashes during the *project* period with the treatment
π: The expected number of target crashes during the *project* period without the treatment

Figure 24: Basic concept of the before-and-after study

Regardless of the corrections made to the BA study, a basic four-step procedure is used (with modifications) to estimate the safety effect of a treatment. In the next subsections, we introduce the four-step procedure for the simple or naïve BA study approach, which is based on the following assumptions:

- Traffic volume, roadway geometry, road user behavior, weather, and many other factors have not significantly changed from the *before* to the *program* period.
- There are no treatments or improvements other than the installation of the speed enforcement cameras during the *program* period.
- The probability that crashes are reported is the same in both periods, and the reporting threshold has not changed.

Step 1: Estimate λ and predict π

The first step is to estimate λ and π. The estimate of λ is equivalent to the sum of the observed number of target crashes in the *program* period. Also, the predicted value of π is equal to the sum of the observed number of crashes in the *before* period. In the simple BA study, these estimates are:

$$\hat{\pi} = \sum_{t=1}^{B} K_t = K \tag{4}$$

and

$$\hat{\lambda} = \sum_{t=B+1}^{B+P} L_t = L, \tag{5}$$

where B and P are the number of durations for the *before* and *program* period respectively, and K_t and L_t are the observed target crash frequencies during the *before* and *program* period.

Step 2: Estimate $\widehat{\sigma}^2[\hat{\lambda}]$ *and* $\widehat{\sigma}^2[\hat{\pi}]$

The second step is to estimate the variance of $\hat{\lambda}$ and $\hat{\pi}$. Suppose that the number of target crashes is Poisson distributed (which is often the case at a single site), then the variance is equal to the mean.

$$\widehat{\sigma}^2[\hat{\lambda}] = \lambda \tag{6}$$

and

$$\widehat{\sigma}^2[\hat{\pi}] = \pi. \tag{7}$$

Of course, the estimate of variance of $\hat{\pi}$ will depend on the method chosen to consider various assumptions.

Step 3: Estimate δ *and* θ

The estimates of treatment effectiveness δ can be estimated:

$$\hat{\delta} = \hat{\pi} - \hat{\lambda} = K - L. \tag{8}$$

The estimator of θ was obtained by using the well-known delta approximation, because θ is a non-linear function of two random variables. Since the applications of the delta method are necessarily brief, the interested reader can refer to two references for a full derivation and justification (Hauer 1997; Shin and Washington 2007a) and consult two of a variety of references for the delta method (Greene 2003; Hines et al. 2003).

$$\hat{\theta} \cong \frac{\left(\hat{\lambda} / \hat{\pi}\right)}{\left\{1 + \widehat{Var}\left[\hat{\pi}\right] / \hat{\pi}^2\right\}} \tag{9}$$

Equation (9) shows that it is also necessary to estimate the variance of $\hat{\pi}$ in order to estimate the index of the effectiveness θ. The variance for $\hat{\pi}$ can be estimated by using the assumption that the number of target crashes is Poisson distributed.

Step 4: Estimate $\hat{\sigma}^2[\hat{\delta}]$ and $\hat{\sigma}^2[\hat{\theta}]$

The final step is to estimate the variance of the effects obtained by using four different methods, which can be used to approximate the "level of confidence" of the results. Equation (10) shows the unbiased estimators for the variances of $\hat{\delta}$ and $\hat{\theta}$, in which the variance of $\hat{\theta}$ is also obtained by using the delta (Hauer 1997; Shin and Washington 2007a).

$$\widehat{Var}[\hat{\delta}]=\hat{\pi}+\hat{\lambda};\ \widehat{Var}[\hat{\theta}]\cong\frac{\hat{\theta}^2\cdot\left(\frac{\widehat{Var}[\hat{\lambda}]}{\hat{\lambda}^2}+\frac{\widehat{Var}[\hat{\pi}]}{\hat{\pi}^2}\right)}{\left(1+\frac{\widehat{Var}[\hat{\pi}]}{\hat{\pi}^2}\right)^2}. \tag{10}$$

Table 17 shows the goal and formulas for each step in simple BA study four-step processes.

Table 17: The four-step procedure for simple before-and-after study

Step	Goals	Formulas for simple before-and-after study
Step 1	Estimate λ and predict π	$\hat{\lambda}=L$ $\hat{\pi}=K$
Step 2	Estimate $\hat{\sigma}^2[\hat{\lambda}]$ and $\hat{\sigma}^2[\hat{\pi}]$	$\hat{\sigma}^2\left[\hat{\lambda}\right]=\hat{\lambda}$ $\hat{\sigma}^2\left[\hat{\pi}\right]=\hat{\pi}$
Step 3	Estimate δ and θ	$\hat{\delta}=\hat{\pi}-\hat{\lambda}=K-L$ $\hat{\theta}\cong\frac{\left(\frac{\hat{\lambda}}{\hat{\pi}}\right)}{\left(1+\frac{\hat{V}[\hat{\pi}]}{\hat{\pi}^2}\right)}=\frac{\left(\frac{L}{K}\right)}{\left(1+\frac{K}{K^2}\right)}$
Step 4	Estimate $\hat{\sigma}^2[\hat{\delta}]$ and $\hat{\sigma}^2[\hat{\theta}]$	$\hat{\sigma}^2\left[\hat{\delta}\right]=\ \hat{\pi}+\hat{\lambda}=K+L$ $\hat{\sigma}^2[\hat{\theta}]\cong\frac{\hat{\theta}^2\cdot\left[\frac{\hat{V}(\hat{\lambda})}{\hat{\lambda}^2}+\frac{\hat{V}(\hat{\pi})}{\hat{\pi}^2}\right]}{\left[1+\frac{\hat{V}(\hat{\pi})}{\hat{\pi}^2}\right]^2}=\frac{\hat{\theta}^2\cdot\left[\frac{L}{L^2}+\frac{K}{K^2}\right]}{\left[1+\frac{K}{K^2}\right]^2}$

4.3 Before-and-After Study with a Comparison Group

The simple BA study assumes that no changes other than the SEP have been implemented from the *before* to the *program* period. However, the assumptions in the simple BA study are often invalid because a number of factors affecting traffic safety can change over time. In general, the factors can be divided into two categories: recognizable and unrecognizable factors (Hauer 1997). While the recognizable factors are measurable and can be modeled directly, unrecognizable factors such as the unobserved changes in driving population, traffic, weather, etc. can not be measured directly. The latter are commonly modeled by accounting for the effect of time trends (Harwood et al. 2002). In this section, the impact of the SEP on safety is estimated by a comparison group approach in order to account for the change in the unrecognizable factors.

4.3.1 Overview of the Before-and-After Study with a Comparison Group

The basic concept of the before-and-after study with a comparison group is illustrated in Figure 25, in which K_t and L_t represent the observed number of target crashes at the treatment entity during the *before* and *program* period respectively, while M_t and N_t represent the observed number of target crashes at the comparison group during the *before* and *program* period respectively.

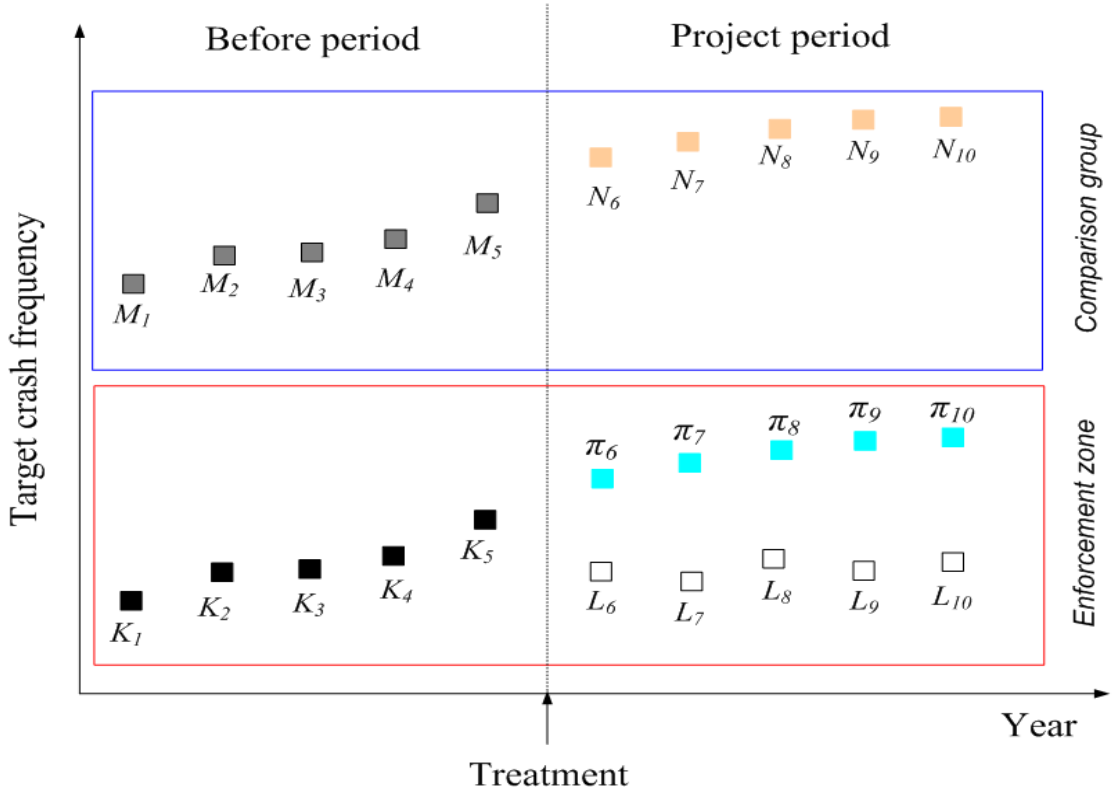

Figure 25: Basic concept of the before-and-after study with comparison group

Again, K, L, M, and N represent the sums of the observed number of crashes during each period. Table 18 shows the observed counts of crashes and the expected crash counts (Greek letters). These quantities are used to obtain the estimates in BA study with a comparison group.

Table 18: Key notations used in the before and after study with a comparison group

	Target crashes at treated sites	Target crashes at comparison sites
Before	K (κ)	M (μ)
After	L (λ)	N (ν)

The key assumption for the BA study with a comparison group is that the crash time series data between the enforcement zone and a comparison group exhibit the same trend in the absence of the treatment (i.e., SEP). If the trends in the two time series data are not statistically different, the value of π can be estimated by using the change in the crash frequency of the comparison group from the *before* to *program* period. Therefore, it is vital that the crash time series data of the comparison group have a similar trend to those of the enforcement zone. It is not necessary for the magnitudes of the crash frequency in the enforcement zone (*K*) to be the same as those of the comparison group (*M*). Consequently, it is more important that the crash time series data in the treated entity change in the same way as the comparison group during the *before* period as shown in Figure 25.

The first step is to estimate λ and predict π. The estimate of λ is equal to the sum of the observed number of crashes during the *program* period. Unlike the simple before-and-after study approach, the comparison ratio can be used in order to estimate π:

$$\left(r_T = \frac{\pi}{\kappa}\right) = \left(r_C = \frac{\nu}{\mu}\right), \tag{11}$$

where these two ratios (r_T and r_C) are identical under the comparison group method assumption. Since the ratio r_C is a random variable consisting of a non-linear combination of two random variables (μ and ν) and the observed counts of target crashes at comparison sites are Poisson distributed, the estimate of π can be represented as Equation (12):

$$\hat{\pi}_C = \hat{r}_T \cdot K = \hat{r}_C \cdot K = \frac{\left(\frac{N}{M}\right)}{\left(1+\frac{1}{M}\right)} \cdot K. \tag{12}$$

The estimate of variance for $\hat{\pi}$ can be obtained by using the delta approximation:

$$\hat{\sigma}^2\left[\hat{\pi}_C\right] = r_T^{\,2} \cdot \hat{\sigma}^2[K] + K^2 \cdot \hat{\sigma}^2[\hat{r}_T] \tag{13}$$

For convenience, the ratio of r_T and r_C is defined as the odds ratio.

$$\omega = r_C / r_T \tag{14}$$

Then, the variance for $\hat{r}_T$ is:

$$\widehat{\sigma}^2[\hat{r}_T] \cong \widehat{r_C}^2 \cdot \left(\frac{1}{M} + \frac{1}{N} + \frac{VAR[\omega]}{E^2[\omega]} \right). \tag{15}$$

By plugging Equation (15) into Equation (13), the estimate of the variance for $\hat{\pi}$ can be rewritten as Equation (16), in which the variance of $\widehat{\pi}_C$ can be approximated by using the estimate of the comparison ratio when the sample size of M and N is large enough:

$$\widehat{\sigma}^2\left[\widehat{\pi}_C\right] = \widehat{\pi}_C^{\,2} \cdot \left\{ \frac{1}{K} + \left(\frac{1}{M} + \frac{1}{N} + \frac{VAR[\omega]}{E^2[\omega]} \right) \right\} \doteq \widehat{r_C}^2 \cdot K. \tag{16}$$

With these corrections to the four-step process, the remaining steps continue as before as shown in Table 19.

Table 19: The four-step procedure for the BA study with a comparison group

Step	Goals	Formulas for simple before-and-after study
Step 1	Estimate λ and predict π	$\hat{\lambda} = L$ $\widehat{\pi} = \widehat{r_C} \cdot K = \dfrac{\left(\dfrac{N}{M}\right)}{\left(1 + \dfrac{1}{M}\right)} \cdot K$
Step 2	Estimate $\hat{\sigma}^2[\hat{\lambda}]$ and $\hat{\sigma}^2[\hat{\pi}]$	$\hat{\sigma}^2\left[\hat{\lambda}\right] = \hat{\lambda}$ $\hat{\sigma}^2\left[\hat{\pi}\right] = \widehat{r_C}^2 \cdot K$
Step 3	Estimate δ and θ	$\hat{\delta} = \hat{\pi} - \hat{\lambda} = K - L$ $\hat{\theta} \cong \dfrac{\left(\dfrac{\hat{\lambda}}{\hat{\pi}}\right)}{\left(1 + \dfrac{\widehat{V}[\hat{\pi}]}{\hat{\pi}^2}\right)}$
Step 4	Estimate $\hat{\sigma}^2[\hat{\delta}]$ and $\hat{\sigma}^2[\hat{\theta}]$	$\hat{\sigma}^2\left[\hat{\delta}\right] = \hat{\pi} + \hat{\lambda} = K + L$ $\hat{\sigma}^2[\hat{\theta}] \cong \dfrac{\hat{\theta}^2 \cdot \left[\dfrac{\widehat{V}(\hat{\lambda})}{\hat{\lambda}^2} + \dfrac{\widehat{V}(\hat{\pi})}{\hat{\pi}^2} \right]}{\left[1 + \dfrac{\widehat{V}(\hat{\pi})}{\hat{\pi}^2} \right]^2}$

4.3.2 Estimating Comparison Ratios

In order to estimate the comparison ratio (i.e., r_C), we used the comparison ratios estimated by using a comparison group instead of using a single comparison section, in which the comparison group is a set of comparison sections. Of course, it is also possible to estimate the comparison ratio by using a single comparison section through one-to-one matching between the enforcement and comparison zones, which is known as the BA study with yoked comparisons (Griffin and Flowers 1997; Harwood et al. 2002). However, the BA study with yoked comparisons is not preferable because there is only one matching comparison zone for the enforcement zone, which also leads to relatively wide confidence intervals for the crash reduction estimates (Harwood et al. 2002). In addition, the variances of the comparison ratios obtained from the comparison group are generally less than those from a single comparison section because of the increased sample size (Harwood et al. 2002; Hauer 1997).

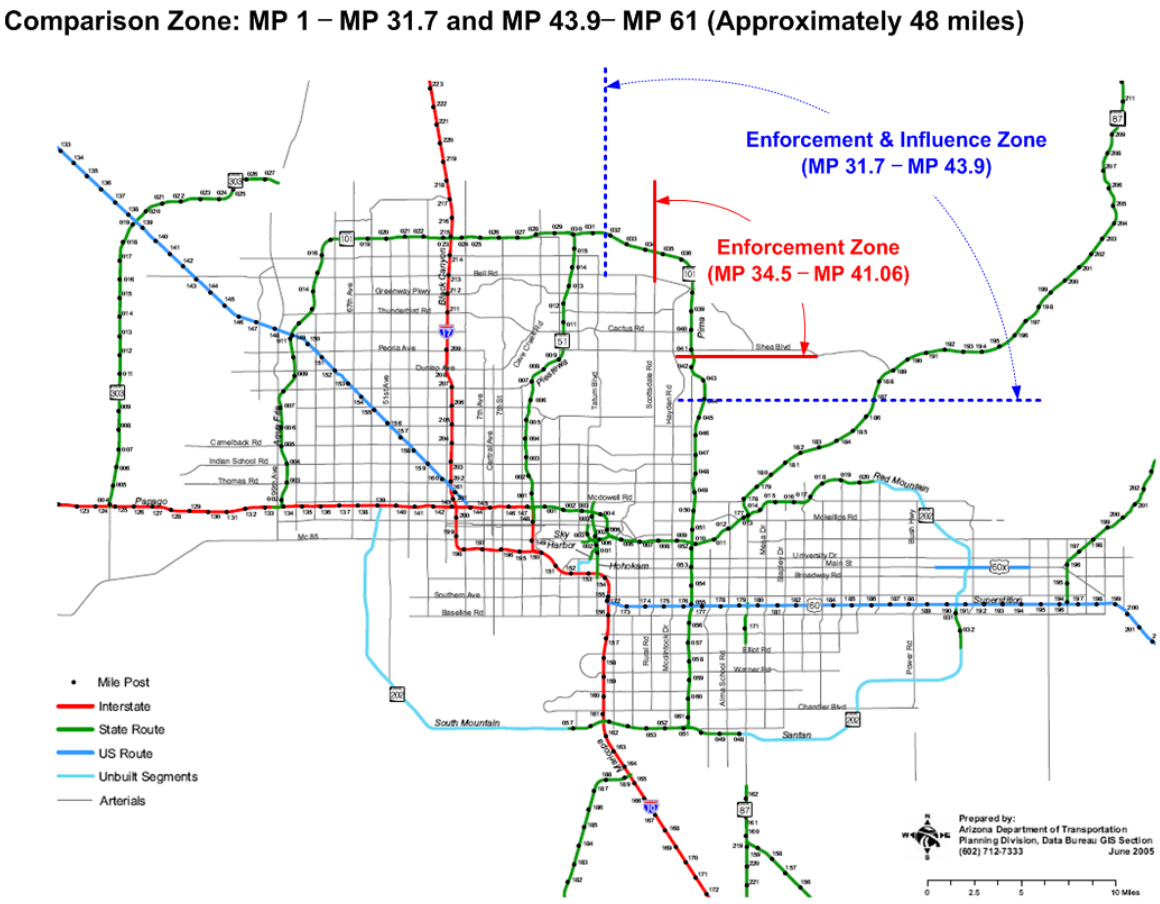

Figure 26: Enforcement zone and comparison group

In this study, the potential sections for the comparison group were limited to the sections on Loop 101 in order to reduce unwanted spatial variability in crashes. However, several sections which are close to the enforcement zone were excluded from the comparison group because it should not be affected by spillover effect. In order to define the sections that can be influenced by the spatial spillover effect, we used a 2.8-mile influence zone, which is devised based on the exponential decay model proposed by Hauer (Hauer et al. 1982). The exponential decay model shows that the effect of enforcement on speed reduction is reduced by half for every 0.56 mile. Thus, we assumed that the spillover effect could almost be eliminated after the 2.8-mile influence zone in each direction. Specifically, the enforcement zone and comparison group (zone) in this analysis illustrated in Figure 26 are:

- Enforcement zone: MP 34.5 – MP 41.06 (6.5 miles)
- Influence zone: MP 31.7—MP 34.5 and MP 41.06 – MP 43.9 (5.6 miles)
- Comparison zone: MP 1 – MP 31.7 and MP 43.9 – MP 61 (48 miles)

Consequently, the comparison zone used in this analysis (approximately a 48-mile stretch on Loop 101) does not include the influence zone in addition to the enforcement zone. Although some of comparison sections in the comparison zone illustrated in Figure 26 can be different in traffic flow and physical characteristics, it is more important that the comparison zone resembles the enforcement zone as a whole (Harwood et al. 2002; Hauer 1997). In other words, the past crash trends of the comparison zone should be similar to those within the enforcement zone.

In order to investigate the degree of agreement in the crash time series data between the enforcement and comparison zone, mean crash frequencies between the two zones were compared over time. Figure 27 shows the change in total target crashes within the two zones by year, in which the average crash frequency in the comparison zone is corrected as "average crash frequency/6.5 miles/244days" for comparison. The two time series show that they moved together and did not stray apart during the *before* period: curves are almost parallel. Note that it is not necessary that the magnitudes of the two time series are the same as discussed in the previous subsection. The findings from the comparison can be summarized:

- Total target crashes in the enforcement zone decreased in 2006, while those in the comparison zone increased in 2006. This inconsistency increases confidence that target crashes in the enforcement zone were reduced by implementing the SEP.
- It is highly unlikely that the expected number of crashes on Loop 101 is constant over time, indicating time-varying κ.
- It is likely that the enforcement zone was not the 'least safe' zone on Loop 101 prior to the SEP program since the observed crash counts from the comparison zone are greater than those from the enforcement zone.

The change in total PDO crashes illustrated in Figure 28 also shows similar movement although they are not perfectly parallel. Consequently, the results of the exploratory analysis suggest that the two crash time series from the comparison and enforcement zone are analogous, which is distinguishable from random fluctuation.

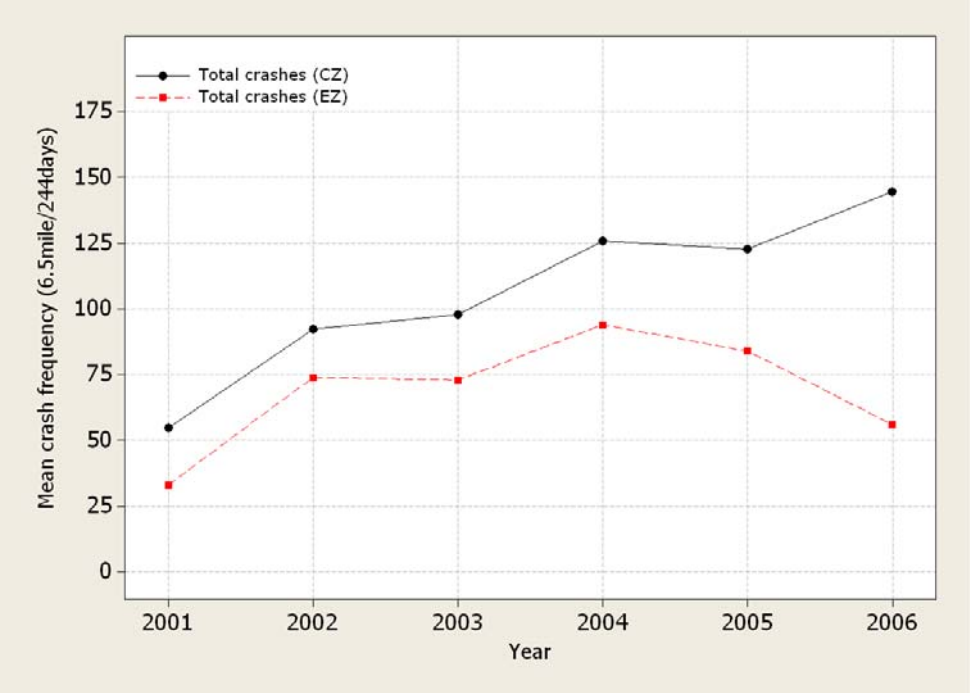

Figure 27: Change in total target crashes by year (comparison group vs. enforcement zone)

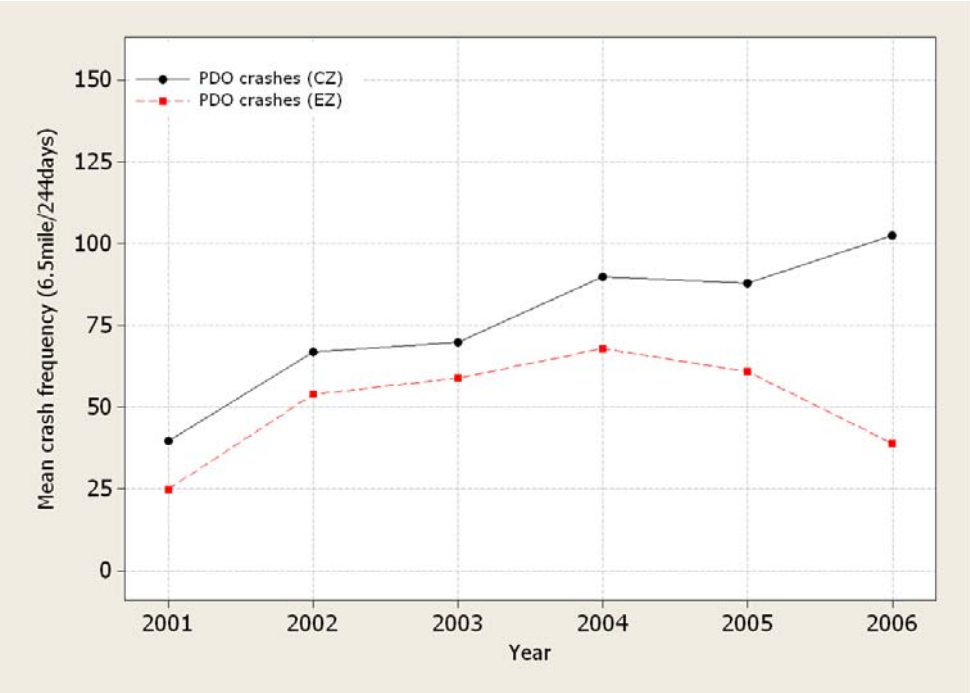

Figure 28: Change in total PDO crashes by year (comparison group vs. enforcement zone)

In order to test whether or not the past crash trends within the comparison zone are statistically similar to those within the enforcement zone, we used the odds ratio as in prior studies (Hauer 1997; Wong et al. 2005). If the past crash trends within the comparison zone are similar to those at the enforcement zone, the population odds ratio defined in Equation (14) should be equal to 1. Since the estimate of the odds ratio is non-linear, an unbiased estimator is obtained using the delta approximation:

$$\hat{\omega}_t = \frac{M_{t+1} \cdot K_t}{K_{t+1} \cdot M_t} \cdot \left(1 + \frac{1}{K_{t+1}} + \frac{1}{M_t}\right)^{-1}, \tag{17}$$

where $\hat{\omega}_t$ is the estimate for the odds ratio during period *t* and the rest of the notation is as defined previously (see 'The Four-Step Procedures for Before-and-After Study' on page 49). Therefore, the average of the estimates for the odds ratios is

$$\overline{\omega} = \frac{1}{B-1} \cdot \sum_{t=1}^{B-1} \hat{\omega}_t, \tag{18}$$

and the variance of the mean of the odds ratios is

$$S^2[\overline{\omega}] = \frac{1}{B-1} \cdot \left[\frac{1}{B-2} \left\{ \sum_{t=1}^{B-1} \hat{\omega}_t^{\,2} - (B-1)\overline{\omega}^2 \right\} \right]. \tag{19}$$

Table 20: Estimates for the odds ratios and 95% CI for the estimates

Crash type and severity		Estimate for the odds ratio	95% confidence interval	
			Lower	Upper
All crashes	Single-Vehicle	1.01	0.94	1.08
	Side-swipe (same)	1.75	0.06	3.44
	Rear-end	0.82	0.57	1.07
	Other	1.14	0.68	1.59
	Total	1.02	0.84	1.20
PDO crashes	Single-Vehicle	1.02	0.88	1.17
	Side-swipe (same)	1.32	0.33	2.32
	Rear-end	0.77	0.52	1.03
	Other	0.92	0.46	1.38
	Total	1.00	0.84	1.16
Injury crashes	Single-Vehicle	1.07	0.04	2.11
	Side-swipe (same)	0.87	-0.09	1.84
	Rear-end	0.87	0.34	1.40
	Other	0.83	0.21	1.45
	Total	1.02	0.65	1.40

Table 20 shows the odds ratio test results for the comparison zone illustrated in Figure 26. Since the estimates for the odds ratios are close to 1 and all 95% CIs contains the expected value 1 under the assumption of the BA study with a comparison group, the comparison ratios from the comparison zone are suitable. Note that the selected

comparison zone should not be employed in the BA study with a comparison group if the confidence interval of the odds ratios does not include 1.

Consequently, we estimated the comparison ratios from the comparison zone. Note that the comparison ratio, (N/M)/(1+1/M), is the ratio of the number of crashes in the before period to the number of crashes in the program period in the comparison zone. Table 21 shows the estimated comparison ratios and associated standard deviations, in which the comparison ratios were estimated by crash type, severity, and year. It is also noteworthy that we used annual comparison ratios instead of using a single comparison ratio because the safety of the enforcement zone changed over time as shown in Figure 27 and Figure 28. For example, the comparison ratio of the single-vehicle crashes in year *t* is:

$$\hat{r}_C(t) = \frac{N_P}{M_t} \cdot \left(1 + \frac{1}{M_t}\right)^{-1}, \tag{20}$$

where M_t is the observed number of the single-vehicle crashes that occurred in the comparison zone in year *t*, and N_P is the observed number of the single-vehicle crashes that occurred in the comparison zone in the *program* period.

The comparison ratios greater than 1 indicate an increase in crashes, while ratios less than 1 indicate a decrease in crashes in the comparison zone during the *program* period. For example, the total number of single-vehicle crashes increased by 58% in the comparison zone from 2001 to 2006, and the total number of single-vehicle crashes increased by 8% in the comparison from 2005 to 2006.

Table 21: Estimates of the comparison ratio

Crash type and severity		Year				
		2001	2002	2003	2004	2005
All crashes	Single-Vehicle	1.58	0.98	1.09	1.02	1.08
	Side-swipe (same)	2.31	1.56	1.36	1.15	1.13
	Rear-end	4.36	2.39	1.86	1.16	1.20
	Other	2.04	1.28	1.28	1.19	1.09
PDO crashes	Single-Vehicle	1.45	0.90	1.03	0.98	1.00
	Side-swipe (same)	2.37	1.66	1.35	1.17	1.14
	Rear-end	4.46	2.57	1.97	1.14	1.25
	Other	1.82	1.03	1.15	1.15	0.92
Injury crashes	Single-Vehicle	1.72	1.16	1.16	1.06	1.18
	Side-swipe (same)	1.48	1.01	1.09	0.87	0.90
	Rear-end	3.46	1.88	1.55	1.13	1.06
	Other	1.51	1.51	1.12	0.91	1.20

4.3.3 Results of the Before-and-After Study with a Comparison Group

Using the estimated comparison ratios shown in Table 21, the predicted values of π for each crash type and severity are obtained. For example, the π for the total single-vehicle crash was predicted as shown in Equation (21):

$$\hat{\pi}_C = r_d \cdot \sum_t^B \hat{r}_C(t) \cdot K_t, \tag{21}$$

where K_t is the observed number of single-vehicle crashes in year t, $\hat{r}_C(t)$ is the estimated comparison ratio for the single-vehicle crashes in year t, B is the total number of years during the *before* period, and r_d is the ratio for duration. Equation (21) is a variation of Equation (12) to account for the change in safety for year, crash type, and severity. Table 22 shows the estimated values for π, λ, δ, and θ as well as the estimated standard deviation for δ and θ of four collision types: single-vehicle, side-swipe (same), rear-end, and other crashes. In addition, the estimates are provided for three categories: total crashes, property-damage-only (PDO) crashes, and injury crashes (all non-PDO crashes). The significance of the estimates was tested with the conditional binomial test as well as the normal approximation test (Griffin and Flowers 1997; Hauer 1996; Przyborowski and Wilenski 1940; Shin and Washington 2007a).

Table 22: Results of the BA study with a comparison group

Crash type and severity		Crash estimates		Impact estimates	
		$\hat{\pi}$	$\hat{\lambda}$	$\hat{\theta}$ [1]	$\hat{\delta}$ [2]
All target crashes	Single-Vehicle	46.53	19	0.41 (0.10)[3]***	27.53 (5.62) ***
	Side-swipe (same)	17.68	12	0.67 (0.21) *	5.68 (4.19) *
	Rear-end	23.36	23	0.96 (0.24)	0.36 (5.85)
	Other	12.47	2	0.16 (0.11) ***	10.47 (2.40) ***
Injury crashes	Single-Vehicle	9.42	6	0.62 (0.27) *	3.42 (2.93) *
	Side-swipe (same)	3.44	2	0.55 (0.39)	1.44 (1.67)
	Rear-end	6.67	8	1.14 (0.46)	-1.33 (3.23)
	Other	3.94	1	0.24 (0.23) **	2.94 (1.48) **
PDO crashes	Single-Vehicle	35.56	13	0.36 (0.10) ***	22.56 (4.71) ***
	Side-swipe (same)	13.38	10	0.73 (0.25)	3.38 (3.78)
	Rear-end	16.23	15	0.90 (0.27)	1.23 (4.84)
	Other	7.46	1	0.13 (0.13) **	6.46 (1.74) **
Total target crashes		100.03	56	0.56 (0.08) ***	44.03 (8.95) ***
Total injury crashes		23.47	17	0.72 (0.19) *	6.47 (4.73) **
Total PDO crashes		72.63	39	0.54 (0.09) ***	33.63 (7.56) ***

Note: * p<0.2;** p<0.1;***p<0.01 for H_0: θ=1 or H_0: δ=0.
[1] Percent change in crash from the *before* to the *program* period is (θ–1)×100.
[2] Positive sign indicates decrease in crash for the *program* period
[3] For parameter estimates, the associated standard deviations are in parentheses.

Figure 29 illustrates the percent changes in target crash for each collision type and category, in which the percent changes are $(\hat{\theta} - 1) \times 100$. Therefore, the negative values indicate the crash reduction, while the positive values indicate the increase in crashes

during the *program* period. For example, the percent change for total single-vehicle crashes (–59%) indicates that the total single-vehicle crashes was reduced by 59%.

Under the assumption for the BA study with a comparison group, the results suggest:

- Total target crash frequency was reduced by 44%. Total injury and PDO crashes were also reduced by 28% and 46% respectively.
- Single-vehicle and side-swipe (same direction) crashes were reduced (27% to 64%) regardless of the severity.
- Total rear-end injury crashes increased (14%), but the changes in rear-end crashes are insignificant.

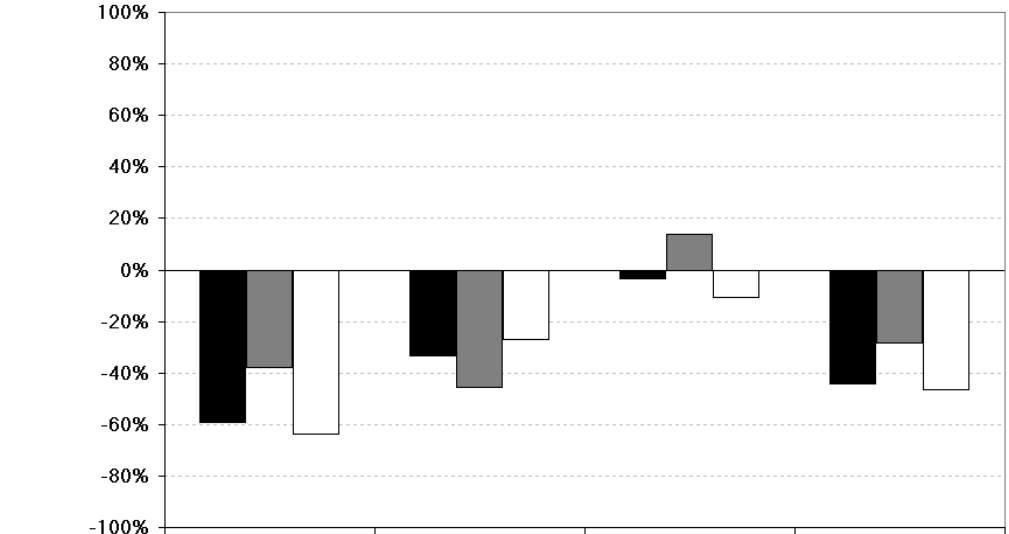

	Single-vehicle	Side-swipe (same direction)	Rear-end	Total
■ Total crashes	-59%	-33%	-4%	-44%
■ Injury crashes	-38%	-45%	14%	-28%
□ PDO crashes	-64%	-27%	-10%	-46%

Figure 29: Results of the BA study with a comparison group

The results should be interpreted while taking into account the assumption that the prediction was modified by using only the trend effects (i.e., comparison ratios). It is necessary to update the prediction procedure if there was an observable change in factors affecting safety other than the SEP in the enforcement zone during the *program* period. For example, if traffic flow in the enforcement zone remarkably changed from the *before* to *program* period, the zone-specific change should be accounted for to predict safety in the *program* period. The comparison zone resembles the enforcement zone as a whole, but some zone-specific changes cannot be captured by using the comparison ratios. In the next sections, this questionable assumption is examined using other analysis methods, and the impact of the SEP on safety is updated to reflect the trend effects as well as the change in a measurable factor from the *before* to *program* period.

4.4 BA Study with Traffic Flow Correction

Traffic flow is one of the most important factors affecting safety. If the changes in traffic flow from the *before* to the *program* period are observable, the prediction procedure should be modified by modeling the change in traffic flow between the two periods. Correction for exposure to risk, or traffic, is essential to account for the increased number of opportunities for conflict and interaction on a roadway. In this section, the impact of the SEP on safety is updated by taking into account the change in traffic flow as well as trend effects.

4.4.1 Overview of the BA Study with Traffic Flow Correction

It is common to use a traffic flow correction factor in order to reflect the change in traffic flow in the treated entity (e.g., the enforcement zone) from the before to program period. However, the change in traffic flow, which can be captured by the traffic flow correction factor, should be distinguishable from the trend effects, which can be captured by the comparison ratios. If they are not appropriately estimated, the countermeasure effects can be overestimated due to the double accounting as discussed in a previous study (Hauer 1997). In this subsection, we described the general procedure for estimating the traffic flow correction factor and expanded the discussion for the procedure to predict π by simultaneously accounting for the change in traffic flow and trend effects.

The first step is to estimate λ and predict π. The estimate of λ is equal to the sum of the observed number of crashes in the program period as shown in Table 17, but the estimate of π is not K in the BA study with traffic flow correction. Let r_{tf} be the ratio of traffic flow in the *before* period to that in the program period. Then, the prediction of π is:

$$\hat{\pi} = \hat{r}_{tf} \cdot K = \frac{F_P}{F_B} \cdot K, \tag{22}$$

where F_P and F_B represent the average traffic flow during the *program* and *before* periods respectively. However, the relationship between traffic flow and safety is not typically proportional in the real world. Thus, the traffic flow correction factor is commonly estimated by using safety performance function (SPF)—a functional relationship between traffic volumes and safety for a specific site or class of sites. Consequently, the prediction of π can be estimated by using the SPFs denoted $f(\cdot)$:

$$\hat{\pi} = \frac{\hat{f}\left(F_P\right)}{\hat{f}\left(F_B\right)} \cdot K. \tag{23}$$

If the traffic flow correction factor should reflect the change in traffic flow as well as trend effects, the safety performance function can be modified:

$$f\left(F_{it}\right) = d_i \gamma_t F_{it}^{\beta}, \tag{24}$$

where d_i is the length of the ith section, γ_t is a parameter for year t, F_{it} is the annual average daily traffic (AADT) of the ith section during the tth year, and β is a parameter for the traffic flow variable. The time-effect parameters $\boldsymbol{\gamma}$ capture the influence of all factors that change from year to year except for the change in traffic flow, while the parameter β captures how the expected crash frequency changes with traffic flow (Hauer 1997). Note that Equation (24) is not chosen arbitrarily, as it has been proven reliable for accounting for the annual changes in safety (Garber et al. 2006; Hauer 1997; Lord and Persaud 2000).

With these corrections to the four-step process, the remaining steps continue as before. Table 23 shows the corrected four-step procedure use in the BA study with traffic flow correction.

Table 23: The four-step procedure for the BA study with traffic flow correction

Step	Goals	Formulas for simple before-and-after study
Step 1	Estimate λ and predict π	$\hat{\lambda} = L$ $\hat{\pi} = \hat{r}_{tf} \cdot K$, where $\hat{r}_{tf} = \frac{\hat{f}\left(F_P\right)}{\hat{f}\left(F_B\right)}$
Step 2	Estimate $\hat{\sigma}^2[\hat{\lambda}]$ and $\hat{\sigma}^2[\hat{\pi}]$	$\hat{\sigma}^2\left[\hat{\lambda}\right] = \hat{\lambda}$ $\hat{\sigma}^2\left[\hat{\pi}\right] = \hat{r}_{tf}^2 \cdot K$
Step 3	Estimate δ and θ	$\hat{\delta} = \hat{\pi} - \hat{\lambda} = K - L$ $\hat{\theta} \cong \frac{\left(\frac{\hat{\lambda}}{\hat{\pi}}\right)}{\left(1 + \frac{\hat{V}[\hat{\pi}]}{\hat{\pi}^2}\right)}$
Step 4	Estimate $\hat{\sigma}^2[\hat{\delta}]$ and $\hat{\sigma}^2[\hat{\theta}]$	$\hat{\sigma}^2\left[\hat{\delta}\right] = \hat{\pi} + \hat{\lambda} = K + L$ $\hat{\sigma}^2[\hat{\theta}] \cong \frac{\hat{\theta}^2 \cdot \left[\frac{\hat{V}(\hat{\lambda})}{\hat{\lambda}^2} + \frac{\hat{V}(\hat{\pi})}{\hat{\pi}^2}\right]}{\left[1 + \frac{\hat{V}(\hat{\pi})}{\hat{\pi}^2}\right]^2}$

4.4.2 Change in Traffic Flow in the Enforcement Zone

In this study, we observed a significant increase in traffic flow in the enforcement zone from the *before* to the *program* period as shown in Table 24 and Figure 30 (e.g., 42% increase on average from the *before* to the *program* period; 66.24% increase in AADT from 2001 to 2006; 60.1% increase in AADT from 2003 to 2006; 16.72% increase in AADT from 2005 to 2006). Therefore, it is evident that the observed number of crashes in the *before* period (K) is not suitable for predicting π.

Table 24: Change in AADT within the enforcement zone

Section		Year					
Start	End	2001	2002	2003	2004	2005	2006
Scottsdale Rd	Princess Dr	-	-	80,000	103,000	124,000	150,000
Princess Dr	Frank Lloyd Wright Blvd	85,000	88,400	90,700	105,000	123,000	144,000
Frank Lloyd Wright Blvd	Raintree Dr	81,000	84,200	86,400	110,000	115,000	120,000
Raintree Dr	Cactus Rd	90,000	93,600	96,000	118,000	123,000	160,000
Cactus Rd	Shea Blvd	90,000	93,600	96,000	119,000	131,000	145,000
Sum		346,000	359,800	449,100	555,000	616,000	719,000
Average		86,500	89,950	89,820	111,000	123,200	143,800

Source: Archived AADT (ADOT, Transportation Planning Division)

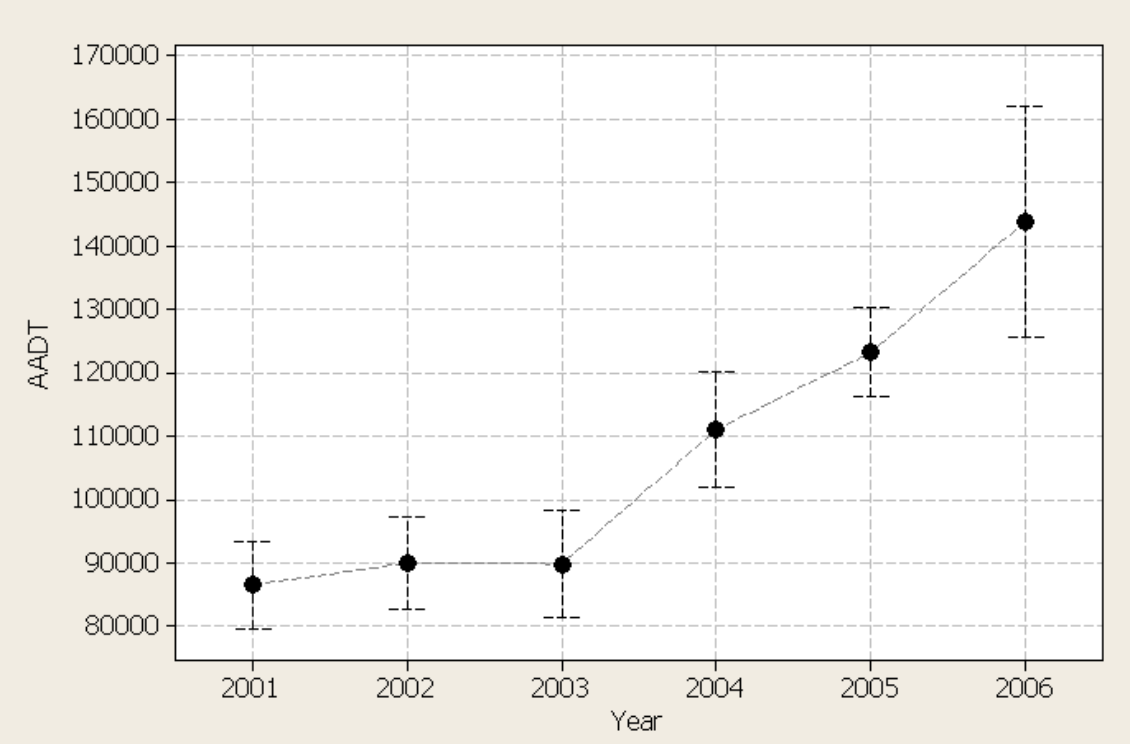

Figure 30: Change in AADT in the enforcement zone from the before (2001–2005) to the program (2006) period (Mean AADT and associated 95% C.I.s)

It was also evident that the trend effects, which can be represented as the comparison ratios, should be accounted for in predicting π as discussed in the previous section. Therefore, the procedure to account for the change in traffic flow should be taken to avoid double accounting (Hauer 1997). In order to determine whether or not the changes in traffic flow were already captured by the trend effects, the changes in AADT from the *before* to *program* period in the enforcement and comparison zone were compared. If the changes in AADT from the *before* to *program* period in the enforcement zone are similar to those in the comparison zone, correcting the change in AADT in the enforcement zone for predicting π may be unnecessary because it is likely that the changes in AADT already have been adjusted by the comparison ratios. Under such circumstances, the impact estimates will be inflated due to the double adjustment if the change in traffic flow is corrected. However, if the changes in AADT from the *before* to *program* period in the enforcement zone are not similar to those in the comparison group, it is necessary to adjust the change in AADT in the enforcement zone because the trend effects cannot capture it. Note that some changes that occurred only in the enforcement zone cannot be captured by the trend effects, although the comparison ratios reflect the trend effects.

Table 25: Summary statistics for AADT in the enforcement and comparison zone

Zone	Year	Mean	Std.dev.	Min.	Median	Max.	N
Comparison zone	2001	90,245	27,841	50,000	83,300	150,000	44
	2002	95,297	30,023	52,000	86,650	156,000	44
	2003	97,709	30,830	53,400	88,900	160,000	44
	2004	138,136	24,681	96,000	140,000	192,000	44
	2005	145,622	23,141	90,000	150,000	196,000	45
	2006	147,340	28,709	92,000	146,000	211,000	45
Enforcement zone	2001	86,500	4,359	81,000	87,500	90,000	4
	2002	89,950	4,550	84,200	91,000	93,600	4
	2003	89,820	6,806	80,000	90,700	96,000	5
	2004	111,000	7,314	103,000	110,000	119,000	5
	2005	123,200	5,675	115,000	123,000	131,000	5
	2006	143,800	14,738	120,000	145,000	160,000	5

Table 25 shows the summary statistics for AADT in the enforcement and comparison zone, and Figure 31 shows the change in average AADT in the enforcement and comparison zone by year. Figure 31 shows that they moved together during the *before* period although they are not perfectly parallel, but the average AADT in the enforcement zone in 2006 is quite close to that of the comparison zone in 2006 (see Figure 31). It indicates that the prediction procedure should be updated to account simultaneously for the change in AADT in the enforcement zone as well as the trend effects. If the prediction procedure is modified only by using the comparison ratios, the π is likely to be under-predicted because the increase in AADT in the enforcement zone during the *program* period is relatively higher than that in the comparison zone. Note that the

average AADT in the enforcement zone increased by 17% from 2005 to 2006, while the average AADT in the comparison zone increased by 1% from 2005 to 2006 (see Table 25). Therefore, we updated the impact of the SEP on safety by simultaneously accounting for the change in AADT and trend effects.

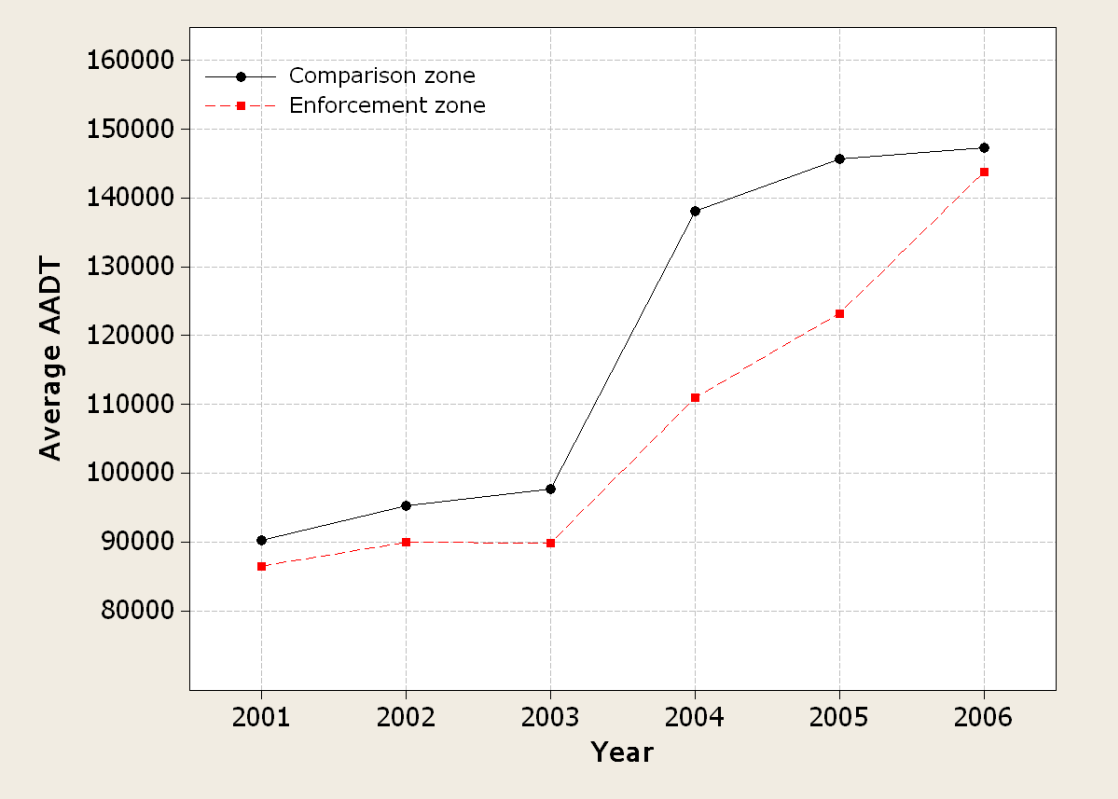

Figure 31: Change in AADT by year (comparison zone vs. enforcement zone)

4.4.3 Developing Safety Performance Functions

In this section, we described the modeling approaches for developing the safety performance functions (SPFs), which need to be developed in order to obtain estimates of traffic flow correction factors. The SPFs were developed using negative binomial regression models, which are provided in the last subsection.

4.4.3.1 Count Models for Developing SPFs

The general approach used to develop SPFs involves the use of count-based models. A common mistake is to model count data as continuous data by applying standard least squares regression. This is not strictly correct because regression models yield predicted values that are non-integers and can also predict values that are negative, both of which are inconsistent with count data. These limitations make standard regression analysis inappropriate for modeling count data without modifying the dependent variables. Count

data are properly modeled using a number of methods, the most popular of which are Poisson and negative binomial regression models (Greene 2003; Washington et al. 2003).

The Poisson regression model is often used to fit models of the number of occurrences of an event. Let $y_i, i = 1, 2, \cdots, N$ be the observations of a discrete and non-negative integer variable, which is assumed to be independently Poisson distributed, with the conditional mean specified as:

$$E\left[y_i \mid \mathbf{x}_i\right] = \lambda_i = \exp(\mathbf{x}_i'\boldsymbol{\beta}) \tag{25}$$

where $\mathbf{x}_i$ is a $k \times 1$ vector of explanatory variables associated with the *i*th observation and $\boldsymbol{\beta}$ is a $k \times 1$ vector of unknown parameters. Equation (25) is called the exponential mean function. The model comprising the Poisson probability distribution and the exponential mean function is typically referred to as the Poisson regression model, although more precisely it is the Poisson regression model with exponential mean function (Cameron and Trivedi 1998).

The density function of y_i given $\mathbf{x}_i$ is:

$$f(y_i \mid \mathbf{x}_i) = \frac{e^{-\lambda_i}\lambda_i^{y_i}}{y_i!}. \qquad y_i = 0, 1, 2, \ldots \tag{26}$$

Therefore, the likelihood function can be obtained by multiplying the density function of y_i across all observations as follows:

$$L(\boldsymbol{\beta}) = \prod_{i=1}^{n} \frac{e^{-\lambda_i}\lambda_i^{y_i}}{y_i!} \tag{27}$$

and the log-likelihood function is

$$\begin{aligned} \ln L(\boldsymbol{\beta}) &= \sum_{i=1}^{n}\left[-\lambda_i + y_i \ln \lambda_i - \ln\left(y_i!\right)\right] \\ &= \sum_{i=1}^{n}\left[-\exp(\mathbf{x}_i'\boldsymbol{\beta}) + y_i\mathbf{x}_i'\boldsymbol{\beta} - \ln\left(y_i!\right)\right]. \end{aligned} \tag{28}$$

The unknown parameters $\boldsymbol{\beta}$ can be estimated by maximizing the log-likelihood function. The maximizing value for $\boldsymbol{\beta}$ denoted as $\hat{\boldsymbol{\beta}}_{ML}$, is derived by computing the first derivatives of the log-likelihood function:

$$\frac{\partial \ln L(\boldsymbol{\beta} \mid y)}{\partial \boldsymbol{\beta}} = \sum_{i=1}^{n}\left[-\mathbf{x}_i' \exp\left(x_i'\boldsymbol{\beta}\right) + y_i\mathbf{x}_i'\right] \tag{29}$$

and then solving the first order conditions for a maximum

$$\sum_{i=1}^{n}\left[-\mathbf{x}_i' \exp\left(\mathbf{x}_i'\boldsymbol{\beta}\right) + y_i\mathbf{x}_i'\right] = 0. \tag{30}$$

The standard errors of the unknown parameters are obtained from the inverse of the Hessian matrix of the log-likelihood function. The Hessian matrix is obtained from the second derivatives of the log-likelihood function with respect to $\boldsymbol{\beta}$.

$$H(\boldsymbol{\beta}; y, x) = \frac{\partial^2 \ln L(\boldsymbol{\beta} \mid y)}{\partial \boldsymbol{\beta}\, \partial \boldsymbol{\beta}'} = \sum_{i=1}^{n} \left[-\mathbf{x}_i' \mathbf{x}_i \exp\left(\mathbf{x}_i' \boldsymbol{\beta}\right) \right] \tag{31}$$

and then the variance of $\hat{\boldsymbol{\beta}}_{ML}$ is given by

$$Var(\hat{\boldsymbol{\beta}}_{ML}) = \left(\sum_{i=1}^{n} -\mathbf{x}_i' \mathbf{x}_i \exp\left(\mathbf{x}_i' \boldsymbol{\beta}\right) \right)^{-1} \tag{32}$$

It is necessary to note that the conditional mean $\lambda_i = \mu_i t_i$, in which μ_i is the incidence rate (probability of a new event per tiny time interval) and t is often referred to as the exposure. Therefore, Equation (25) can be rewritten:

$$E\left[y_i \mid \mathbf{x}_i \right] = \lambda_i t_i = t_i \exp(\mathbf{x}_i' \boldsymbol{\beta}), \tag{33}$$

where the coefficient of t_i is 1. However, the coefficient of t_i can also be estimated by inserting it into the exponential mean function: $E\left[y_i \mid \mathbf{x}_i \right] = \exp(\gamma t_i + \beta_1 + \cdots + \beta_k x_{ik})$. Notice that if t_i is the same for every observation, this term can be absorbed into the intercept.

The Poisson regression model rarely fits in practice since the conditional variance is greater than the conditional mean in many applications. If this equality ($E\left(y_i\right) = V\left(y_i\right)$), which is assumed in the Poisson regression model, does not hold, the data are said to be under-dispersed ($E\left(y_i\right) > V\left(y_i\right)$) or over-dispersed ($E\left(y_i\right) < V\left(y_i\right)$). The most common is the negative binomial model, which arises from a natural formulation of unobserved heterogeneity (Greene 2003). By introducing the unobserved heterogeneity into the conditional mean, Equation (25) can be rewritten:

$$E\left[y_i \mid \mathbf{x}_i, v_i \right] = \lambda_i^* = \lambda_i v_i = \exp(\mathbf{x}_i' \boldsymbol{\beta} + u_i), \tag{34}$$

where v_i is $\exp(u_i)$ and u_i reflects either specification error or the kind of the unobserved heterogeneity. Therefore, the conditional density of y_i is:

$$f(y_i \mid \mathbf{x}_i, v_i) = \frac{e^{-\lambda_i^*} \lambda_i^{*y_i}}{y_i!} = \frac{e^{-\lambda_i v_i} \left(\lambda_i v_i\right)^{y_i}}{\Gamma(y_i + 1)}. \tag{35}$$

Since it is impossible to condition on the unobserved v_i, the marginal density of $f(y_i \mid \mathbf{x}_i)$ is obtained by integrating the joint distribution over v_i:

$$f(y_i \mid \mathbf{x}_i) = \int_0^\infty f(y_i \mid \mathbf{x}_i, v_i) g(v_i) dv_i, \tag{36}$$

where v_i>0. Thus, a specific choice of $g(\bullet)$ defines the marginal density of $f(y_i \mid \mathbf{x}_i)$.

There have been three distributions for $g(\bullet)$: the gamma distribution, the inverse Gaussian distribution, and the log-normal distribution (Winkelmann 2003). In this analysis, we chose the gamma mixture that is widely used in traffic safety studies. In the gamma mixture model, the density function of v_i is Gamma(a,b):

$$g(v_i) = \frac{v_i^{a-1} \cdot \exp(-v_i / b)}{b^a \cdot \Gamma(a)}, \quad \text{for } v_i > 0 \tag{37}$$

where a is the shape parameter and b is the scale parameter of the gamma distribution. In order to reduce the number of parameters from two to one (for mathematical convenience), the model usually assumes that $v_i \sim \text{Gamma}(1/\alpha, \alpha)$.

$$g(v_i) = \frac{v_i^{\frac{(1-\alpha)}{\alpha}} \cdot \exp(-v_i / \alpha)}{\alpha^{1/\alpha} \cdot \Gamma(1/\alpha)}, \quad \text{for } v_i > 0 \tag{38}$$

As a result, the gamma distribution can be expressed by one parameter, and the mean and variance of the gamma distribution of the v_i are $E[v] = 1$ and $Var[v] = \alpha$.

By using Equations (36) and (38), the marginal density of $f(y_i \mid \mathbf{x}_i)$ can be obtained:

$$f(y_i \mid \mathbf{x}_i) = \frac{\Gamma(1/\alpha + y_i)}{\Gamma(y_i + 1)\Gamma(1/\alpha)} \left(\frac{1}{1+\alpha\lambda_i}\right)^{1/\alpha} \left(\frac{\alpha\lambda_i}{1+\alpha\lambda_i}\right)^{y_i}, \tag{39}$$

which is one form of the negative binomial distribution (Winkelmann 2003) and it is defined as NB2. Therefore,

$$E\left[y_i \mid \mathbf{x}_i, v_i\right] = \lambda_i \tag{40}$$

and

$$Var\left[y_i \mid \mathbf{x}_i, v_i\right] = \lambda_i(1 + \alpha\lambda_i) \tag{41}$$

Under this model, the ratio of the variance to the mean is $(1+\alpha\lambda_i)$, which can vary by individuals. The log-likelihood function is

$$\begin{aligned} \ln L(\boldsymbol{\theta} \mid y) = \sum_{i=1}^{n} \Big[& \ln\Gamma\left(\alpha^{-1} + y_i\right) - \ln\Gamma\left(\alpha^{-1}\right) - \ln\Gamma\left(y_i + 1\right) \\ & + y_i \ln\alpha + y_i x_i'\beta - \left(\alpha^{-1} + y_i\right)\ln\left(1 + \alpha\lambda_i\right) \Big]. \end{aligned} \tag{42}$$

The unknown parameters, $\boldsymbol{\beta}$ and α (over-dispersion parameter), can be estimated by maximizing the log-likelihood function and derived by computing the first derivatives of the log-likelihood function with respect to $\boldsymbol{\beta}$ and α:

$$\frac{\partial \ln L(\boldsymbol{\beta} \mid y)}{\partial \boldsymbol{\beta}} = \sum_{i=1}^{n} \left[\frac{(y_i - \lambda_i)}{1 + \alpha \lambda_i} \mathbf{x}_i' \right] \tag{43}$$

$$\begin{aligned} \frac{\partial \ln L(\boldsymbol{\beta} \mid y)}{\partial \alpha} = \sum_{i=1}^{n} \Bigg[& -\frac{1}{\alpha^2} \Psi\left(\frac{1}{\alpha} + y_i\right) + \frac{1}{\alpha^2} \Psi\left(\frac{1}{\alpha}\right) + \frac{y_i}{\alpha} \\ & + \frac{1}{\alpha^2} \ln(1 + \alpha \lambda_i) - \left(\frac{1}{\alpha} + y_i\right) \frac{\lambda_i}{1 + \alpha \lambda_i} \Bigg] \end{aligned} \tag{44}$$

where $\lambda_i = \exp(\mathbf{x}_i' \boldsymbol{\beta})$ and $\Psi(x)$ is a digamma function:

$$\Psi(x) = \frac{d \ln \Gamma(x)}{dx} = \frac{\Gamma'(x)}{\Gamma(x)}.$$

The standard errors of the parameters $\hat{\boldsymbol{\beta}}_{ML}$ and $\hat{\alpha}_{ML}$, are obtained from the inverse of the Hessian matrix. The Hessian matrix is obtained from the second derivatives of the log-likelihood function with respect to $\boldsymbol{\beta}$ and α. The (2×2) Hessian matrix is given by:

$$H(\boldsymbol{\beta}, \alpha; y, \mathbf{x}) = \begin{bmatrix} \dfrac{\partial^2 \ln L(\boldsymbol{\beta} \mid y)}{\partial \boldsymbol{\beta} \, \partial \boldsymbol{\beta}'} & \dfrac{\partial^2 \ln L(\boldsymbol{\beta} \mid y)}{\partial \boldsymbol{\beta} \, \partial \alpha} \\ \dfrac{\partial^2 \ln L(\boldsymbol{\beta} \mid y)}{\partial \alpha \, \partial \boldsymbol{\beta}} & \dfrac{\partial^2 \ln L(\boldsymbol{\beta} \mid y)}{\partial \alpha \, \partial \alpha'} \end{bmatrix}. \tag{45}$$

4.4.3.2 Modeling Results

In order to establish SPFs, the AADT and target crash data (from 2001 to 2006) from a total of 60 sections (1-mile sections) on the Loop 101 were used. Out of the panel dataset, we eliminated the AADT and crash data from the enforcement and influence zone, since the SPFs should reflect the relationship between traffic flow and crashes without the SEP. The data used in the analysis have the unbalanced panels due to missing data, in which the sample sizes differ across year. Table 26 shows the summary statistics for the variables used in the full model.

The SPFs were estimated by crash type and severity in order to obtain traffic flow correction factors for each crash type and severity (e.g., the traffic flow correction factor for the PDO single-vehicle crashes). In addition, time-effect covariates were included in the model to reflect the trend effects. Consequently, the expected number of crashes per year for each section was estimated:

$$\kappa_{it} = d_i \gamma_t F_{it}^{\beta}. \tag{46}$$

- κ_{it} : the expected number of crashes for the *i*th section during the *t*th year
- d_i : the length of the *i*th section, which is often referred to as the exposure variable in count models

- γ_t : the time-effect parameter, capturing the influence of all factors that change from year to year (except for the change in traffic flow)
- F_{it} : the AADT of the *i*th section during the *t*th year
- β : an estimable parameter for the traffic flow variable.

Although the model form is quite simple, it has been proven reliable for simultaneously accounting for the change in AADT and trend effects (Garber et al. 2006; Hauer 1997; Lord and Persaud 2000). Table 27 shows the developed SPFs estimated by using the NBRM. All estimated coefficients of independent variables and the log-likelihood ratio test for global test (H_0: the estimated model is not appropriate) are significant at α=0.1. In addition, the results of the log-likelihood ratio test for investigating that the over-dispersion is 0 in the negative binomial regression model indicate that the negative binomial regression model is preferable to the Poisson regression model at α=0.2. In all estimated models, the signs for AADT are greater than 0, which suggests that a certain percentage increase in AADT will result in an increase in the number of crashes. The time-effect parameters are also significant at α=0.1, reflecting the fact that the expected number of crashes changes from year to year.

Table 26: Summary statistics for variables in the full model [N=348]

Variable		Mean	Std. Dev.	Min	Q1	Q2	Q3	Max
Total target crashes*	Total frequency	24.5	13.7	1	15	21	33.5	82
	Single-vehicle	9.31	4.74	0	6	9	12	27
	Side-swipe (same)	3.84	2.72	0	2	4	5.5	16
	Rear-end	9.57	9.09	0	3	7	13	54
	Other	1.79	1.5	0	1	2	3	8
Total injury crashes	Total frequency	7.19	4.61	1	4	6	9	23
	Single-vehicle	2.46	1.85	0	1	2	3	11
	Side-swipe (same)	0.93	1.05	0	0	1	1	5
	Rear-end	3.33	3.33	0	1	2	5	18
	Other	0.47	0.74	0	0	0	1	4
Total PDO crashes	Total frequency	17.5	9.81	1	11	15	23	59
	Single-vehicle	6.92	3.72	0	4	7	9	22
	Side-swipe (same)	2.94	2.32	0	1	3	4	14
	Rear-end	6.33	6.29	0	2	4.5	9	36
	Other	1.34	1.26	0	0	1	2	7
AADT (vehicles/day)		117604	34239	56710	86619	120140	144180	202450

* Crash frequency used in the analysis is the number of crashes per mile per year

Table 27: Estimated safety performance functions for BA studies [n=335]

Crash Type and Severity		ln(AADT) (veh/day)	Time-effect parameter						LR Test Statistic (χ^2)	Over-dispersion Parameter (α)
			ln(γ_1)	ln(γ_2)	ln(γ_3)	ln(γ_4)	ln(γ_5)	ln(γ_6)		
Single-vehicle	All	0.6737***	-5.7872***	-5.3592***	-5.4719***	-5.6184***	-5.7484***	-5.6576***	7754.0***	0.1124***
	Injury	0.5314***	-5.4300**	-5.1525**	-5.2339**	-5.2813**	-5.4479**	-5.1971**	545.1***	0.1147***
	PDO	0.6881***	-6.2459***	-5.7969***	-5.9210***	-6.0780***	-6.2062***	-6.1747***	5361.2***	0.0982***
Side-swipe (same direction)	All	1.1203***	-12.0769***	-11.6352***	-11.5354***	-11.7347***	-11.7751***	-11.6393***	1918.3***	0.0984***
	Injury	0.8854***	-10.7030***	-10.1840***	-10.4307***	-10.3390***	-10.4383***	-10.3948***	22.92***	0.1172**
	PDO	1.1806***	-13.0502***	-12.6626***	-12.4534***	-12.7272***	-12.7591***	-12.5928***	1047.6***	0.1123***
Rear-end	All	1.8012***	-19.3112***	-18.7977***	-18.5895***	-18.7894***	-18.9611***	-18.6873***	2930.9***	0.4491***
	Injury	1.6193***	-18.1867***	-17.6743***	-17.5023***	-17.7472***	-17.8475***	-17.6902***	732.5***	0.4174***
	PDO	1.9240***	-21.1583***	-20.6892***	-20.4826***	-20.6252***	-20.8395***	-20.5186***	2018.5***	0.3997***
Other	All	0.7506***	-8.5236***	-8.0564***	-7.9830***	-8.2254***	-8.2097***	-8.0038***	270.5***	0.0446*
	Injury	1.5941***	-19.5714***	-19.3824***	-19.1445***	-19.3823***	-19.6471***	-19.2705***	88.8***	0.1609*
	PDO	0.4648**	-5.5236**	-4.9989**	-4.9712**	-5.2040**	-5.0953**	-4.9552**	67.83***	0.0680*
Total	All	1.1822***	-10.9089***	-10.4484***	-10.4187***	-10.5924***	-10.7129***	-10.5352***	19047.9***	0.1357***
	Injury	1.1374***	-11.5808***	-11.1901***	-11.1848***	-11.2914***	-11.4240***	-11.2460***	4816.9***	0.1297***
	PDO	1.1791***	-11.2022***	-10.7465***	-10.7139***	-10.8843***	-11.0126***	-10.8378***	15705.5***	0.1161***

Note: * p<0.2;** p<0.1;***p<0.01

4.4.4 Results of the Before-and-After Study with Traffic Flow Correction

Using the estimated SPFs shown in Table 27, the predicted values of π are estimated by year, section, crash type, and severity. For example, the prediction of π for the single-vehicle crashes using the traffic flow correction ($\hat{\pi}_{tf}$) is:

$$\hat{\pi}_{tf} = r_d \cdot \sum_{i}^{E} \sum_{t}^{B} \frac{\hat{f}(F_{ip})}{\hat{f}(F_{it})} \cdot K_{it}, \tag{47}$$

where K_{it} is the observed number of single-vehicle crashes in the *i*th section during the *t*th before period, F_{it} is the AADT in the *i*th section during the *t*th before period, F_{ip} is the AADT in the *i*th section during the *program* period, E is the total number of sections in the enforcement zone, B is the total number of years during the *before* period, and r_d is the ratio for duration. Note that Equation (47) is an expansion of Equation (23) to account for the change in AADT for year, section, crash type, and severity. Consequently, the impact of the SEP on safety for a crash type was estimated using all predicted values for each section as well as each year. The estimation results are summarized in Table 28, and the percent change in crashes for each crash type and category are summarized in Figure 32.

Table 28: Results of the BA study with traffic flow correction

Crash type and severity		Crash estimates		Impact estimates	
		$\hat{\pi}$	$\hat{\lambda}$	$\hat{\theta}$ [1]	$\hat{\delta}$ [2]
All target crashes	Single-Vehicle	51.18	19	0.37 (0.09) [3]***	32.18 (5.88)***
	Side-swipe (same)	21.85	12	0.54 (0.17)**	9.85 (4.55)**
	Rear-end	30.43	23	0.74 (0.18)*	7.43 (6.41)*
	Other	15.28	2	0.13 (0.09)***	13.28 (2.79)***
Injury crashes	Single-Vehicle	10.37	6	0.56 (0.24)*	4.37 (3.02)*
	Side-swipe (same)	4.83	2	0.39 (0.27)*	2.83 (1.89)*
	Rear-end	9.30	8	0.82 (0.33)	1.30 (3.57)
	Other	6.61	1	0.14 (0.13)***	5.61 (2.11)**
PDO crashes	Single-Vehicle	39.60	13	0.33 (0.09)***	26.60 (4.97)***
	Side-swipe (same)	16.82	10	0.58 (0.20)**	6.82 (4.13)**
	Rear-end	21.01	15	0.69 (0.21)*	6.01 (5.33)*
	Other	9.19	1	0.10 (0.10)***	8.19 (2.02)***
Total target crashes		118.74	56	0.47 (0.07)***	62.74 (10.50)***
Total injury crashes		31.12	17	0.54 (0.14)**	14.12 (5.43)**
Total PDO crashes		86.62	39	0.45 (0.08)***	47.62 (8.93)***

Note: * p<0.2;** p<0.1;***p<0.01 for H_0: θ=1 or H_0: δ=0.
[1] Percent change in crash from the *before* to the *program* period is (θ–1)×100.
[2] Positive sign indicates decrease in crash for the *program* period
[3] For parameter estimates, the associated standard deviations are in parentheses.

Note that the estimated impacts in the BA study with traffic flow correction are higher than those in the BA study with a comparison group because the BA study with traffic flow correction accounted for the increase in AADT as well as the trend effects.

The results of the BA study with traffic flow correction suggest that:

- Total target crash frequency was reduced by 53%. Total injury and PDO crashes were also reduced by 46% and 55% respectively.
- Unlike the results of the BA study with a comparison group, all types of crashes were reduced (18% to 67%).
- However, the decrease in the total number of rear-end injury crashes (18%) is insignificant (p-value=0.377).

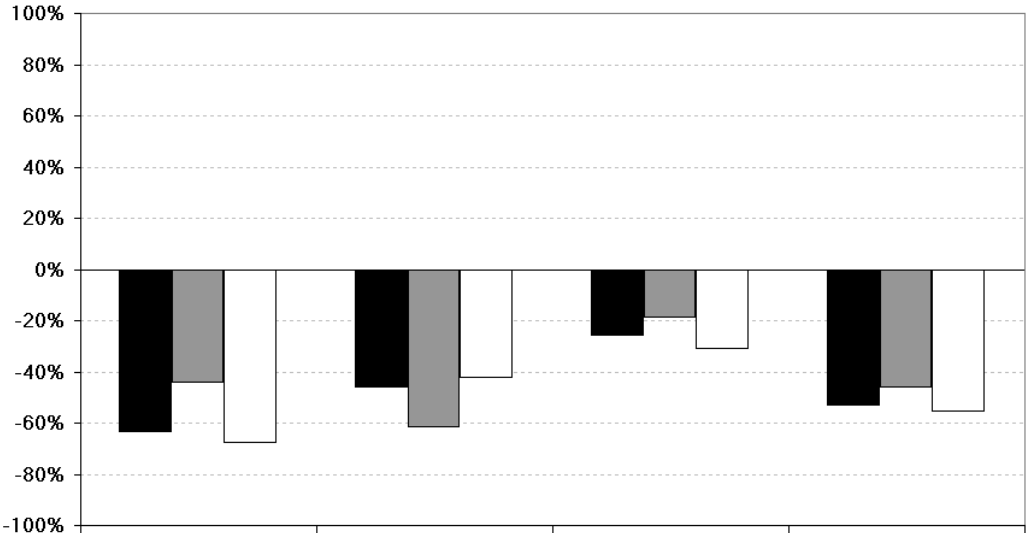

	Single-vehicle	Side-swipe (same direction)	Rear-end	Total
■ Total crashes	-63%	-46%	-26%	-53%
▒ Injury crashes	-44%	-61%	-18%	-46%
□ PDO crashes	-67%	-42%	-31%	-55%

Figure 32: Results of the BA study with traffic flow correction

In general, the results of the BA study with traffic flow correction, which accounts for both the change in traffic flow and trend effects, are more desirable than those of the BA study with a comparison group because the trend effects do not capture the zone-specific change in traffic flow from the *before* to *program* period. However, the BA study with traffic flow correction shown in this section assumes that the expected number of crashes in the *before* period (i.e., κ) can be estimated solely by using the observed number of crashes in the *before* period (i.e., K). The assumption is often violated in traffic safety studies. In the subsequent sections, the assumption is modified by using another analysis method.

4.5 Empirical Bayes' Before-and-After Study

In the previous approach the observed crash count in the before period (*K*) plays a key role in estimating π with the correction factor. However, it is often necessary to consider the possible regression-to-the-mean (RTM) bias in safety studies, although the impacts were estimated by accounting for the change in traffic flow and the trend effects in the previous section. In this section, the RTM bias is described, and the empirical Bayes' before-and-after study approach is applied to the crash data in order to account simultaneously for the change in traffic flow, trend effect, and the RTM bias.

4.5.1 Regression-to-the-Mean Phenomenon

In the 19th century, Sir Francis Galton observed that the offspring of tall parents were, on average, shorter than their progenitors—this phenomenon became known as the regression-to-the-mean (RTM). The RTM is a statistical phenomenon that occurs when two repeated measurements for a random variable are imperfectly correlated (Campbell and Kenny 1999). The RTM is ubiquitous in numerous researches since the perfect correlation between two measures is rarely observed.

Hauer and Persaud (1983) investigated the RTM phenomenon in traffic safety data by examining seven observed datasets from Canada, Israel, the UK, and the United States. They found that if an entity is treated because its before accident count (K) was abnormally high or low, then the same K can not be a good estimate of κ. Hauer (1997) stressed that K tends to overestimate κ if the entity has been selected because it had an unusually high number of crashes. He also stated that K is not a good estimate of κ, even if the entities were not selected because of abnormally high or low accident counts. He explained the RTM phenomenon (Hauer 1997):

> *If K was a good estimator of* κ *then, entities which recorded K accidents in one period would record, on the average, K accidents in a subsequent period of equal duration if* κ *remained unchanged. However, this is not born out by empirical evidence. It follows that K is not a good estimator of* κ.

The conclusion above has been unanimously used to explain the RTM bias in traffic crashes, and the RTM bias is a well-known source of error when analyzing the traffic safety treatment effect.

In order to investigate the RTM phenomenon, the crash data of Loop 101 from 2001 to 2006 are compared. Table 29 shows the mean crash frequency per mile on Loop 101 from 2001 to 2006. Again, the crashes that occurred in the enforcement and influence zone in 2006 were excluded in this analysis in order to eliminate the impact of the SEP.

All crashes in this analysis are the mainline crashes that occurred during the non-peak-period (see '4.1.1 Determining Target Crashes' on page 45). We found that the mean crash frequency between 2002 and 2003 was not statistically different (p-value from a paired *t* test is 0.18), although the mean crash frequency in 2003 was slightly greater than that in 2002. The test results indicate that the observed number of crashes for a section in 2002 is a good estimator for predicting the expected number of crashes for the same section in 2003. In order to test the assumption, we regressed the number of crashes for each section in 2003 against the number of crashes for each section in 2002, leading to a regression model with a lagged dependent variable.

Table 29: Summary statistics for mean crash frequency per mile by year

Year	Mean	Std.dev.	Min.	Median	Max.	N
2001	12.91	8.55	1	11.5	40	56
2002	21.17	11.91	2	18.5	59	60
2003	22.80	10.69	2	19.5	56	60
2004	29.40	14.63	2	26	69	60
2005	27.97	13.97	5	27	82	60
2006	33.98	12.35	6	34	66	47

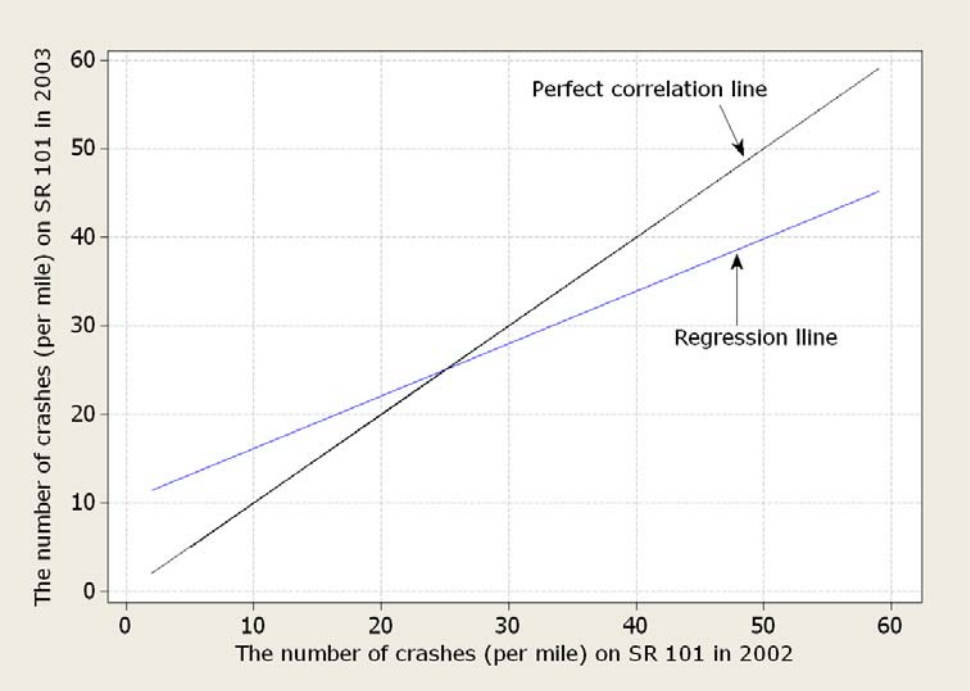

Figure 33: Regression-to-the-mean phenomenon on Loop 101 from 2002 to 2003

Figure 33 shows a regression plot for investigating the RTM effect, in which the horizontal line indicates the number of crashes (per 1-mile section) on Loop 101 in 2002 and the vertical line indicates the number of crashes (per 1-mile section) on Loop 101 in

2003. Figure 33 shows the regression line is not close to the perfect correlation line, although we could infer from the statistically same mean that no treatment was applied to Loop 101 in 2003. The regression line in Figure 33 indicates that the sections with a high crash frequency in 2002 tended to have fewer crashes in 2003 (or vice versa) as prior studies revealed. Therefore, the K_{2002} is not the best predictor for estimating the crash frequency in 2003 (κ_{2003}) due to the RTM phenomenon.

The RTM still exists although the expected number of crashes (κ) changes over time, which was also revealed in a simulation study (Shin and Washington 2007b)—the random fluctuation around κ_t (not a single κ) eventually leads to the RTM phenomenon. Figure 34 illustrates the RTM phenomenon that occurred on Loop 101 from 2005 to 2006. Note that the mean crash frequency significantly increased from 2005 to 2006 (p-value from a paired *t* test is <0.001). The regression line in Figure 34 indicates that the number of crashes for a section in 2006 tends to be less exceptional in 2006 if the number of crashes for the section in 2005 was exceptionally high due to the RTM phenomenon (or vice versa). It is possible that the regression line can be fitted another way (e.g., parallel to the perfect correlation line) if the change in safety between two years is remarkably large. However, the RTM bias is ubiquitous when we analyze the observed dataset because it is caused by the random fluctuation around κ_t.

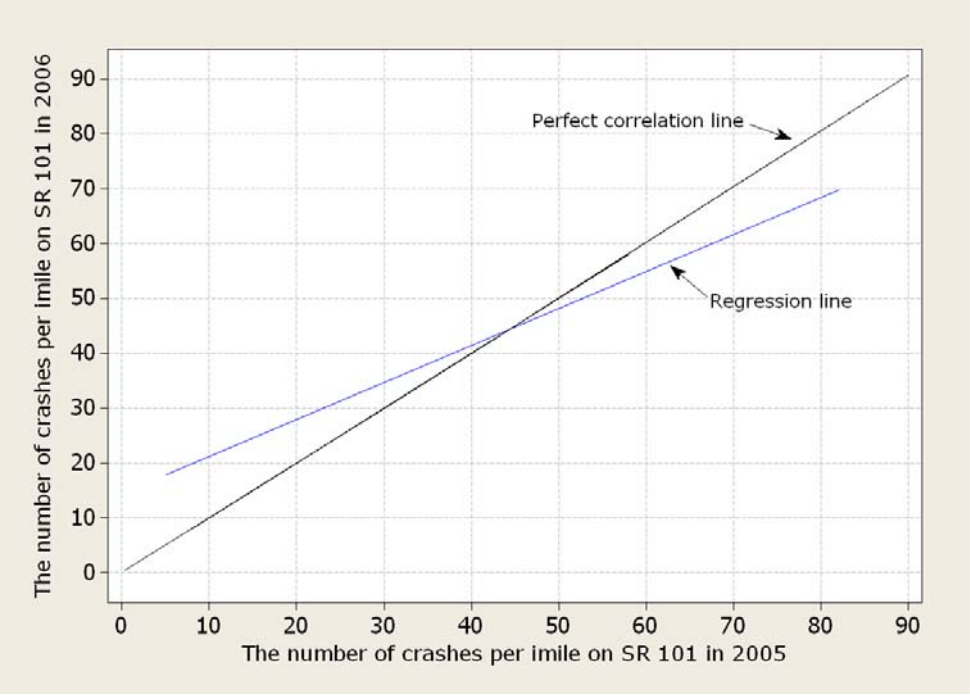

Figure 34: Regression-to-the-mean phenomenon on Loop 101 from 2005 to 2006

In addition, the RTM exists in the uninterrupted facility. Washington and Shin (2005) examined the RTM phenomenon in the crash data at 218 intersections in the city of Scottsdale from 1995 to 1996. The researchers also observed the RTM phenomenon from the dataset. If the crash frequency in 1995 at a particular site was less than the average crash frequency in 1995, the average crash frequency in 1996 increased on average (or vice versa). For other empirical examples, the interested reader can consult a variety of references (Hauer 1997; Hauer and Persaud 1983).

Consequently, the RTM bias should be eliminated from the results of the previous BA studies. If the enforcement zone was selected due to its high crash history, the impact of the SEP on safety will be overestimated. On the contrary, if the enforcement zone's crash frequency in the *before* period was relatively lower than that in the corresponding reference group, its expected number of crashes in the *before* period is likely to be higher than the observed number of crashes in the *before* period. In the next subsection, we described how to use K in order to eliminate the RTM bias.

4.5.2 Overview of Empirical Bayes' Before-and-After Study

Since the RTM bias is caused by random fluctuation around κ, the RTM bias can be reduced if we have a sufficiently large sample (i.e., large T) under the *independent and identically distributed* (iid) *κ assumption* as revealed in previous studies (Cheng and Washington 2005; Sharma and Datta 2007). However, it is often difficult to collect crash data from several consecutive years, and it is questionable to assume the observed number of crashes for each year was from identical distribution. In this study, we have six years of crash data, which is generally recognized as being a sufficient sample size for reducing the RTM bias, but the time-constant κ assumption is dubious due to the trend in safety as discussed in the previous sections. Thus, we used the modified empirical Bayes' method to take into account simultaneously the change in traffic flow, the trend effect, and the RTM bias. In this subsection, we described the empirical Bayes' BA study approaches with two assumptions (i.e., time-constant κ and time-varying κ) in order to provide an insight into the modified empirical Bayes' BA study.

4.5.2.1 Empirical Bayes' BA Study with Time-constant κ

Generally, the expected number of crashes in the before period (κ) is assumed to be constant over time:

$$\kappa_t \equiv \kappa \text{ for } t = 1, 2, \cdots, B, \tag{48}$$

where κ_t is the expected number of crashes (per year) during the tth year in the *before* period, and κ is the time-constant expected number of crashes (per year) during the

before period. In such circumstances, the best estimate of κ is conditionally defined as E(κ|K), in which the observed crash K and the expected value κ are thought of as a *sample* and as a *prior* respectively in the Bayesian model. Then, the Bayesian theorem is expressed:

$$f(\kappa \mid K) = \frac{f(K \mid \kappa) \cdot f(\kappa)}{f(K)}, \tag{49}$$

where $f(\kappa \mid K)$ is the posterior density of parameter κ given sample K, $f(\kappa)$ is the prior density of parameter (κ) in which κ is considered as a random variable, and $f(K \mid \kappa)$ is the likelihood of sample K. Suppose that the distribution of sample K and parameter κ are Poisson and Gamma distributed respectively. Then, the posterior density of κ given K is calculated using the Bayesian theorem.

For a random sample of a segment, the likelihood of the sample element given κ, is

$$f(K \mid \kappa) = \frac{e^{-\kappa} \cdot \kappa^{K}}{K!}.$$

The prior distribution for κ is a Gamma distribution with parameters α and β:

$$f(\kappa) = \frac{\beta^{\alpha}}{\Gamma(\alpha)} \cdot \kappa^{\alpha-1} \cdot e^{-\kappa\beta} \text{ for } \kappa \geq 0,$$

where α and β are chosen depending on the exact knowledge or the degree of belief we have about the value of κ. In addition, the parameters are denoted:

$$\alpha = \frac{E(\kappa)^2}{V(\kappa)}, \ \beta = \frac{E^2(\kappa)}{V(\kappa)} \tag{50}$$

The joint density of the sample (K) and κ is

$$f(K \mid \kappa) \cdot f(\kappa) = \frac{\kappa^{K+\alpha-1} \beta^{\alpha} e^{-\kappa(1+\beta)}}{K!\Gamma(\alpha)},$$

and the marginal density of the sample (K) is

$$f(K) = \frac{\beta^{\alpha}}{K!\Gamma(\alpha)} \left(\frac{1}{1+\beta} \right)^{K+\alpha} \Gamma(K+\alpha).$$

In conjunction with "the joint density of the sample (K) and κ" and "the marginal density of the sample (K)", the posterior density for κ is

$$f(\kappa \mid K) = \frac{(1+\beta)^{K+\alpha} \kappa^{K+\alpha-1} e^{-\kappa(1+\beta)}}{\Gamma(K+\alpha)}, \tag{51}$$

and we see that the posterior density for κ is a Gamma distribution with parameters $\alpha + K$ and $1 + \beta$. As a result, the Bayesian expected value of κ and the Bayesian variance of κ are obtained:

$$E(\kappa \mid K) = \frac{K + \alpha}{1 + \beta},\ V(\kappa \mid K) = \frac{K + \alpha}{(1 + \beta)^2}$$

By plugging parameters α and β expressed by E(κ) and V(κ) in the prior distribution of κ (Equation (50)), they can be rewritten:

$$\begin{aligned} E(\kappa \mid K) &= w \cdot E(\kappa) + (1 - w) \cdot K; \\ V(\kappa \mid K) &= (1 - w) \cdot E(\kappa \mid K), \end{aligned} \tag{52}$$

where the term w is a weight between 0 and 1.

$$w = \frac{E(\kappa)}{E(\kappa) + V(\kappa)} \tag{53}$$

In addition, if we update *T*-year data instead of 1 year data, the posterior distribution of κ is modified (Abbess et al. 1981):

$$f(\kappa \mid K) = \frac{(T + \beta)^{K+\alpha}\, \kappa^{K+\alpha-1} e^{-\kappa(T+\beta)}}{\Gamma(K + \alpha)}. \tag{54}$$

Consequently, the empirical Bayes' weight is modified:

$$w = \frac{E(\kappa)}{E(\kappa) + TV(\kappa)}. \tag{55}$$

Equation (55) indicates that the weight for the observed number of crashes (K) increases as the number of years for the sample data increases.

In Equation (52), E(κ|K) is interpreted as the expected number of crashes for a segment given observed crash frequency K, and E(κ) is the average crash frequency of the reference group, which is similar to the comparison group, but the reference group should have data about crashes as well as other covariates for the safety performance functions used in the EB method (will be discussed in the next subsection). In addition, V(κ|K) is the variance of crashes for a segment given observed crash frequency K. They are determined after obtaining the weight term shown in the Equation (53). The weight *w* consists of the average crash frequency of the reference group (i.e., E(κ)) and the variation around E(κ) (i.e., V(κ)). If *w* is estimated to be near 1, then the E(κ|K) of the segment of interest is close to the mean of its reference group (E(κ)). On the contrary, if *w* is estimated to be near 0, then the E(κ|K) of the intersection of interest is mainly affected by the observed crash frequency (K).

The two components E(κ) and V(κ) play a pivotal role in obtaining the Bayesian estimator E(κ|K) as shown in Equation (53). In fact, the two components can be expressed by using the two parameters for the *prior*, which can be empirically estimated by the actual data (Carlin and Louis 2000). In the empirical Bayes' approach, it is common to assume that the crash frequency serves as data from a negative binomial distribution (Hauer 1992; Hauer 1997; Hauer et al. 2002; Hauer and Persaud 1987; Lord 2006). It is usually assumed that the heterogeneity term in the negative binomial regression model is gamma distributed with a mean equal to 1 and a variance 1/α. By using a negative binomial regression model, the two pivotal components can be estimated:

$$\widehat{E}(\kappa) = f(\text{covariates});\ \widehat{V}(\kappa) = \frac{\widehat{E}^2(\kappa)}{\alpha};\ \ \widehat{w} = \frac{\widehat{E}(\kappa)}{\widehat{E}(\kappa) + \widehat{V}(\kappa)}, \tag{56}$$

where the estimate of E(κ) and an over-dispersion parameter α can be obtained by using the safety performance functions for the EB correction, which are discussed in the next subsection. Again, the four steps to estimate the impacts of the SEP on safety can be corrected by using the results of the empirical Bayes' estimates. The first step is to estimate λ and predict π. Again, the estimate of λ is equal to the sum of the observed number of crashes during the program period, and the EB estimate of π is given by:

$$\widehat{\pi}_{EB} = \widehat{E}\left(\kappa \middle| K\right) = \widehat{w}\widehat{E}(\kappa) + (1 - \widehat{w})K. \tag{57}$$

The time-constant κ, which also remains the same during the *program* period, is discussed in this subsection. However, the prediction of π should be modified when κ≠π. For example, if there is a significant change in traffic flow or if a comparison group exists, the corresponding correction factors can be applied to predict π. the remaining steps continue as before as shown in Table 19. Table 30 shows the corrected four-step procedure, which can be used in the EB BA study with time-constant κ.

Table 30: The four-step procedure for the empirical Bayes' BA study (Time-constant κ)

Step	Goals	Formulas for the EB BA study
Step 1	Estimate λ and predict π	$\hat{\lambda} = L$ $\hat{\pi} = \widehat{w}\widehat{E}(\kappa) + (1-\widehat{w})K \; ; \; \widehat{w} = \frac{\widehat{E}(\kappa)}{\widehat{E}(\kappa) + \widehat{V}(\kappa)}$
Step 2	Estimate $\hat{\sigma}^2[\hat{\lambda}]$ and $\hat{\sigma}^2[\hat{\pi}]$	$\hat{\sigma}^2(\hat{\lambda}) = \hat{\lambda}$ $\sigma^2(\widehat{\pi}) = (1-\widehat{w})\widehat{E}\left(\kappa \middle| K\right)$
Step 3	Estimate δ and θ	$\hat{\delta} = \hat{\pi} - \hat{\lambda} = K - L$ $\hat{\theta} \cong \frac{\left(\frac{\hat{\lambda}}{\hat{\pi}}\right)}{\left(1 + \frac{\widehat{V}[\hat{\pi}]}{\hat{\pi}^2}\right)}$
Step 4	Estimate $\hat{\sigma}^2[\hat{\delta}]$ and $\hat{\sigma}^2[\hat{\theta}]$	$\hat{\sigma}^2\left[\hat{\delta}\right] = \hat{\pi} + \hat{\lambda} = K + L$ $\hat{\sigma}^2(\hat{\theta}) \cong \frac{\hat{\theta}^2 . \left[\frac{\widehat{V}(\hat{\lambda})}{\hat{\lambda}^2} + \frac{\widehat{V}(\hat{\pi})}{\hat{\pi}^2}\right]}{\left[1 + \frac{\widehat{V}(\hat{\pi})}{\hat{\pi}^2}\right]^2}$

4.5.2.2 Empirical Bayes' Before-and-After Study with Time-varying κ

The assumption that the expected number of crashes for the enforcement zone are invariant during the *before* period shown in Equation (48) is invalid. When the safety changes over time, the π cannot be accurately predicted if we used the EB BA study with time-constant κ. However, the change in κ is not entirely unpredictable, although the κ changes over time. The predictable κ indicates that the κ of the enforcement zone changes from one year to the next, but there must be some discipline and orderliness to this change as Hauer described (Hauer 1997). Moreover, the fact that important features in the enforcement zone remain largely unchanged over time, change slowly, or change predictably indicates that the change in κ is predictable.

The change in the expected number of crashes can be modeled by using the correction factor, which is similar to the traffic flow correction factor r_{tf}:

$$C_{it} = \frac{\kappa_{it}}{\kappa_{i1}}, \tag{58}$$

and

$$\kappa_{it} = C_{it}\kappa_{i1}, \tag{59}$$

where κ_{it} is the expected number of crashes (per year) in the *i*th section during the *t*th year within the *before* period. Equation (59) indicates that the expected number of crashes at section *i* during the *t*th year can be predicted by multiplying the correction factor (C_{it}) by the expected number of crashes at section *i* during the base year. Note that in Equation (58)the κ_{i1} was chosen as the base year arbitrarily to reflect the relative change in safety in the *t*th year to the first year. Although we use any year as the base year, the final EB estimation results are the same (Garber et al. 2006; Hauer 1997).

If the correction factor C_{it} is equal to 1, it indicates that no change in safety from the base year to the *t*th year occurred (i.e., $\kappa_{i1} = \kappa_{it} \equiv \kappa$). On the contrary, if the correction factor C_{it} is unequal to 1, it indicates the underlying safety for section *i* in the *t*th year is no longer the same as that in the base year, which can be attributed to the change in AADT as well as the change in all the other factors affecting safety from the base year to the *t*th year.

Since the true expected number of crashes is often unattainable, the C_{it} can be estimated by SPFs:

$$\widehat{C}_{it} = \frac{\widehat{E}\left(\kappa_{it}\left|\mathbf{x}_{it}\right.\right)}{\widehat{E}\left(\kappa_{i1}\left|\mathbf{x}_{i1}\right.\right)} = \frac{\widehat{E}\left(\kappa_{it}\right)}{\widehat{E}\left(\kappa_{i1}\right)}, \tag{60}$$

where $\widehat{E}\left(\kappa_{it}\left|\mathbf{x}_{it}\right.\right)$ is the estimate of the expected number of crashes at section *i* in the *t*th year given covariates $\mathbf{x}_{it}$, and the term is often expressed as $\widehat{E}\left(\kappa_{it}\right)$ without the conditional component.

If we directly multiply the correction factors in Equation (60) by the observed crashes (K) in order to predict π, the predictions are essentially equivalent to those of the BA study with traffic flow correction from the previous section. However, the observed crashes (K) are likely to be influenced by regression-to-the-mean phenomenon as revealed in the previous subsection. Therefore, it is necessary to estimate κ_{it} by using the empirical Bayes' approach in order to eliminate the RTM bias.

Hauer (1997) proposed a method to account for the change in traffic flow, trend effect, and RTM bias simultaneously. When we analyze the time-varying κ, the Bayes' theorem described in Equation (49) can be modified:

$$f(\kappa_{i1} \mid K_{i1}, K_{i2}, \cdots, K_{iB}) = \frac{f(K_{i1}, K_{i2}, \cdots, K_{iB} \mid \kappa_{i1}) \cdot f(\kappa_{i1})}{f(K_{i1}, K_{i2}, \cdots, K_{iB})}, \tag{61}$$

In the case of the time-constant κ, the sum of the observed number of crashes during the *before* period (K) was treated as a single observation (i.e., sample). However, if the κ is not constant over time, it is necessary to treat the observed number of crashes for each year as one independent observation. By repeatedly updating the observed number of crashes for each year, the posterior distribution of κ_{i1} can be obtained:

$$f\left(\kappa_{i1} \mid K_{i1}, K_{i2}, \cdots, K_{iB}\right) = \frac{\left(\beta_i + \sum_{t=1}^{B} C_{it}\right)^{\alpha + \sum_{t=1}^{B} K_{it}} \cdot \kappa_{i1}^{\alpha + \sum_{t=1}^{B} K_{it} - 1} \cdot e^{-\kappa_{i1}\left(\beta_i + \sum_{t=1}^{B} C_{it}\right)}}{\Gamma\left(\alpha + \sum_{t=1}^{B} K_{it}\right)}, \tag{62}$$

where α and β_i are the parameters of the prior Gamma distribution for κ_{i1}, and the rest of the notation is as previously defined. Note that Equation (62) is the same as the Equation (54) when the κ is constant over time.

The posterior distribution of κ_{i1} given all available crash history $\{K_{i1}, K_{i2}, \cdots, K_{iB}\}$ is also gamma distributed (see Equation (62)). Therefore, the expected number of crashes and the variance of the crashes can be estimated by using the properties of the gamma distribution. The EB estimate is:

$$\widehat{E}\left(\kappa_{i1} \middle| K_{i1}, K_{i2}, \cdots, K_{iB}\right) = \frac{\widehat{\alpha} + \sum_{t=1}^{B} K_{it}}{\frac{\widehat{\alpha}}{\widehat{E}\left(\kappa_{i1}\right)} + \sum_{t=1}^{B} \widehat{C}_{it}}, \tag{63}$$

where $\widehat{\alpha}$ is the estimate of the over-dispersion parameter in the NBRM and the rest of the notation is as previously defined. The variance of the EB estimate is:

$$\widehat{V}\left(\kappa_{i1} \middle| K_{i1}, K_{i2}, \cdots, K_{iB}\right) = \frac{\widehat{\alpha} + \sum_{t=1}^{B} K_{it}}{\left\{\frac{\widehat{\alpha}}{\widehat{E}\left(\kappa_{i1}\right)} + \sum_{t=1}^{B} \widehat{C}_{it}\right\}^2}. \tag{64}$$

The EB estimate in Equation (63) can be extended to estimate the EB estimate for the *t*th year (i.e., $\widehat{E}\left(\kappa_{it}\left|K_{i1},K_{i2},\cdots,K_{iB}\right.\right)$) by using the relationship described in Equation (60):

$$\widehat{E}\left(\kappa_{it}\left|K_{i1},K_{i2},\cdots,K_{iB}\right.\right)=\widehat{C}_{it}\,\widehat{E}\left(\kappa_{i1}\left|K_{i1},K_{i2},\cdots,K_{iB}\right.\right). \tag{65}$$

In addition, the variance of the EB estimate for the *t*th year is:

$$\widehat{V}\left(\kappa_{it}\left|K_{i1},K_{i2},\cdots,K_{iB}\right.\right)=\widehat{C}_{it}^{2}\,\widehat{V}\left(\kappa_{it}\left|K_{i1},K_{i2},\cdots,K_{iB}\right.\right). \tag{66}$$

In order to predict π, Equations (65) and (66) can be used, but the correction factor needs to be clearly stated:

$$\widehat{C}_{it}=\frac{\widehat{E}\left(\kappa_{it}\left|\mathbf{x}_{it}\right.\right)}{\widehat{E}\left(\kappa_{i1}\left|\mathbf{x}_{i1}\right.\right)}=\frac{\widehat{E}\left(\kappa_{it}\right)}{\widehat{E}\left(\kappa_{i1}\right)}\ \text{for } t>B, \tag{67}$$

where *B* is the number of durations for the *before* period. Equation (67) indicates that the numerator should reflect the relationship between the number of crashes and covariates during the *program* period without treatment. As a result, the predicted value of π is:

$$\widehat{\pi}=\sum_{t=B+1}^{p}\widehat{C}_{it}\,\widehat{E}\left(\kappa_{i1}\left|K_{i1},K_{i2},\cdots,K_{iB}\right.\right), \tag{68}$$

and the variance of $\widehat{\pi}$ is

$$\widehat{V}\left(\widehat{\pi}\right)=\sum_{t=B+1}^{p}\widehat{C}_{it}^{2}\,\widehat{V}\left(\kappa_{it}\left|K_{i1},K_{i2},\cdots,K_{iB}\right.\right). \tag{69}$$

The remaining steps are as previously stated.

Table 31 shows the modified four-step procedure for the empirical Bayes' method, which can simultaneously account for the change in traffic flow, trend effect, and the RTM bias. The discussion in this report makes it clear that on conceptual and theoretical ground the modified EB approach is the most defensible of the four approaches.

Table 31: The four-step procedure for the empirical Bayes' BA study (Time-varying κ)

Step	Goals	Formulas for the EB BA study
Step 1	Estimate λ and predict π	$\hat{\lambda} = L$ $\hat{\pi} = \widehat{C}_{it}\,\widehat{E}\left(\kappa_{i1}\middle\vert K_{i1}, K_{i2}, \cdots, K_{iB}\right)$ for $t > B$; where $\widehat{E}\left(\kappa_{i1}\middle\vert K_{i1}, K_{i2}, \cdots, K_{iB}\right) = \dfrac{\widehat{\alpha} + \sum_{t=1}^{B} K_{it}}{\dfrac{\widehat{\alpha}}{\widehat{E}\left(\kappa_{i1}\right)} + \sum_{t=1}^{B} \widehat{C}_{it}}$; $\widehat{C}_{it} = \dfrac{\widehat{E}\left(\kappa_{it}\right)}{\widehat{E}\left(\kappa_{i1}\right)}.$
Step 2	Estimate $\hat{\sigma}^2[\hat{\lambda}]$ and $\hat{\sigma}^2[\hat{\pi}]$	$\hat{\sigma}^2\left[\hat{\lambda}\right] = \hat{\lambda}$ $\hat{\sigma}^2\left[\hat{\pi}\right] = \widehat{C}_{ip}^2\,\widehat{V}\left(\kappa_{it}\middle\vert K_{i1}, K_{i2}, \cdots, K_{iB}\right)$ for $t > B$ where $\widehat{V}\left(\kappa_{i1}\middle\vert K_{i1}, K_{i2}, \cdots, K_{iB}\right) = \dfrac{\widehat{\alpha} + \sum_{t=1}^{B} K_{it}}{\left\{\dfrac{\widehat{\alpha}}{\widehat{E}\left(\kappa_{i1}\right)} + \sum_{t=1}^{B} \widehat{C}_{it}\right\}^2}.$
Step 3	Estimate δ and θ	$\hat{\delta} = \hat{\pi} - \hat{\lambda} = K - L$ $\hat{\theta} \cong \dfrac{\left(\dfrac{\hat{\lambda}}{\hat{\pi}}\right)}{\left(1 + \dfrac{\widehat{V}[\hat{\pi}]}{\hat{\pi}^2}\right)}$
Step 4	Estimate $\hat{\sigma}^2[\hat{\delta}]$ and $\hat{\sigma}^2[\hat{\theta}]$	$\hat{\sigma}^2\left[\hat{\delta}\right] = \hat{\pi} + \hat{\lambda} = K + L$ $\hat{\sigma}^2(\hat{\theta}) \cong \dfrac{\hat{\theta}^2 \cdot \left[\dfrac{\widehat{V}(\hat{\lambda})}{\hat{\lambda}^2} + \dfrac{\widehat{V}(\hat{\pi})}{\hat{\pi}^2}\right]}{\left[1 + \dfrac{\widehat{V}(\hat{\pi})}{\hat{\pi}^2}\right]^2}$

4.5.3 Results of the EB Before-and-After Study

Using the estimated SPFs shown in Table 27 and the EB procedure with time-varying κ described in the previous subsection, the predicted values of π are estimated by year, section, crash type, and severity. For example, the prediction for single-vehicle crashes is:

$$\hat{\pi}_{EB} = \sum_{i=1}^{E} \sum_{t=B+1}^{p} \hat{C}_{it} \hat{E}\left(\kappa_{i1} \left| K_{i1}, K_{i2}, \cdots, K_{iB} \right.\right), \tag{70}$$

where E is the total number of sections in the enforcement zone, and the rest of the notation is as previously defined. Again, note that the modified empirical Bayes' BA study with time-varying κ was used to take into account all confounding factors such as the change in traffic flow, trend effect, and the RTM bias.

Table 32 shows the results of the EB BA study. The predicted values of π in the EB BA study are slightly greater than those in the BA study with traffic flow correction (except for the single-vehicle injury crashes). It indicates that the enforcement zone was not the 'least safe' on Loop 101 prior to the SEP program since the expected number of crashes from the reference group is greater than the observed number of crashes from each section in the enforcement zone. In addition, the similarity of the predictions between the EB BA study and the BA study with traffic flow correction indicates that the bias from the regression-to-the-mean is relatively small when estimating the impact of the SEP on safety.

Table 32: Results of the EB BA study

Crash type and severity		Crash estimates		Impact estimates	
		$\hat{\pi}$	$\hat{\lambda}$	$\hat{\theta}$ [1]	$\hat{\delta}$ [2]
All target crashes	Single-Vehicle	50.97	19	0.37 (0.09)[3]***	31.97 (8.36)***
	Side-swipe (same)	22.61	12	0.52 (0.16)**	10.61 (5.88)**
	Rear-end	30.77	23	0.74 (0.18)*	7.77 (7.33)*
	Other	15.70	2	0.12 (0.09)***	13.70 (4.21)***
Injury crashes	Single-Vehicle	10.15	6	0.57 (0.25)*	4.15 (4.02)*
	Side-swipe (same)	5.27	2	0.36 (0.25)**	3.27 (2.70)*
	Rear-end	9.93	8	0.77 (0.30)	1.93 (4.23)
	Other	6.66	1	0.14 (0.13)***	5.66 (2.77)**
PDO crashes	Single-Vehicle	39.64	13	0.33 (0.09)***	26.64 (7.26)***
	Side-swipe (same)	17.14	10	0.57 (0.20)**	7.14 (5.21)**
	Rear-end	21.13	15	0.69 (0.20)*	6.13 (6.01)*
	Other	9.36	1	0.10 (0.10)***	8.36 (3.22)***
Total target crashes		120.05	56	0.46 (0.07)***	64.05 (13.27)***
Total injury crashes		32.02	17	0.52 (0.14)**	15.02 (7.00)**
Total PDO crashes		87.28	39	0.44 (0.08)***	48.28 (11.24)***

Note: * p<0.2;** p<0.1;***p<0.01 for H_0: θ=1 or H_0: δ=0.
[1] Percent change in crash from the *before* to the *program* period is (θ–1)×100.
[2] Positive sign indicates decrease in crash for the *program* period
[3] For parameter estimates, the associated standard deviations are in parentheses.

Figure 35 illustrates the percent change in target crashes for each crash type and severity. Again, the percent change is $(\hat{\theta}_{-1})\times 100$. The EB before-and-after study results suggest:

- The impacts of the SEP on safety estimated by the EB BA study are larger than those from the previous approaches when accounting for the RTM bias because the enforcement zone was 'safer than average' prior to the SEP. Specifically,
  - Total target crash frequency was reduced by 54%. Total injury and PDO crashes were also reduced by 48% and 56% respectively.
  - All types of crashes were reduced, but the decrease in rear-end injury crashes was not significant (p-value=0.325).

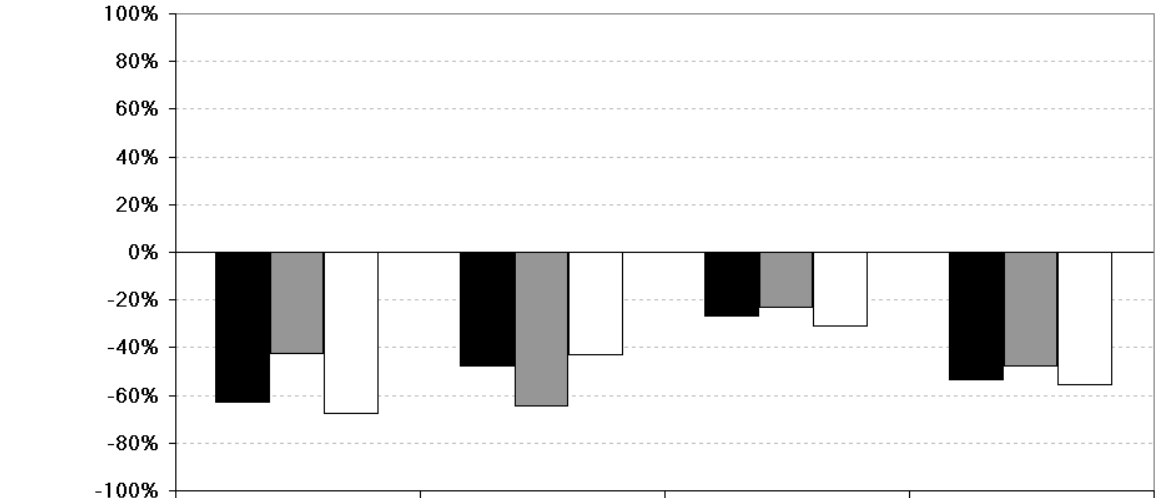

	Single-vehicle	Side-swipe (same direction)	Rear-end	Total
■ Total crashes	-63%	-48%	-26%	-54%
▒ Injury crashes	-43%	-64%	-23%	-48%
□ PDO crashes	-67%	-43%	-31%	-56%

Figure 35: EB before-and-after study results

The results from the EB BA study (time-varying κ) are the most defensible of the four approaches for two reasons. First, the modified EB BA study eliminated the possibility of double accounting, which can occur when we account for both the change in traffic flow and trend effect simultaneously. Second, the modified EB BA study reduced another source of error called regression-to-the-mean bias, which often contributes to over/underestimating the effectiveness of the countermeasure.

4.6 Economic Analysis

In this section, the estimated changes in safety due to the SEP are translated into economic impacts. The conversion of crashes to crash costs is extremely beneficial and insightful because different crash types have different cost implications, with some crash types costing more than others. In order to quantify the economic impacts, the Arizona-

specific crash costs were developed based on the crash costs obtained from several Arizona freeways, and the economic benefits from the SEP were estimated by using the crash costs and the estimated changes in safety (δ).

4.6.1 Arizona-specific Crash Costs

Crash costs are obtained from extensive national research on full costs of motor vehicle crashes (Blincoe et al. 2002). In this analysis, the crash costs are updated to reflect Arizona-specific costs such as hospital charges by injury severity category and to reflect crashes on Arizona high-speed freeways.

Table 33: Estimated Arizona-specific crash costs per crash

Collision type	Crash severity	Final Medical Cost	Total Other Cost	Quality of Life Cost	Total Cost
Single-vehicle	K	$162,870	$1,340,063	$2,111,828	$3,614,761
	A	$122,790	$200,291	$361,020	$684,101
	B	$24,104	$61,295	$88,104	$173,503
	C	$13,545	$34,771	$45,343	$93,659
	O	$15,527	$41,402	$50,277	$107,206
Side-swipe (same direction)	K	$119,065	$1,651,039	$2,496,842	$4,266,946
	A	$133,636	$301,959	$442,205	$877,801
	B	$27,504	$80,482	$86,291	$194,277
	C	$16,354	$65,398	$64,673	$146,425
	O	$15,826	$62,247	$50,530	$128,604
Rear-end	K	$71,037	$1,608,206	$2,441,687	$4,120,929
	A	$70,820	$162,469	$239,725	$473,013
	B	$39,899	$100,244	$152,827	$292,971
	C	$28,785	$77,037	$113,695	$219,517
	O	$30,643	$77,278	$117,022	$224,942
Other Crashes	K	$77,949	$1,200,900	$1,784,243	$3,063,092
	A	$97,374	$236,524	$310,713	$644,611
	B	$15,431	$62,216	$60,957	$138,604
	C	$8,557	$42,965	$43,917	$95,439
	O	$3,421	$34,919	$11,019	$49,359

We utilized inflation adjusted costs from National Hospital Discharge Survey, National Health Interview Survey, AZ hospital cost/charge information, CHAMPUS data on physician costs, National Medical Expenditure Survey, National Council on Compensation Insurance, and Crashworthiness Data System.

All crash costs for each crash type are estimated by using a large sample of crashes that occurred on Arizona high-speed freeways (SR 101, 202, and 51). Table 33 shows the estimated Arizona-specific crash costs for each target crash by severity level, in which

the crash severity is classified by using the KABCO severity scale (K = killed; A = disabling injury; B = evident injury; C = possible injury; O = property damage only). The crash costs have three cost items:

- Medical Costs: Professional, hospital, emergency department, drugs, rehabilitation, long-term care
- Other Costs: Police/ambulance/fire, insurance administration, loss of wages, loss of household work, legal/court costs, property damage
- Quality of Life Costs: Based on Quality Adjusted Life Years (approximately $92k/QALY)

4.6.2 Economic Benefits

The economic benefits from SEP are quantified using the unit costs and the changes in safety (δ). Crash benefits were obtained by multiplying the estimated crash costs by the estimates of the change in safety (δ). Since it is necessary to estimate the change in safety by crash type as well as severity, the predicted total number of injury crashes for each crash type was divided by crash type. The division was conducted by multiplying the predicted total number of injury crashes by the proportion of crashes with a certain crash type calculated using the observed data. However, the changes in safety for the PDO crashes were directly extracted from the predicted value for the PDO crashes for more reliable results. The estimates are summarized by the type of crash and the 5 severity levels (i.e., KABCO scale). Table 34 shows the estimated change in safety by crash type and severity.

Table 34: Changes in safety by severity

Analysis method	Collision type	Crash severity					
		Fatal Crashes (K)	Disabling Injury (A)	Evident Injury (B)	Possible Injury (C)	Property Damage (O)	Total
BA study with traffic flow correction	Single-Vehicle	0.28	0.13	5.28	-1.31	26.60	30.97
	Side-swipe (same)	0.26	0.00	1.64	0.93	6.82	9.65
	Rear-end	0.00	-1.21	2.32	0.19	6.01	7.31
	Other	0.38	0.38	1.78	3.07	8.19	13.81
EB BA study with time-varying κ	Single-Vehicle	0.27	0.09	5.17	-1.37	26.64	30.80
	Side-swipe (same)	0.28	0.00	1.79	1.20	7.14	10.41
	Rear-end	0.00	-1.16	2.61	0.47	6.13	8.06
	Other	0.38	0.38	1.79	3.10	8.36	14.03

Note that the economic benefits from the BA study with a comparison group are not quantified in this report because the estimates do not reflect the change in traffic flow from the *before* to *program* period. By multiplying the unit costs by the changes in safety,

the economic benefits ($) are obtained. Table 35 shows the economic benefits per year, which are $16.50 M and $17.05 M per year.

Table 35: Summary of crash benefits per year ($1,000)

Analysis method	Collision type	Crash severity					
		Fatal Crashes (K)	Disabling Injury (A)	Evident Injury (B)	Possible Injury (C)	Property Damage (O)	Total
BA study with traffic flow correction	Single-Vehicle	$1,503	$134	$1,370	-$184	$4,266	$7,088
	Side-swipe (same)	$1,651	$0	$476	$204	$1,312	$3,643
	Rear-end	$0	-$859	$1,018	$63	$2,021	$2,243
	Other	$1,748	$368	$369	$438	$605	$3,529
	Total	$4,902	-$358	$3,234	$521	$8,204	$16,503
EB BA study with time-varying κ	Single-Vehicle	$1,471	$87	$1,341	-$192	$4,273	$6,980
	Side-swipe (same)	$1,803	$0	$520	$263	$1,373	$3,960
	Rear-end	$0	-$822	$1,145	$155	$2,064	$2,543
	Other	$1,762	$371	$372	$443	$618	$3,565
	Total	$5,036	-$364	$3,379	$669	$8,328	$17,048

The crash benefits should be interpreted with caution because the analysis was based on the brief *program* period. Random fluctuations in crashes are commonly observed, and can influence the results significantly. In particular, severe crashes including fatal crashes will significantly influence the benefit estimates associated with the analysis.

Chapter 5 Effect of SEP on Travel Times

In this chapter, the effects of the SEP on transportation systems are analyzed. Specifically, the effects are measured by the change in total travel time and travel time uncertainty resulting from the SEP. A microscopic traffic simulation tool, which models the acceleration and speed choice behavior of individual vehicles in detail, was used to capture the effects under numerous traffic conditions. In the following sections, all relevant simulation procedures and analysis results are discussed in detail.

5.1 Background

5.1.1 Motivation and Study Objectives

Transportation system investments are often targeted towards one or more goals; to improve travel times, to improve safety, to reduce air pollution or noise, or to reduce travel time variability. When safety investments are considered, often there is a tradeoff between travel times and safety, or mobility and driving risk. In fact, many safety initiatives such as speed enforcement are politically unpopular due to their perceived negative impact on mobility. Consider, for example, the setting of national and state speed limits on freeways and highways—perceived mobility is reduced while safety is improved (in theory). Little research to date has rigorously examined the travel time impacts of photo speed enforcement.

In this chapter, we described the results of a combined empirical and simulation-based analysis of automated photo speed enforcement on safety and travel times. The impact of the SEP on travel times and travel time uncertainty—the focus of this chapter—was estimated by simulating network traffic conditions with and without the SEP. Travel time impacts resulting from changes in average travel speeds and non-recurrent congestion (by-products of the SEP and its impact on crashes) were estimated by simulating the enforcement zone within the broader Loop 101 freeway network in Scottsdale, AZ. Specifically, the objectives of this study are to:

- Examine the change in travel time distribution resulting from the SEP or crashes;
- Estimate daily travel time uncertainty caused by the change in average travel speeds and non-recurrent congestion;
- Assess the change in total travel time resulting from the SEP or crashes;
- Estimate total travel time savings as a potential byproduct of the SEP.

Since it is often difficult to estimate the change in travel time distribution and total travel time from the observed data directly, a microscopic traffic simulation tool was used.

5.1.2 Past Studies

A number of studies have revealed that speed enforcement has reduced speeding and crashes, see an extensive review in Kweon and Kockelman (2005); Lave and Lave (1998); Skszek (2004); Stuster et al. (1998). Several observational studies that evaluated the impact of speed enforcement on driving behavior disclosed that the reductions in speed and crash frequency resulting from speed enforcement have limited temporal and spatial spillover effects, with revealed inconsistencies over time and space (Champness and Folkman 2005; Ha et al. 2003; Hauer et al. 1982; Sisiopiku and Patel 1999; Vaa 1997; Waard and Rooijers 1994). Few simulation studies have been conducted to estimate the impact of speed enforcement on driver behavior and network-wide impacts (Liu and Tate 2004; Toledo et al. 2007). These simulation studies used microscopic traffic simulation models to analyze the network-wide impacts of one of the speed limiters, which is an electronic device to regulate the maximum speed of equipped vehicle.

More specifically, Liu and Tate (2004) analyzed the impact of an intelligent speed adaptation system (ISAS) on network total travel times and other traffic externalities in an urban network during peak and non-peak periods. In the study network of 70 traffic analysis zones consisting of 120 nodes and 245 links, two levels of speed limiter settings were assumed: 64 kph (40 mph) and 48 kph (30 mph). The authors found that the ISAS changed the shape of speed distributions by reducing the travel times at speeds exceeding the speed limit, and that the ISAS is more effective during the non-peak than during the peak periods. Although the authors concluded that the ISAS does not significantly affect the travel time of the slower drivers, they also found that there is a 2.4% average increase in network total travel time between 0% and 100% ISAS penetration. However, the significant increase in network total travel time should be viewed as the product of a network-wide installation of the ISAS.

Toledo et al. (2007) examined the effects of an active speed limiters on average speed, speed variability, and lane change frequency in a freeway network using a microscopic simulation model. The authors used a 10% equipment rate at various congestion levels with three levels of speed limiter settings: no limiting, 100 kph (62 mph), and 120kph (75 mph). Although they concluded that the active speed limiter generally contributes to reduced mean speeds and speed variability, they also found that speed variability and lane-change frequency increased during free flow conditions, attributed to a bi-modal distribution of slow and fast vehicles. The authors also estimated potential crash reduction using the estimated reduction in mean speed (40% reduction in fatal crashes and 25% reduction in injury crashes).

While these papers discussed travel time impacts from reduced speeds, they did not attempt to account for the travel time impacts from reduced crashes and resultant congestion (non-recurrent congestion). Of course the non-recurrent congestion impacts of a safety program cannot be ignored and in theory could have a significant impact on travel time and travel time variability.

On the contrary, it is noteworthy that numerous studies have examined travel time uncertainty, although the impact of speed enforcement on travel time caused by reduced crash frequencies has not been estimated (Al-Deek and Emam 2006; Bell and Iida 1997; FHWA 2007; Ikhrata and Michell 1997; Lam and Wong 2003; Levinson and Zhang 2003; Li et al. 2006; Oh and Chung 2006; Rakha et al. 2006; Recker et al. 2005; Sumalee and Watling 2003).

In general, the measures for assessing travel time uncertainty are divided into two categories (Levinson and Zhang 2003): *travel time variability* and *travel time reliability*. Travel time variability estimates the magnitude of the dispersion of travel time by treating early and late arrivals with equal weight (Levinson and Zhang 2003; Li et al. 2006; Oh and Chung 2006; Rakha et al. 2006), while travel time reliability measures the probability that a trip can reach its destination within a given period of time (Al-Deek and Emam 2006; Bell and Iida 1997; FHWA 2007; Ikhrata and Michell 1997; Lam and Wong 2003; Recker et al. 2005; Sumalee and Watling 2003).

From the literature review, several lessons were learned that could be useful in designing a reliable simulation study. These are itemized below:

- *Travel time impacts resulting from reduced crashes*: The impact of the SEP on travel time should be estimated by taking into account the delay resulting from the reduction in crashes. To the best of the authors' knowledge, no past studies account for the travel time impact resulting from the reduction in the total number of crashes, which are estimated by using a rigorous before-and-after study.
- *Change in travel time distribution*: It is necessary to carefully examine how the distribution of travel time shifted as a result of the SEP. Specifically, the travel time distribution with and without the SEP needs to be compared by using travel time reliability rather than travel time variability, since it is necessary to explore the impact of the SEP on faster drivers independently.
- *Estimate daily travel time uncertainty*: It is also necessary to convert the change in travel time reliability per day into annual daily travel time uncertainty in order to measure how the travel time reliability during the *before* period differs from that of the *program* period.
- *Change in total travel time*: Since the non-recurrent congestion caused by the reduced number of crashes can affect traffic in the enforcement zone as well as adjacent arterials in Scottsdale, it is desirable to measure the change in total travel time on the Scottsdale network as a system-wide effect.

5.2 Data Preparation

Numerous sources of data were utilized as sources of inputs to the simulation of the photo speed enforcement program on the Scottsdale Loop 101 freeway: 2006 Maricopa Association of Governments (MAG) transportation planning data, Arizona Department of Transportation (ADOT) and the City of Scottsdale's speed and traffic volume data collected during the *before* period, speed data collected from the enforcement zone during the *program* period by Redflex (the vendor of Scottsdale's enforcement cameras during the program), and 2006 ADOT freeway incident log files. In the following subsections, the overall procedures for data preparation are described in detail.

5.2.1 MAG Transportation Network and Travel Demand Data

Since the microscopic traffic simulation model should simulate Scottsdale's transportation system during the non-peak period, the MAG data only for the non-peak period (9:00 AM –15:00 PM) were collected:

- 2006 MAG transportation network (EMME/2 format) including link length, direction, number of lanes, link type, etc
- 2006 off-peak period 35 volume-delay functions
- 2006 off-peak period OD matrix (1995×1995)

The highway network and demand data were directly imported to TransCAD, but the volume-delay functions were added to TransCAD by joining database because of the different database structure. Figure 36 shows the imported 2006 MAG transportation network, in which all links are divided into 5 areas: CBD, outlying CBD, mixed urban, rural, and suburban.

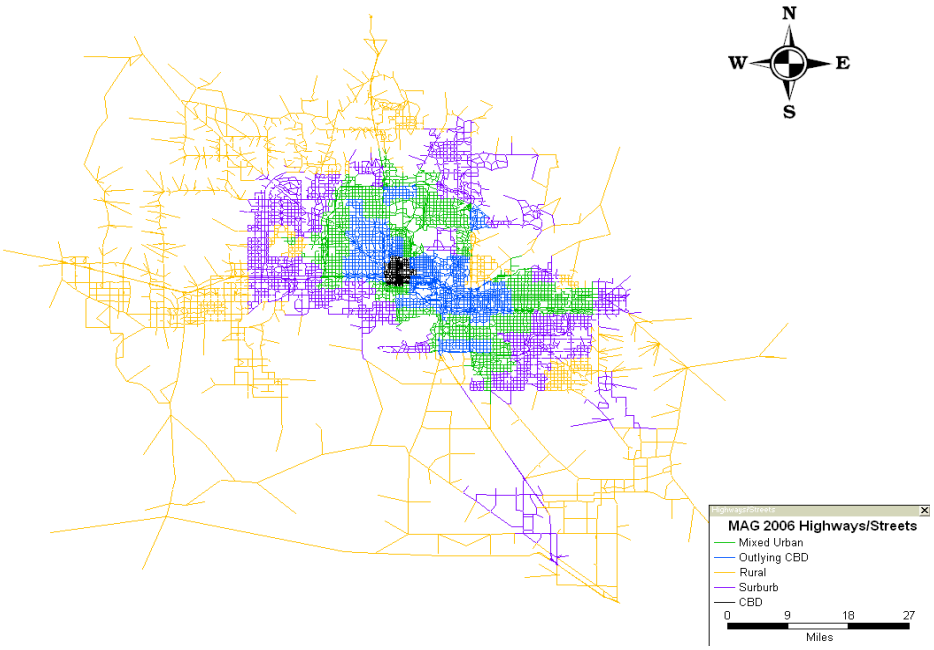

Figure 36: 2006 MAG Transportation Network

For each area, MAG uses 10 volume-delay functions (VDFs) for each facility type, which are a slightly modified version of the BPR (Bureau of Public Roads) congestion function:

$$t_i = \eta_i \cdot l_i \cdot \left\{1 + \alpha \left(\frac{v_i}{c_i}\right)^{\beta}\right\} = t_i^0 \cdot \left\{1 + \alpha \left(\frac{v_i}{c_i}\right)^{\beta}\right\}, \tag{71}$$

where t_i is congested travel time on link i, t_i^0 is the free-flow travel time on link i, η is the free-flow travel time coefficient on link i, l_i is the length of link i, c_i is capacity of link i, v_i is flow on link i, and α and β are estimable parameters. The VDFs were used to extract the target network. Table 36 (next page) shows the VDFs used in this study for the non-peak period (when V/C<2).

Table 36: MAG volume-delay function coefficients during non-peak period (when v/c<2)

Area	VDF	Free-flow travel time coefficient (η)	Capacity (pce/6hr/lane)	α	β	Link Type
CBD	10	0.882	7275	0.1	8	HOV
	11	0.882	7275	0.1	8	Freeway
	12	1.5	3593	0.15	6	Expressway
	13	1.875	2086	0.15	6	Collector
	14	2.007	1934	0.15	6	6-legged expressway
	15	4				Centroid Connector
	16	1.893	3040	0.15	6	Major Arterial
	17	4	6509	0.15	6	Un-metered Ramp
Outlying CBD	20	0.882	7275	0.1	8	HOV
	21	0.882	7275	0.1	8	Freeway
	22	1.5	3593	0.15	6	Expressway
	23	1.714	2086	0.15	6	Collector
	24	1.881	1934	0.15	6	6-legged expressway
	25	3				Centroid Connector
	26	1.644	3040	0.15	6	Major Arterial
	27	4	6509	0.15	6	Un-metered Ramp
Mixed urban	30	0.882	7275	0.1	8	HOV
	31	0.882	7275	0.1	8	Freeway
	32	1.5	3520	0.15	6	Expressway
	33	1.714	2086	0.15	6	Collector
	34	1.875	1934	0.15	6	6-legged expressway
	35	2.4				Centroid Connector
	36	1.604	2957	0.15	6	Major Arterial
	37	4	6509	0.15	6	Un-metered Ramp
Rural	40	0.882	7275	0.1	8	HOV
	41	0.882	7275	0.1	8	Freeway
	42	1.277	3520	0.15	6	Expressway
	43	1.5	1441	0.15	6	Collector
	44	1.84	1771	0.15	6	6-legged expressway
	45	2.4				Centroid Connector
	46	1.508	2773	0.15	6	Major Arterial
	47	4	6509	0.15	6	Un-metered Ramp
Suburban	50	0.882	7275	0.1	8	HOV
	51	0.882	7275	0.1	8	Freeway
	52	1.054	3281	0.15	6	Expressway
	53	1.5	1441	0.15	6	Collector
	54	1.818	1771	0.15	6	6-legged expressway
	55	2				Centroid Connector
	56	1.376	1678	0.15	6	Major Arterial
	57	4.0	5234	0.15	6	Un-metered Ramp

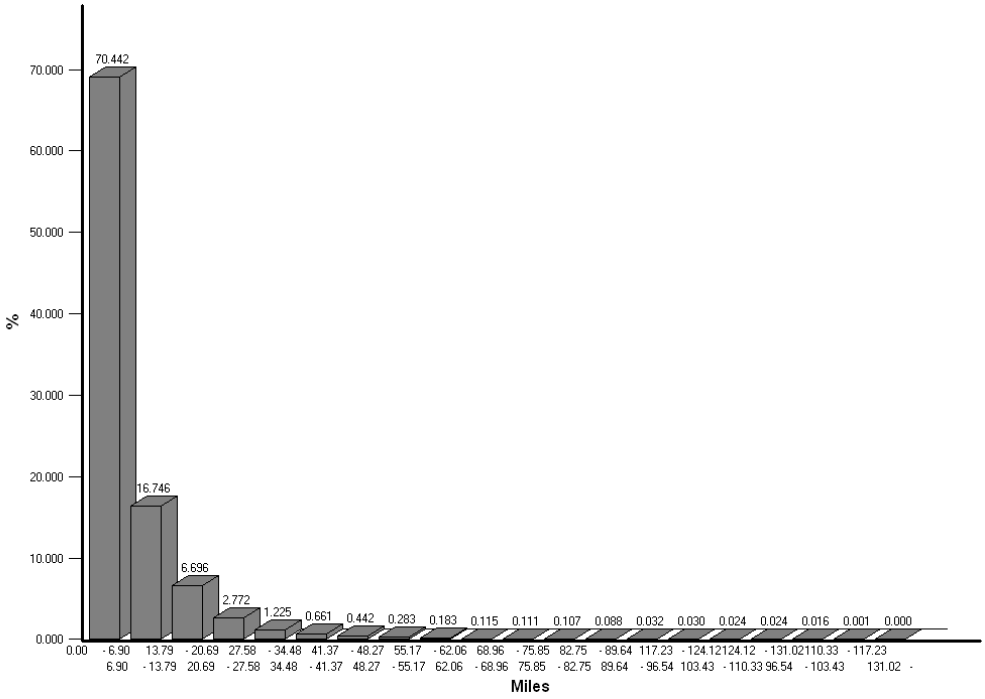

Figure 37: Trip length distribution of all non-peak trips

In addition to the network and VDFs, the '1995×1995' OD matrix by five modes (low occupancy auto, high occupancy auto, heavy truck, mid-size truck, and other trunk) was also imported to TransCAD. Figure 37 shows the trip length distribution (TLD), which was created by using the shortest path matrix based on the physical length of each highway segment. The TLD shows that the average trip length in MAG area is 6.57 miles and standard deviation for the trip length is 9.89 miles for '5,099,363.45 trips/6 hours' during the non-peak period.

5.2.2 Multi-Class Sub-area Analysis

Since the MAG transportation network shown in Figure 36 is not suitable for microscopic simulation due to large network size, we extracted a sub-area from the MAG transportation network, which encompasses the 101 enforcement zone as well as the adjacent area. In this study, the sub-area was extracted by using the multi-class sub-area analysis, which is usually employed to perform a more detailed investigation of traffic patterns within a sub-area. Specifically, the multi-class sub-area analysis is used to extract the selected sub-area network and to regenerate OD matrix of the sub-area by using the traffic flow loaded from traffic assignment method that users choose.

Figure 38 shows the multi-class sub-area analysis procedure in TransCAD. The user equilibrium traffic assignment technique being used in MAG was applied to the sub-area analysis, and the modified BPR delay functions shown in Table 36 were used. In addition, the exclusive set was applied to each mode (class). For example, heavy truck (i.e., MDHTRK) trips should not be loaded to the high occupancy vehicle (HOV) lane. Although MAG is currently not using passenger car equivalent (PCE) for any mode, we adjusted heavy truck trips by using PCE 1.5, which is utilized for trucks and buses in HCM (Transportation Research Board 2000).

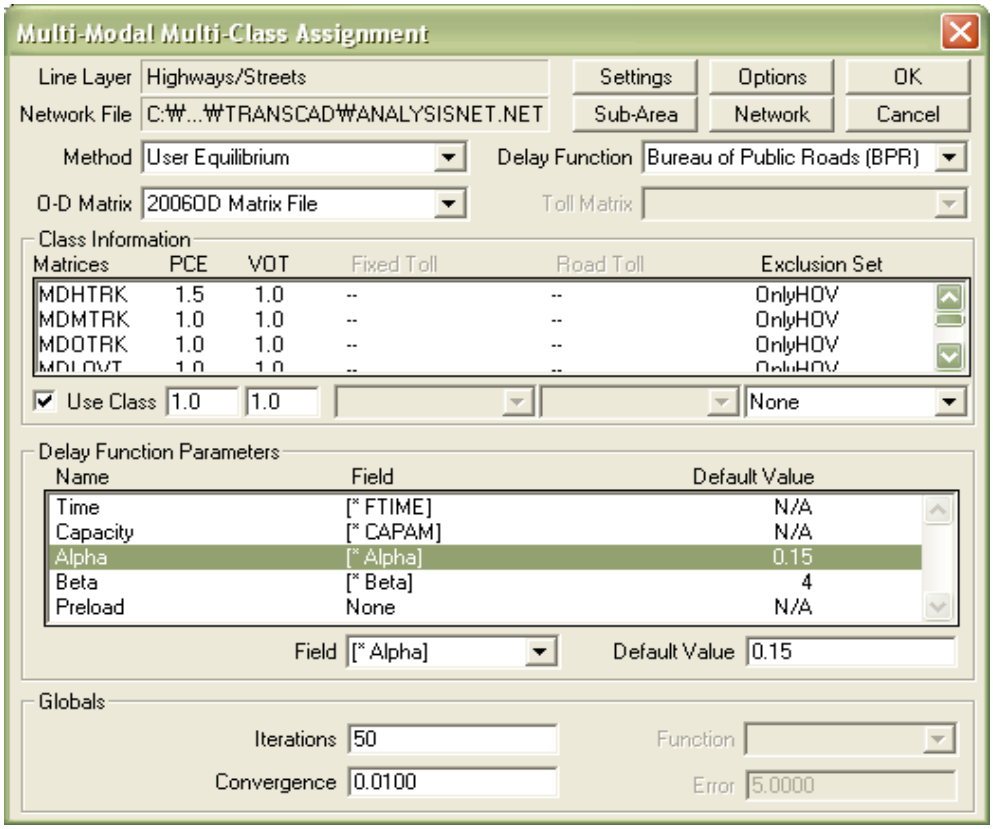

Figure 38: Multi-Class sub-area analysis procedure

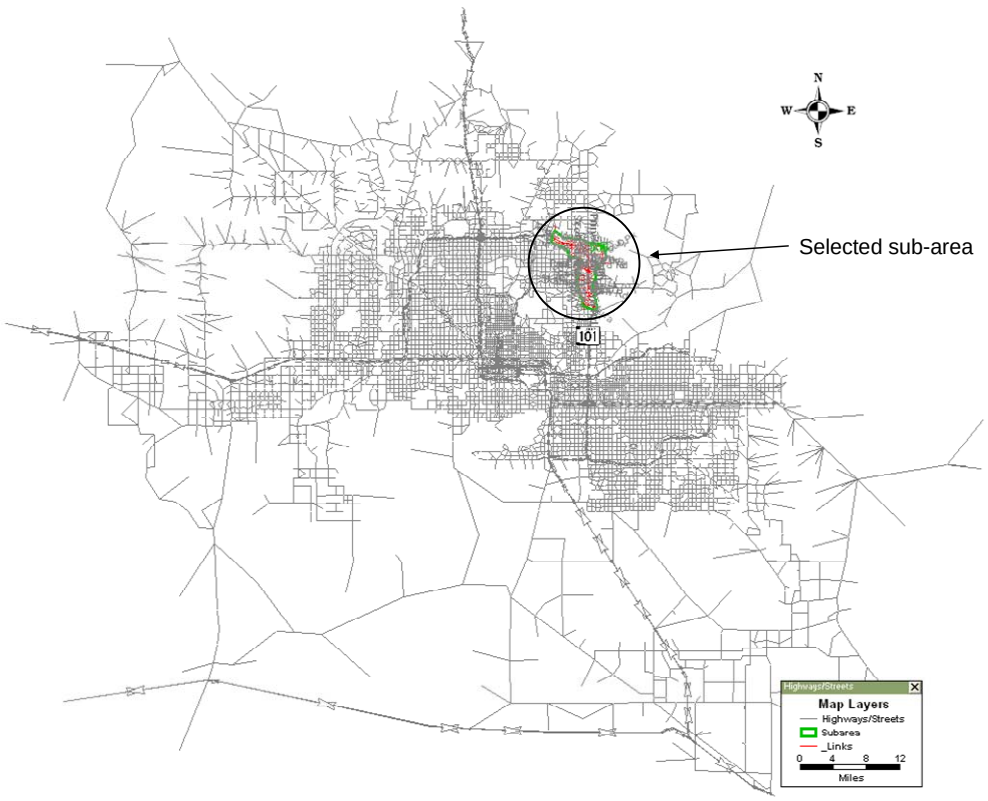

Figure 39: Selected sub-area

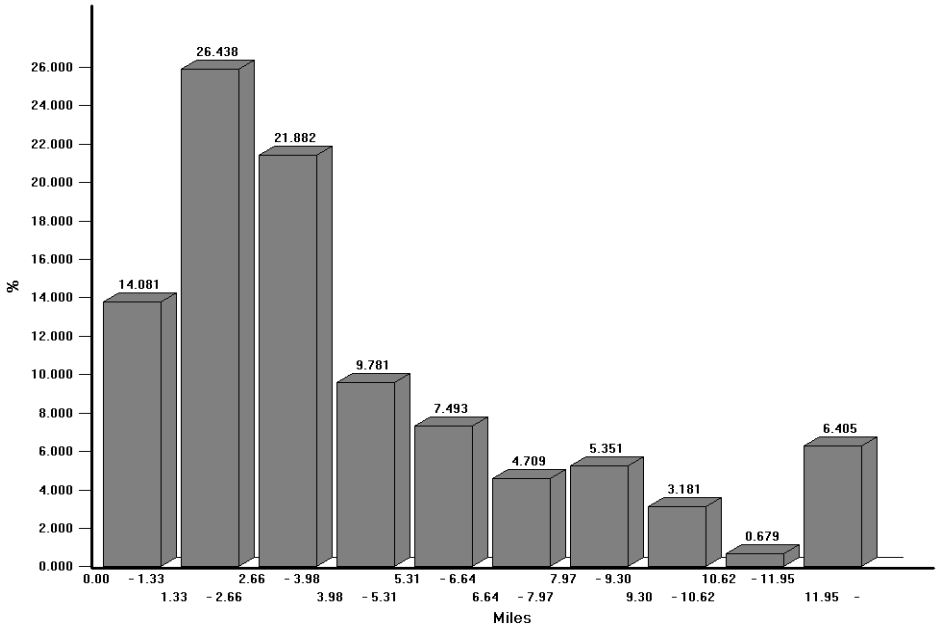

Figure 40: Trip length distribution of non-peak trips within sub-area

Figure 39 shows the selected sub-area in the MAG highway network, while Figure 41 shows the extracted sub-area network, which encompasses the 13-mile stretch of the Loop 101 segment including the enforcement zone as well as adjacent arterials that can be used

as alternative routes for the Loop 101 in Scottsdale. A total of 231,136.43 trips were estimated for the sub-area during six non-peak hours, which is 4.5% of total 5,099,363.45 trips in the MAG area during six non-peak hours. Figure 40 shows the trip length distribution (TLD) of the trips associated with the sub-area. The TLD is also created by using the shortest path matrix based on the physical length. The average trip length during non-peak period was 4.27 miles and standard deviation for the trip length was 3.22 miles.

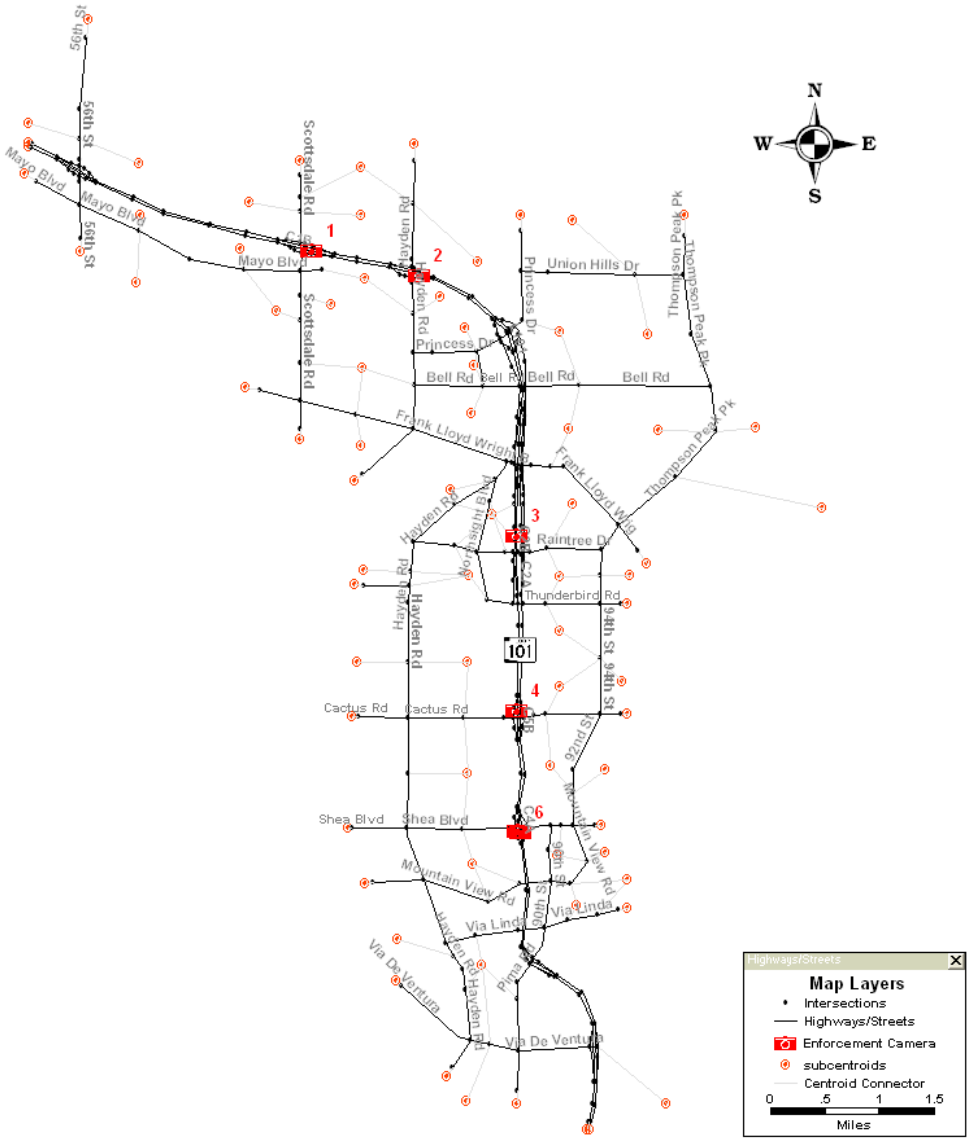

Figure 41: Extracted Sub-area Network (75 TAZs)

5.2.3 Additional Input Data

In addition to transportation network and demand data, the observed traffic volume and speed data that was collected from within the enforcement zone were used to validate the output data of microscopic traffic simulation tool or to create the input parameters of the

tool. Also, the information of traffic incidents that occurred within the enforcement and comparison zones during the *program* period was used to create incident input data. In the following subsections, the descriptive statistics for the additional input data are described in detail.

5.2.3.1 Speed and Traffic Volume Data

In order to validate the simulation runs' results, the traffic volume and speed data collected from the 8 reference sites during the *before* period were used (see Table 37). The middle of the day (24 hours) was consistently used (i.e., 4/14/2005; 4/20/2005; 6/28/2005; 1/5/2006) in order to reduce the variance from the different measurement dates.

Table 37: Description of the eight validation sites for the *before* period

ID	Direction	Location	Measurement date		
1	NB	CACTUS RD & SHEA BLVD	4/13/2005	4/14/2005	4/15/2005
2	SB	CACTUS RD & SHEA BLVD	4/13/2005	4/14/2005	4/15/2005
3	NB	RAINTREE DR & CACTUS RD	4/19/2005	4/20/2005	4/21/2005
4	SB	RAINTREE DR & CACTUS RD	4/19/2005	4/20/2005	4/21/2005
5	NB	SCOTTSDALE RD & PIMA/PRINCESS DR	6/27/2005	6/28/2005	6/29/2005
6	SB	SCOTTSDALE RD & PIMA/PRINCESS DR	6/27/2005	6/28/2005	6/29/2005
7	WB	SCOTTSDALE RD & HAYDEN RD	1/4/2006	1/5/2006	
8	EB	SCOTTSDALE RD & HAYDEN RD	1/4/2006	1/5/2006	

Only the traffic volume and speed data collected during the MAG non-peak six hours (09:00 AM–15:00 PM) were analyzed. In addition, we again used the concept of the LOS in order to eliminate the oversaturated regime. The 70 mph speed was used as the free flow speed for determining the LOS, and the LOS A, B, C, and D are selected based on the given criteria in Table 13 (i.e., 'speed for LOS D: 62.2 mph' was used).

Table 38: Summary statistics for speed by reference site (mph)

Site ID	Mean	Std.dev	Min.	Median	Max.	n
1	72.02	4.50	62	72	78	52
2	73.33	2.64	67	73	79	72
3	73.04	3.39	66	73	79	72
4	75.68	2.99	70	75	82	72
5	70.07	3.69	63	69	77	72
6	71.01	2.67	66	71	78	72
7	72.64	4.22	64	72	82	72
8	71.62	3.79	62	72	78	69

The descriptive statistics for the speed data are summarized in Table 38, in which an individual speed data observation is the aggregated mean speed in each lane during 15 minute intervals. The traffic flow rates (vehicle/lane/hour) for each reference site that was

collected during the same analysis period are summarized in Table 39, which are also summarized by the aggregated flow rate in each lane during the same 15 minute intervals. The aggregated mean speeds are summarized in Table 40. Note that the mean speeds in Table 38 and Table 40 are slightly different than those in Table 12 and Table 14 due to the different analysis period (i.e., 9:00 AM –15:00 PM).

Table 39: Summary statistics for traffic flow rate by reference site (veh/lane/hr)

Site ID	Mean	Std.dev	Min.	Median	Max.	n
1	1321.2	148.3	988	1350	1556	52
2	1409.4	249.3	972	1436	1904	72
3	1216.4	171.0	852	1256	1500	72
4	1404.7	241.4	904	1476	1768	72
5	1109.4	201.1	584	1170	1568	72
6	1032.5	243.2	632	998	1628	72
7	996.8	209.6	708	940	1596	72
8	1160.1	218.4	712	1196	1708	69
Average	1202.4	261.8	584	1208	1904	553

In addition to the speed and flow rate data during the *before* period for validation, the speed data collected during the *program* period were re-analyzed for creating the speed distribution input parameter of microscopic simulation. Among the speed data collected from the enforcement zone during the *program* period, which were described in '3.2 Changes in the Mean Speed' on page 34, only 922 intervals collected during the study period (i.e., 9:00 AM –15:00 PM) were extracted as shown in Table 40.

Table 40: Summary statistics for the speed (mph) during the before and program periods

Period	Mean	Std.Dev.	Min	Median	Max	N
Before	72.45	3.84	62	72	82	553
Program	64.21	1.46	62	64	69	992

By using the speed data described in Table 40, empirical cumulative distribution of speeds during the both periods was generated as shown in Figure 42. Note that the median speed during the *before* period was 72 mph, while the median speed during the *program* period was 64 mph. In this analysis, the vehicles' speeds during the *before* and *program* periods were used for developing the desired speed distribution. The desired speed is the speed which would be maintained on a roadway given no impedance from other vehicles (Toledo et al. 2007; Toledo et al. 2005; Wicks and Lieberman 1980). If the time headway between the subject vehicle and leading vehicle is large enough (e.g., 1.15 sec –1.75 sec), the subject vehicle will start to accelerate to achieve its desired speed. If the current speed is higher than the desired speed, the vehicle will decelerate to the desired speed. Since desired speeds are assumed to vary across the driving population (i.e., some drivers tend to travel faster than others, while others are more conservative), a

vehicle's desired speed in the simulation model was assigned by using the empirical cumulative distribution function (CDF) for the observed mean speed shown in Figure 42.

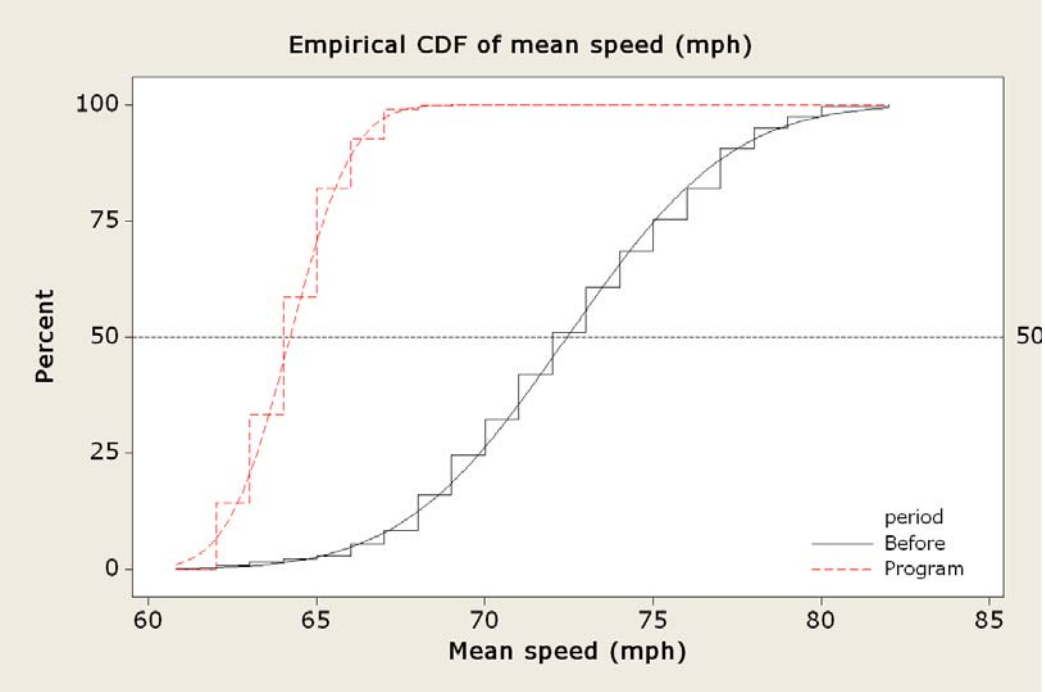

Figure 42: Empirical CDF of mean speed during the before and program period

5.2.3.2 Incident Data on Loop 101

In addition to the speed and traffic flow rate data, the information of freeway incidents that occurred on the comparison and enforcement sections during the *program* period (see Figure 43) were analyzed in order to develop a more specific highway incident simulation scenario.

- Comparison section: MP 6 – MP 10.3 (Bethany Home Road to Peoria Avenue section)
- Enforcement section: MP 34.5 – MP 42.4 (Tatum Blvd to Via de Ventura section)

Since the highway log file provided by ADOT only includes the duration of incidents as well as the duration of recurring events, the log data for the recurring events were eliminated. Also, the events that were not categorized as incident/accident events were excluded for analysis (i.e., road maintenance, road conditions, obstruction hazards, lane restrictions, information, and traffic equipment status categories were excluded).

Consequently, all possible scenarios due to incidents were analyzed. The remaining 477 incidents revealed mean and median time durations of 94 and 68 minutes respectively as shown in Table 41.

Table 41: Summary statistics for incident duration (minutes)

Section	Mean	Std.Dev.	Min.	Median	Max.	N
Comparison	93.17	94.48	14	69	787	191
Enforcement	94.92	99.90	15	68	797	286
Total	94.22	97.67	14	68	797	477

(1) Enforcement zone: MP 34.51– MP 41.06 (Approximately 6.5 miles)
(2) Comparison zone: MP 3.5 – MP 10 (6.5 miles)

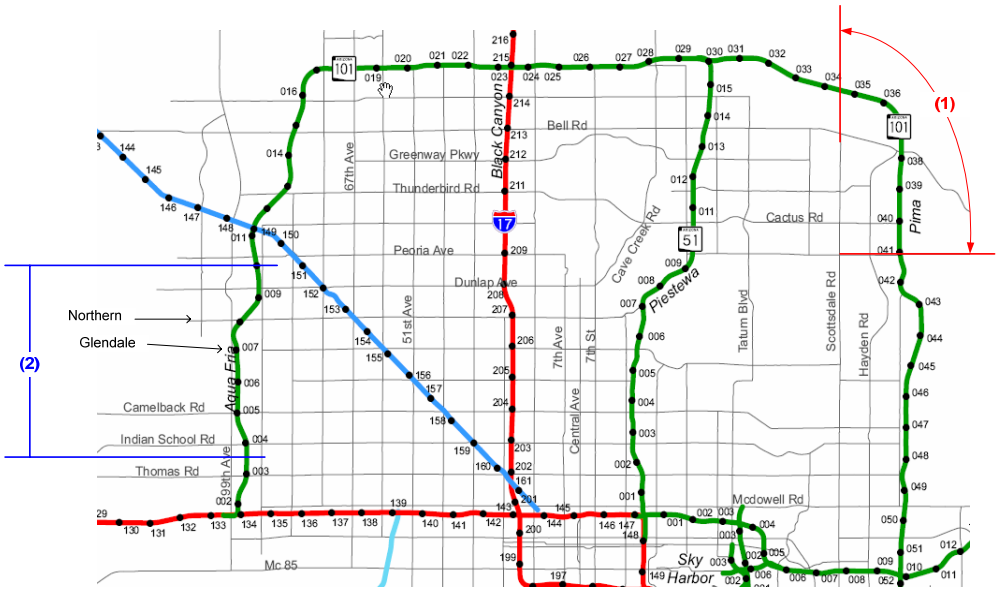

Figure 43: Enforcement zone and comparison section

Although the analyzed median incident duration is relatively small because the incident data includes all freeway incidents rather than only major freeway incidents, the distribution of incident duration is highly skewed (see Figure 44) as investigated in the previous studies (Skabardonis et al. 1996; Ullman and Ogden 1996). In other words, most incidents last considerably less than the average duration.

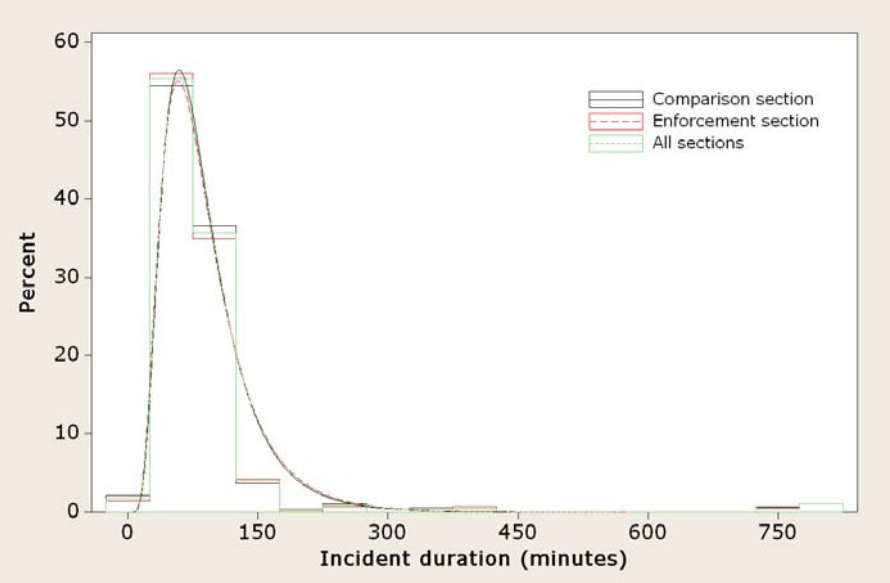

Figure 44: Histogram of incident duration (minutes)

5.2.4 Model Validation

In this study, TransModeler (www.caliper.com) was used as a microscopic traffic simulation tool, in which the movement of vehicles is determined by various driver behavior models including car-following and lane-change models (Caliper 2006a; Caliper 2006b; Yang and Morgan 2006). TransModeler is a path-based model, indicating that every vehicle has a habitual path before departure which can be determined by one of the route choice models. Although a modified multinomial logit model such as the path-size logit model can be applied for modeling the route choice behavior, the stochastic algorithm (with 10% perturbation) was used in this study due to the lack of information for logit parameters.

Therefore, it is important to obtain reliable travel times for each segment before running simulation since the route choice models use the generalized path costs, which is a function of individual segment travel time. Although a static traffic assignment can be used as one alternative for estimating segment travel time, multiple simulations with feedback were used in this study because a static traffic assignment cannot capture the stochastic drivers' behavior and the analysis network was modified for microscopic simulation. The feedback results were also used to validate the simulation model by comparing the simulation outputs to the observed speed and traffic flow rate data. In the next subsections, the feedback procedure and results are described and the validation results are provided.

5.2.4.1 Feedback Results

When running multiple simulations with feedback, the travel times from previous simulations are used as inputs to the route generation and choice models of subsequent runs. The segment travel time for the iteration i+1 is:

$$X_{i+1} = (1-\alpha_i) X_i + \alpha_i f(X_i), \tag{72}$$

where X_i is segment travel time input to the ith feedback run, $f(X_i)$ is segment travel time output from the ith feedback run, and α_i is a weight used to obtain X_{i+1}. In order to determine the weighting factor α_i, the method of successive average (MSA) was used:

$$\alpha_i = \frac{1}{i+1}. \tag{73}$$

For the segment travel time for the first run, the free-flow travel time was employed, and a 130-minute non-peak simulation period (9:50 AM–12:00 PM) was used, but only a 120-minute period after 10-minute warming-up period was analyzed for testing convergence. All simulation runs were based on the base condition (i.e., with the speed distribution during the *before* period; see Figure 42).

- Simulation Period: 9:50 AM–12:00 PM (130 minutes)
  - Analysis Period: 10:00 AM–12:00 PM (120 minutes)
  - Warming-up Period: 09:50 AM –10:00 AM (10 minutes)

Table 42 shows the simulation output and percent change in vehicle miles traveled (VMT) and vehicle hours traveled (VHT) for each feedback run during the 120-minute analysis period:

- VMT: the sum total distance (miles) traveled by all vehicles that complete or incomplete their trips during the analysis period
- VHT: the sum total travel time (hours) experienced by all vehicles that complete or incomplete their trips during the analysis period

Table 42: Simulation output and percent change in output for each feedback run

Feedback	Simulation output		Percent change in output	
	VMT (miles)	VHT (hours)	VMT (miles)	VHT (hours)
1	283709.17	12552.61		
2	292534.87	11367.59	3.11%	-9.44%
3	291797.00	10991.39	-0.25%	-3.31%
4	292428.45	10659.14	0.22%	-3.02%
5	292060.81	10467.26	-0.13%	-1.80%
6	291496.56	10272.95	-0.19%	-1.86%
7	292143.96	10290.45	0.22%	0.17%
8	292471.51	10302.56	0.11%	0.12%
9	293435.69	10325.98	0.33%	0.23%
10	292510.23	10344.43	-0.32%	0.18%
11	292415.53	10179.10	-0.03%	-1.60%
12	293843.21	10408.72	0.49%	2.26%
13	292539.11	10180.92	-0.44%	-2.19%
14	293857.74	10220.43	0.45%	0.39%
15	292841.90	10268.33	-0.35%	0.47%
16	291932.36	10270.66	-0.31%	0.02%
17	292650.94	10237.98	0.25%	-0.32%
18	293780.54	10291.67	0.39%	0.52%
19	293635.87	10231.91	-0.05%	-0.58%
20	294212.54	10142.21	0.20%	-0.88%
21	293327.48	10136.40	-0.30%	-0.06%
22	292414.41	10112.79	-0.31%	-0.23%
23	293957.33	10134.29	0.53%	0.21%
24	293374.47	10064.72	-0.20%	-0.69%
25	293150.93	10188.16	-0.08%	1.23%
26	292441.04	10249.80	-0.24%	0.61%
27	293161.98	10311.57	0.25%	0.60%
28	291915.26	10288.73	-0.43%	-0.22%
29	292261.86	10348.17	0.12%	0.58%
30	292679.53	10235.47	0.14%	-1.09%

The results of feedback runs (conducted by using the distribution of the desired speeds during the *before* period) were repeatedly compared to the observed speed and traffic volume data collected during the *before* period in order to search for reliable simulation input data. As a result of the repeated comparisons, a final set of 30 feedback runs were obtained, in which the percent change in simulation outputs such as vehicle hours traveled (VHT) and vehicle miles traveled (VMT) were converged to 0 after several feedback runs as shown in Figure 45 (next page).

Note that VHT decreased with feedback runs, while VMT increased with feedback runs. The results indicate that the shortest paths based on free-flow travel time are not optimal in minimizing drivers' travel time. In addition, the results suggest that drivers tend to

choose the path having shortest travel time, although the travel length of the chosen path can be longer than that of the shortest path based on free-flow travel time. Therefore, the feedback results show that drivers determine their habitual travel time based on both free-flow travel time and the updated segment travel time from their previous experience as they do in the real world.

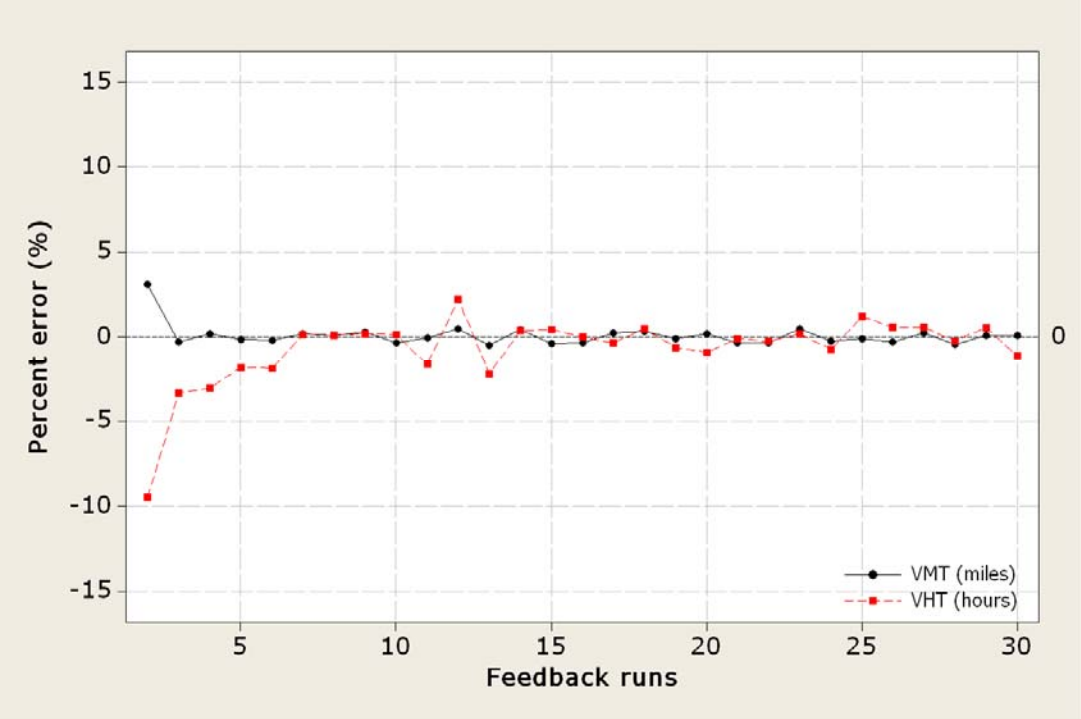

Figure 45: Percent change in simulation outputs by feedback run

5.2.4.2 Model Validation

Validation is the task of ensuring that the model behaves the same as the real system, which is a common procedure in simulation modeling (Horiguchi and Kuwahara 2005; Kelton et al. 2004). In this study, the speed and traffic flow rate outputs for the reference sites simulated from the last feedback run (the 30th run) were compared to the corresponding observed data. The analysis results from all feedback runs are summarized in Table 44 to Table 49.

The results show that the root-mean-square error (RMSE) of the simulated speed is 2.12 mph to 2.31 mph, and the RMSE of the simulated traffic flow is 82 veh/lane/hr to 104 veh/lane/hr, which provides a good fit between the observed and simulated data. In addition, the paired *t* test results revealed that the mean difference between paired observations was insignificant at $\alpha=0.05$ (see Table 43). Consequently, the input data of

the 30th simulation feedback were used for analyzing the effect of SEP on transportation system.

Table 43: Paired *t*-test results for comparing simulated and observed data

	Difference in Mean	T-value (associate p-value)	95% CI for mean difference
Speed	0.83	1.05 (0.328)	(-1.04, 2.704)
Flow rate	24.94	0.76 (0.475)	(-53.12, 33.01)

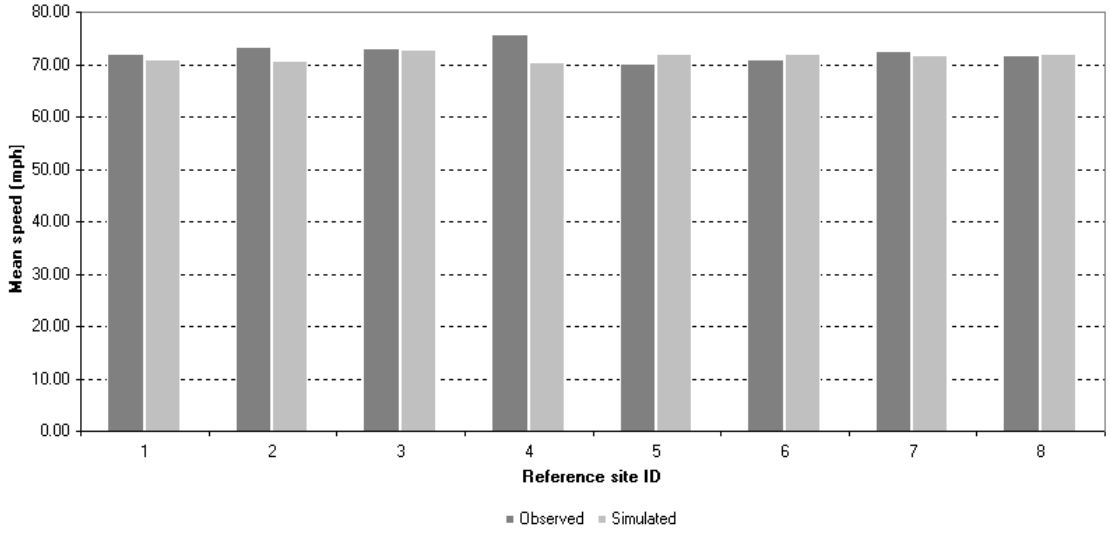

Figure 46: Comparison of observed and simulated speeds at eight reference sites

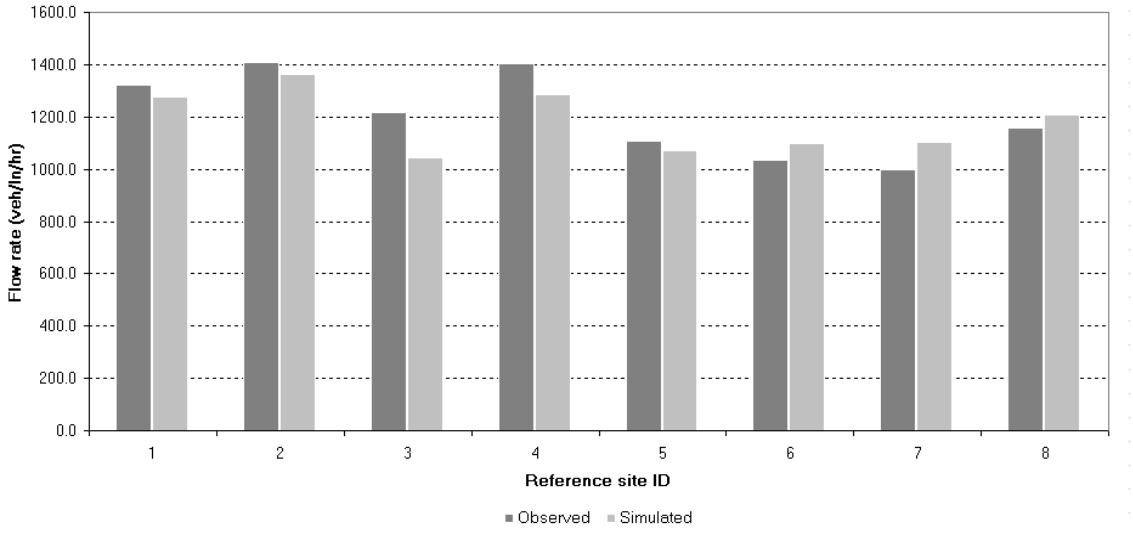

Figure 47: Comparison of observed and simulated traffic flow at eight reference sites

Table 44: Speed comparison by feedback run (feedback 1–10)

Site ID	Simulated speed (mph) by feedback run										Observed speed
	1	2	3	4	5	6	7	8	9	10	
1	70.81	71.07	71.52	70.94	71.27	70.94	70.95	71.07	70.87	71.03	72.02
2	71.09	70.66	70.95	70.85	70.80	70.73	70.92	70.99	70.62	71.33	73.33
3	72.65	72.80	72.88	72.88	72.93	72.93	72.91	72.87	72.93	72.87	73.04
4	70.54	70.74	70.69	70.55	70.70	70.50	70.66	70.58	70.49	70.48	75.68
5	72.24	71.95	72.19	71.94	72.12	71.96	72.18	72.01	71.92	72.13	70.07
6	72.29	72.22	72.05	72.37	72.21	72.12	72.07	72.13	71.97	71.95	71.01
7	72.32	71.81	72.12	71.98	71.79	71.69	72.08	71.84	71.94	71.91	72.64
8	71.91	71.86	71.87	71.87	71.89	71.96	71.75	72.04	71.95	71.91	71.62
Mean	71.73	71.64	71.78	71.67	71.71	71.61	71.69	71.69	71.59	71.70	72.43
MAE	1.63	1.62	1.49	1.62	1.59	1.66	1.56	1.61	1.62	1.55	
MAPE	2.23	2.21	2.04	2.22	2.17	2.26	2.13	2.19	2.21	2.11	
RMSE	2.22	2.19	2.14	2.22	2.19	2.25	2.18	2.19	2.25	2.17	
RMSPE	2.99	2.94	2.88	2.99	2.94	3.03	2.94	2.94	3.02	2.92	

Table 45: Speed comparison by feedback run (feedback 11–20)

Site ID	Simulated speed (mph) by feedback run										Observed speed
	11	12	13	14	15	16	17	18	19	20	
1	70.84	71.01	71.05	70.77	70.87	70.77	70.83	70.75	70.90	70.92	72.02
2	71.17	70.54	70.79	71.07	70.89	70.63	71.03	71.06	70.75	70.81	73.33
3	72.85	72.84	72.86	72.80	72.70	72.65	72.84	72.64	72.90	72.67	73.04
4	70.54	70.40	70.54	70.47	70.58	70.63	70.52	70.66	70.44	70.56	75.68
5	72.08	72.15	71.89	72.04	71.75	72.10	71.94	72.14	72.14	72.07	70.07
6	72.09	72.12	71.95	72.23	72.12	72.07	72.29	71.87	72.11	72.17	71.01
7	71.93	71.97	71.85	71.79	71.68	72.20	72.15	71.87	72.22	71.72	72.64
8	71.71	71.69	71.79	71.94	71.84	71.95	72.02	71.82	71.75	71.98	71.62
Mean	71.65	71.59	71.59	71.64	71.55	71.63	71.70	71.60	71.65	71.61	72.43
MAE	1.57	1.65	1.57	1.66	1.62	1.66	1.61	1.61	1.6	1.69	
MAPE	2.14	2.25	2.14	2.27	2.21	2.26	2.2	2.19	2.18	2.31	
RMSE	2.18	2.31	2.2	2.24	2.19	2.24	2.2	2.17	2.26	2.24	
RMSPE	2.94	3.11	2.95	3.01	2.94	3.01	2.96	2.93	3.04	3.02	

Table 46: Speed comparison by feedback run (feedback 21–30)

Site ID	Simulated speed (mph) by feedback run										Observed speed
	21	22	23	24	25	26	27	28	29	30	
1	70.98	71.08	70.80	71.10	70.63	71.06	71.02	70.87	70.89	70.99	72.02
2	70.68	70.93	70.68	70.74	70.75	71.18	70.69	70.96	70.75	70.75	73.33
3	72.93	72.95	72.83	72.84	72.93	72.87	72.99	72.95	72.86	72.89	73.04
4	70.65	70.45	70.65	70.68	70.69	70.70	70.43	70.50	70.48	70.46	75.68
5	71.64	72.04	72.01	71.97	71.94	72.06	71.91	71.96	72.07	71.94	70.07
6	72.13	72.06	71.97	72.21	72.04	72.03	72.11	71.99	72.15	72.09	71.01
7	71.73	72.05	72.11	71.99	71.76	72.01	72.08	71.90	71.87	71.70	72.64
8	71.91	71.83	71.78	71.74	71.83	71.64	71.88	71.67	71.94	71.93	71.62
Mean	71.58	71.68	71.60	71.66	71.57	71.69	71.64	71.60	71.62	71.59	72.43
MAE	1.59	1.56	1.59	1.57	1.63	1.49	1.59	1.56	1.66	1.65	
MAPE	2.17	2.12	2.16	2.14	2.23	2.03	2.16	2.12	2.27	2.25	
RMSE	2.18	2.22	2.2	2.18	2.2	2.12	2.25	2.21	2.26	2.25	
RMSPE	2.93	2.98	2.96	2.94	2.97	2.84	3.02	2.96	3.05	3.03	

Table 47: Traffic flow rate comparison by feedback run (feedback 1–10)

Site ID	Simulated flow rate (vehicle/lane/hr) by feedback run										Observed flow rate
	1	2	3	4	5	6	7	8	9	10	
1	1225	1243	1234	1258	1257	1257	1262	1254	1262	1269	1321.2
2	1319	1298	1354	1355	1358	1339	1357	1356	1383	1359	1409.4
3	1027	1051	1030	1039	1050	1037	1058	1027	1047	1052	1216.4
4	1275	1266	1272	1282	1284	1276	1286	1288	1313	1287	1404.7
5	1043	1075	1051	1071	1056	1051	1060	1073	1067	1077	1109.4
6	1083	1079	1089	1092	1088	1105	1111	1102	1114	1114	1032.5
7	1051	1126	1094	1117	1091	1084	1078	1109	1095	1089	996.8
8	1181	1192	1196	1214	1190	1209	1219	1211	1217	1214	1160.1
Mean	1151	1166	1165	1179	1172	1170	1179	1178	1187	1183	1206
MAE	87.18	92.01	88.68	86.26	79.47	88.55	82.01	86.72	78.10	80.68	
MAPE	7.07	7.58	7.36	7.24	6.63	7.36	6.86	7.28	6.65	6.78	
RMSE	100.27	103.82	100.24	97.32	89.95	97.59	89.51	98.65	88.45	90.35	
RMSPE	8.02	8.56	8.26	8.21	7.47	8.06	7.46	8.30	7.56	7.58	

Table 48: Traffic flow rate comparison by feedback run (feedback 11–20)

Site ID	Simulated flow rate (vehicle/lane/hr) by feedback run										Observed flow rate
	11	12	13	14	15	16	17	18	19	20	
1	1260	1277	1278	1279	1273	1269	1270	1275	1268	1287	1321.2
2	1375	1379	1349	1358	1357	1349	1355	1352	1361	1378	1409.4
3	1049	1071	1056	1056	1064	1055	1052	1075	1046	1070	1216.4
4	1303	1300	1276	1282	1279	1297	1303	1292	1300	1303	1404.7
5	1058	1084	1076	1091	1092	1056	1075	1096	1069	1082	1109.4
6	1109	1111	1091	1102	1090	1092	1101	1116	1108	1104	1032.5
7	1071	1094	1089	1117	1113	1091	1099	1104	1095	1107	996.8
8	1211	1213	1201	1218	1210	1211	1210	1224	1218	1208	1160.1
Mean	1180	1191	1177	1188	1185	1178	1183	1192	1183	1192	1206
MAE	76.93	72.35	77.22	80.26	77.60	79.97	78.26	78.10	81.22	71.26	
MAPE	6.47	6.14	6.42	6.77	6.50	6.70	6.59	6.59	6.85	6.08	
RMSE	86.31	82.14	88.35	92.36	89.40	87.91	87.85	87.06	90.60	82.26	
RMSPE	7.23	7.01	7.30	7.85	7.53	7.36	7.44	7.41	7.66	7.09	

Table 49: Traffic flow rate comparison by feedback run (feedback 21–30)

Site ID	Simulated flow rate (vehicle/lane/hr) by feedback run										Observed flow rate
	21	22	23	24	25	26	27	28	29	30	
1	1276	1276	1276	1271	1275	1259	1275	1270	1279	1276	1321.2
2	1363	1344	1369	1369	1345	1355	1359	1343	1323	1365	1409.4
3	1053	1049	1055	1063	1076	1041	1051	1056	1063	1046	1216.4
4	1300	1287	1299	1300	1283	1281	1280	1282	1266	1286	1404.7
5	1087	1073	1073	1077	1080	1076	1075	1075	1067	1072	1109.4
6	1106	1101	1123	1103	1103	1110	1110	1089	1091	1098	1032.5
7	1099	1094	1083	1102	1104	1100	1101	1086	1085	1102	996.8
8	1210	1215	1221	1213	1211	1209	1214	1206	1202	1206	1160.1
Mean	1187	1180	1187	1187	1185	1179	1183	1176	1172	1181	1206
MAE	75.80	81.60	78.35	76.14	78.80	84.76	82.05	78.39	81.35	79.10	
MAPE	6.40	6.83	6.63	6.44	6.61	7.10	6.90	6.50	6.71	6.66	
RMSE	86.94	91.31	87.77	85.43	87.13	95.44	92.46	88.23	91.23	90.80	
RMSPE	7.38	7.63	7.44	7.28	7.33	7.99	7.78	7.27	7.42	7.64	

5.2.5 Simulation Scenarios

In this study, the simulation scenarios were developed for reflecting two major network states: free-flow (FF) and non-recurrent congestion (NR) states. The former represents the network in the absence of congestion, while the latter represents the network with incident-based congestion only (no recurrent congestion). Two conditions were modeled for each major network state (see Figure 48):

- Free-flow State: *Base* and *SEP* conditions
- Non-recurrent Congestion State: one-lane blockage and two-lane blockage conditions (as a result of crashes)

The two conditions for the FF state were devised to reflect network traffic conditions with and without the SEP since the travel time in the FF state is relatively sensitive to the presence of the SEP. For the NR state, the two conditions were developed to examine the impact of crash severity (and subsequent emergency response) on travel times. So, comparisons of simulation results within the FF state provide information about the impact of the SEP on travel times in the absence of incidents, whereas comparisons across states allow an accounting for non-recurrent congestion events on travel times.

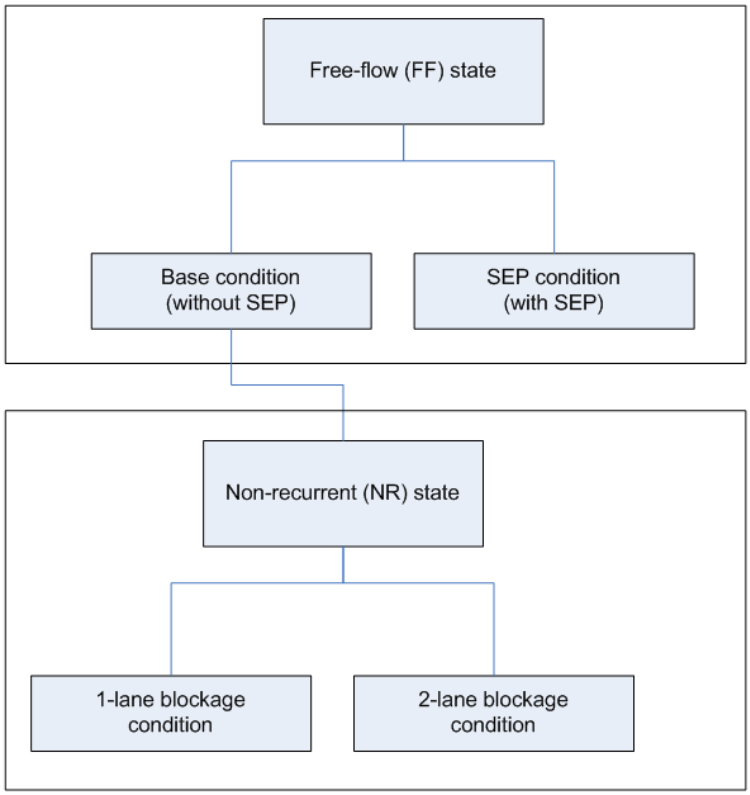

Figure 48: Simulation scenarios

5.2.5.1 Free-Flow State

The FF state represents the network state without any recurrent or non-recurrent congestion. The *Base* condition represents various operational performance measures expected during the before period, while the SEP condition represents the operational performance measures expected during the program period. All parameter settings for the *Base* condition were set to equal those for the last feedback run described previously.

The SEP condition is also based on the same simulation parameters, but the empirical distribution of the desired speed for the *program* period was applied to an appropriate subset of segments within the enforcement zone. Since the assumption that all segments within the enforcement zone will be equally influenced by the speed enforcement cameras is incongruous with a limited spatial spillover effect revealed in previous studies (Champness and Folkman 2005; Ha et al. 2003; Hauer et al. 1982; Hess 2004), a 0.56-mile influence area assumption was devised based on the exponential decay model proposed by Hauer (Hauer et al. 1982).

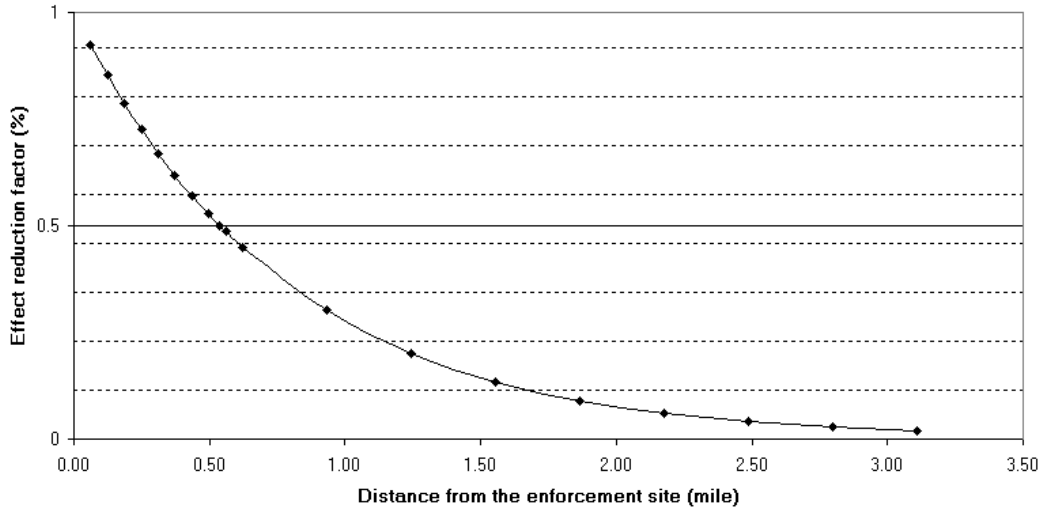

Figure 49: Effect reduction by distance [Source: Hauer et al. 1982]

The exponential decay model shows that the effect of enforcement on speed reduction is reduced by $e^{-0.8L}$ at L kilometer downstream from the enforcement site (see Figure 49). Thus, the effect of enforcement on speed reduction is reduced by half for every 0.56 mi (0.9 km). Although the model suggests that the different desired speed distributions for each L kilometer downstream from the enforcement site are needed to simulate precisely the spatial spillover effects, it is difficult to estimate all desired speed distributions unless rigorous field studies are conducted. Therefore, we aggregated all spatial spillover effects into the 0.56-mile influence area by applying the empirical distribution of the desired speed during the program period to the 0.56-mile influence area. However, it should be noted that this assumption is an approximation.

5.2.5.2 Non-recurrent Congestion State

The NR state reflects the network state with only non-recurrent congestion, assumed to be caused by crashes that occur during the non-peak period. The NR conditions are simulated to capture the impact of crash occurrence on various operational performance measures, which may be converted into travel time impacts. Since it is not possible to simulate all possible crash scenarios, we used the two aforementioned types of NR congestion conditions (i.e., *one-lane blockage* and *two-lane blockage*). For each condition, the median incident duration (68 min: 10:00 AM–11:08 AM) was used as the blocking duration, since the distribution of incident duration is highly skewed to the right as shown in previous studies (Skabardonis et al. 1996; Ullman and Ogden 1996). In addition, each condition was simulated at the six enforcement camera sites (three sites per direction) in order to reflect the level of influence across sites within the enforcement zone.

The NR conditions have the same parameters as the *Base* condition, except the parameter associated with updating path en route. The updating path behavior en route was modeled to represent more realistic driver behavior in the NR conditions. As in a previous study (Chu et al. 2004), a total of 20% of the drivers were within the informed driver group, who will update their paths en route when experiencing unexpected delay. This percentage has been noted as an optimal level of market penetration for traveler information provision (Oh and Jayakrishnan 2002).

5.2.5.3 Additional Information

A total of 180 simulation runs were conducted with different random number seeds to establish a distribution of the simulation output results: 60 simulation replications for the FF states (30 replications for each condition) and 120 simulation replications for the NR states (60 replications for each condition). The 130-minute simulation period (9:50 AM–12:00 PM) was assumed to capture the delays during the incident clearance time as well as the recovery time. The first 10 minutes of the simulation period were used as a warming–up (burn in) period, thus the simulation output data obtained from vehicles that departed from their origin before 10:00 AM were not used in the analysis.

5.3 Change in Travel Time Distribution

5.3.1 Preliminary Analysis

The changes in travel time distribution were examined in order to reveal how the distribution of travel time shifted as a result of the SEP. Only trips that thoroughly passed all 101 segments within the sub-area were extracted for analyzing the change in the travel time distribution, eliminating drivers (and their associated travel times) with truncated trips. The selected

trips are divided by travel direction: 'northbound trips' from Via De Ventura to 56th Street on Loop 101 and 'southbound trips' from 56th Street to Via De Ventura on the Loop 101.

Table 50 shows summary statistics for the travel time of the selected trips by direction. The mean travel time was greater in the SEP and NR conditions than in the *Base* condition, and the measures for dispersion such as the standard deviation, interquantile range, and range of the travel time in the NR conditions were greater than those in the *Base* condition. However, the travel time dispersion in the SEP condition was less than that in the *Base* condition, indicating that the SEP may lead to reduced travel time uncertainty.

Table 50: Summary Statistics for the Travel Time of the Selected Trips (minute)

Direction	Simulated Network State	N	Mean	Std. Dev.	Min.	10%th Percentile	99%th Percentile	Max.	IQR	Range
Northbound Trips	Base	53104	10.71	0.29	9.69	10.34	11.40	11.98	0.40	2.30
	SEP	52221	10.84	0.26	9.78	10.49	11.41	11.99	0.37	2.22
	1-lane Blockage Crash	52653	10.91	0.37	9.69	10.47	12.05	12.82	0.46	3.13
	2-lane Blockage Crash	53011	31.93	15.92	10.84	14.87	69.75	74.58	26.71	63.74
Southbound Trips	Base	62127	10.64	0.32	9.63	10.24	11.44	12.15	0.44	2.51
	SEP	61931	10.75	0.29	9.75	10.38	11.44	12.15	0.40	2.40
	1-lane Blockage Crash	62043	11.02	0.83	9.71	10.36	14.65	17.89	0.65	8.18
	2-lane Blockage Crash	58526	20.36	11.51	9.7	11.01	65.68	74.02	11.07	64.32

In order to test the change in travel time distribution, two statistical tests were used. First, the Kruskal–Wallis (KW) tests were conducted to examine the equality of population, which is equivalent to the rank *F* test (Kutner et al. 2005; Washington et al. 2003).

$$H = \frac{12}{n_T(n_T+1)}\sum_{i=1}^{s}\frac{R_i^2}{n_s} - 3(n_T+1), \tag{74}$$

where n_T is the total number of simulated travel times for the selected trips, n_i is the number of observations for the *i*th simulation state, s is the number of simulation states, and R_i^2 is the sum of the ranks from the *i*th scenario. The statistic *H* is approximately χ^2 distributed with the degree of freedom *s*-1 under the null hypothesis (H_o: all samples are drawn from the same population). Second, the Brown-Forsythe (BF) tests were conducted to investigate as to whether or not the variance of travel time in each simulation state is the same (Kutner et al. 2005). Equation (75) shows the BF test, which is insensitive to departures from normality.

$$F_{BF} = \frac{(n_T - s)\sum_i n_i(\bar{d}_{i\cdot}^m - \bar{d}_{\cdot\cdot}^m)^2}{(s-1)\sum_i\sum_j\sum_k (d_{ijk}^m - \bar{d}_{i\cdot}^m)^2}, \tag{75}$$

where d_{ijk}^{m} is the absolute deviations of the t_{ijk}^{d} (the travel time for the *k*th trip for trip direction *m* at the *j*th simulation replication for the *i*th simulation state) about their respective simulation state medians $\tilde{T}_{i\cdot}^{m}$, $\bar{d}_{i\cdot}^{m}$ ($\bar{d}_{\cdot\cdot}^{m}$) indicates an aggregation of the absolute deviations over the *j* index (over the *j* and *i* indexes), and the rest of the notation is as previously stated. Under the null hypothesis (H_0: $\sigma_i^2 = \sigma^2 \ \forall i$), the F_{BF} follows approximately an *F* distribution with $s-1$ and $n_T - s$ degree of freedom. In both tests, the observation unit is the travel time for the *k*th trip for trip direction *m* at the *j*th simulation replication for the *i*th simulation state, and the *Base* condition was considered consistently as the reference group.

Table 51: Results of the BF and KW Tests

Direction	Simulated Network State	*H* (p-value.) H_0: Equal Distribution	F_{BF} (p-value.) H_0: Equal Variance
Northbound Trips	Base	–	–
	SEP	5556.31 (<0.001)	335.21 (<0.001)
	1-lane Blockage Crash	8551.53 (<0.001)	1475.48 (<0.001)
	2-lane Blockage Crash	79548.62 (<0.001)	84871.24 (<0.001)
Southbound Trips	Base	–	–
	SEP	3759.65 (<0.001)	381.33 (<0.001)
	1-lane Blockage Crash	9666.82 (<0.001)	5741.97 (<0.001)
	2-lane Blockage Crash	71393.04 (<0.001)	32794.40 (<0.001)

The test results are summarized in Table 51. Figure 50 to Figure 52 show the cumulative distribution of the travel time in each simulation condition, where the distribution of the travel time in the *Base* condition was compared to those in other conditions. The findings from the preliminary analyses are summarized below:

- The KW and BF test results show not only that the shape of the travel time distribution for the SEP and NR conditions is altered from the *Base* condition, but also that the variance of travel time for each simulation condition is significantly different at α=0.05.
- The distributions of the travel time in the SEP and NR conditions were shifted to the right, leading to an increase in the mean travel time.
- However, it is noteworthy that the right tails of the distribution of travel time in the *Base* and SEP conditions converged at a similar location, while the right tails of the distribution of travel time in the *Base* and NR conditions did not converge at a similar location—the long-tail distribution in the NR conditions.
- These exploratory data analysis results show that the drivers in the left tail of the travel time distribution (i.e., faster drivers) are more likely to be affected by the SEP than those on the right side of the travel time distribution, while the NR conditions changed the overall shape of the travel time distribution.

In the next subsection, the changes in travel time distribution are statistically tested, and the results are discussed in detail.

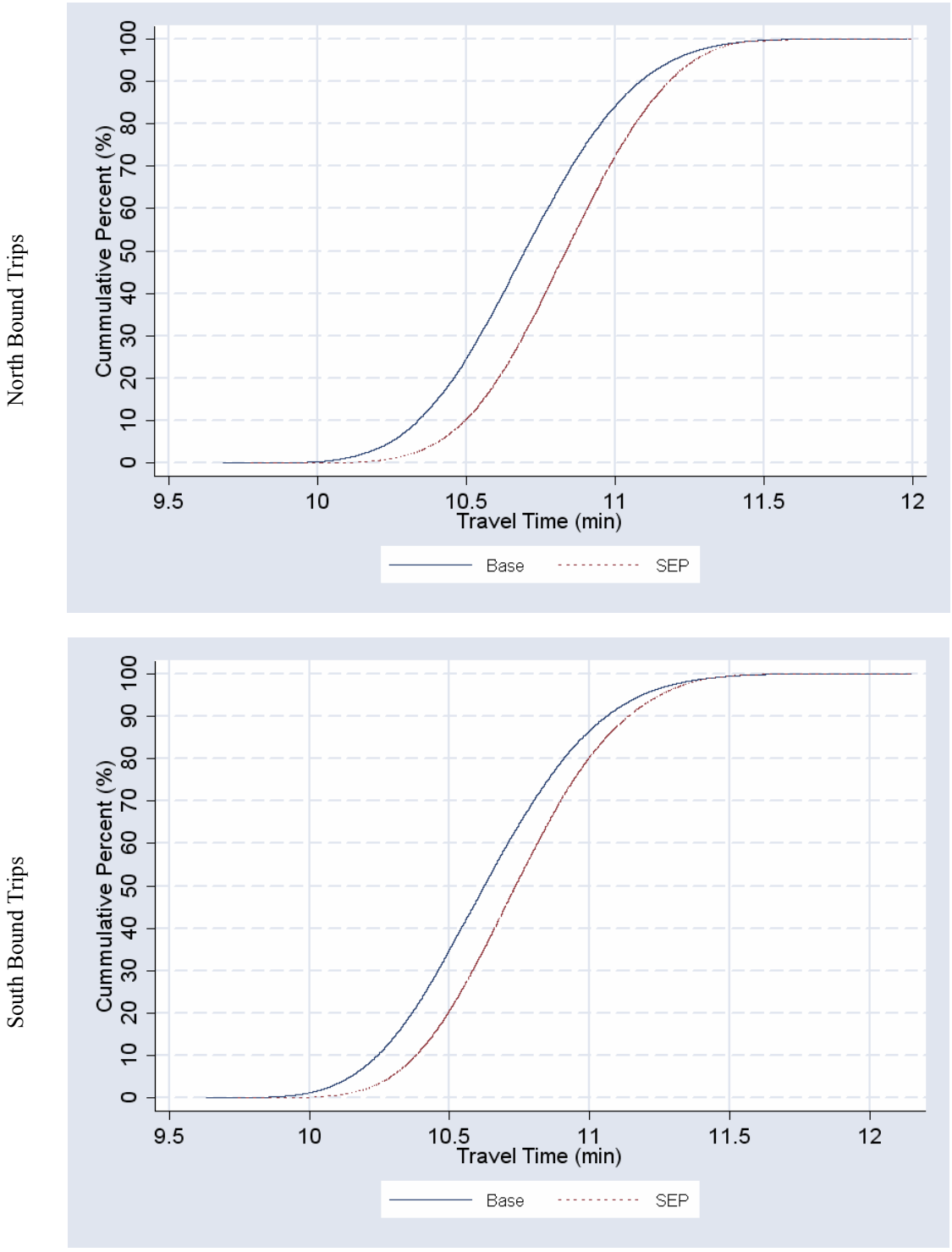

Figure 50: Change in travel time distribution (Base vs. SEP)

North Bound Trips

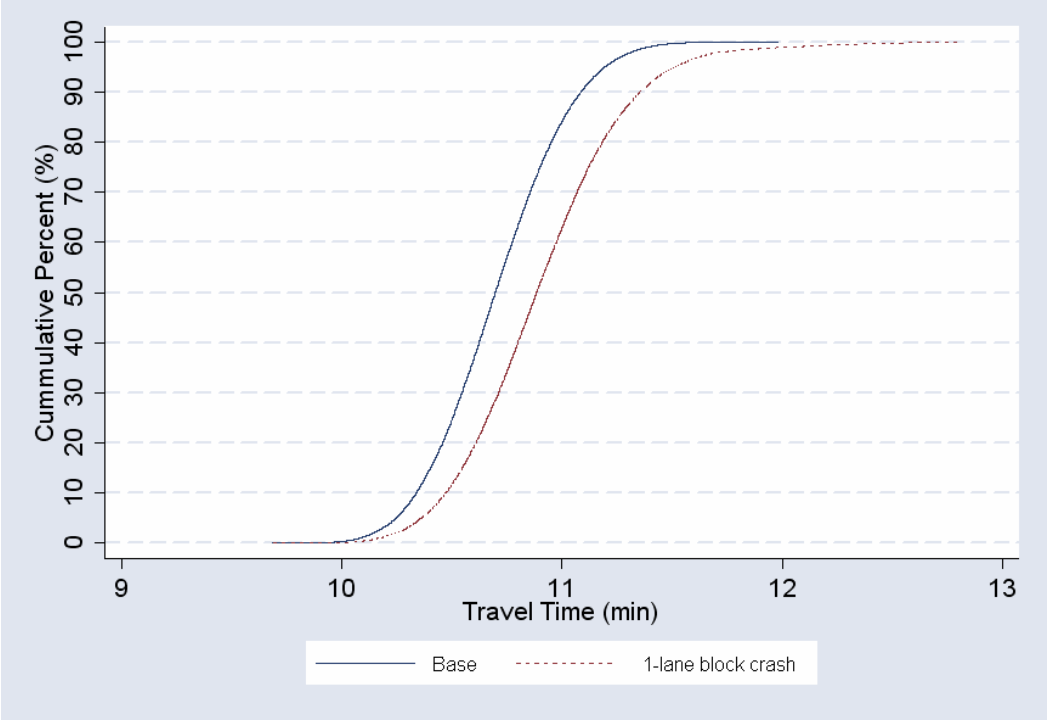

South Bound Trips

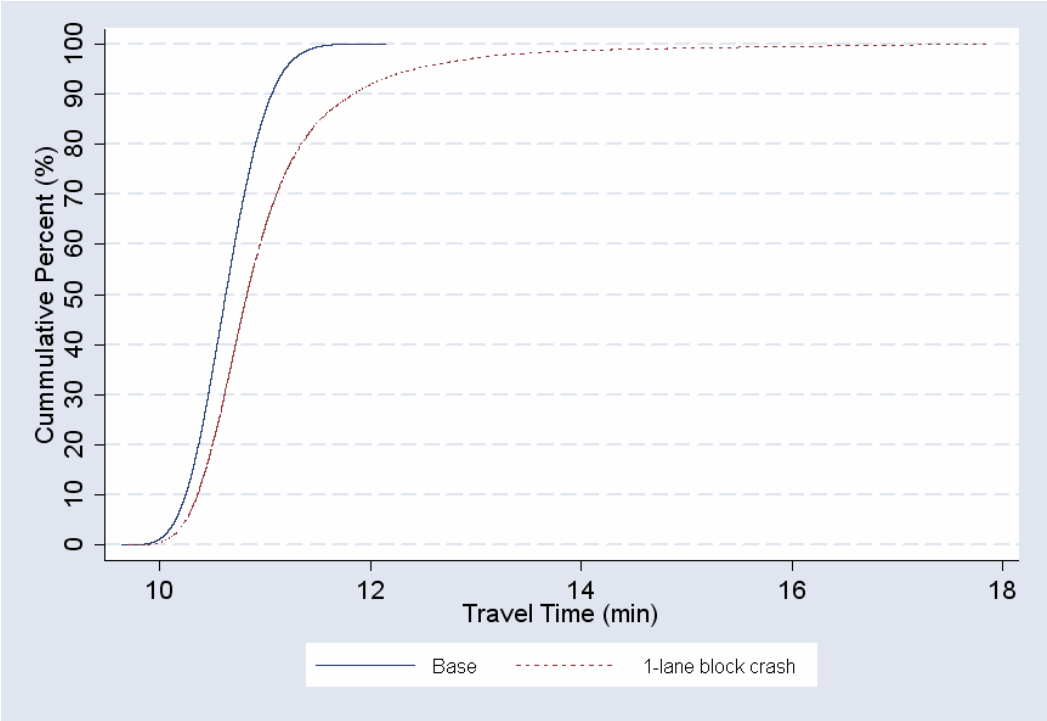

Figure 51: Change in travel time distribution (Base vs. one-lane blockage)

North Bound Trips

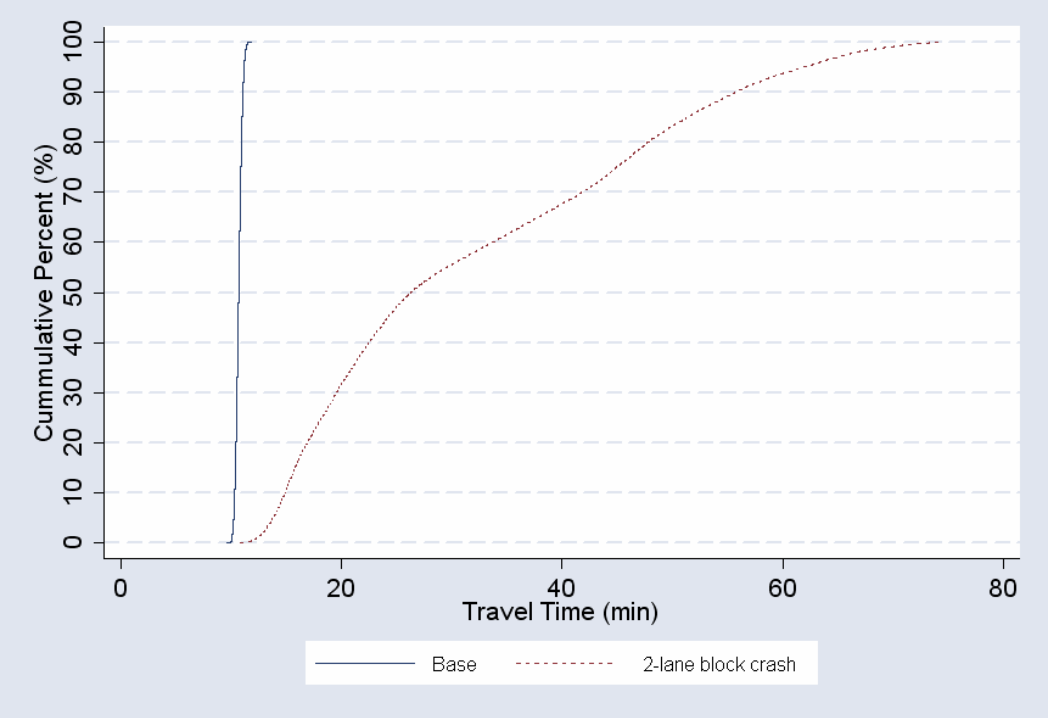

South Bound Trips

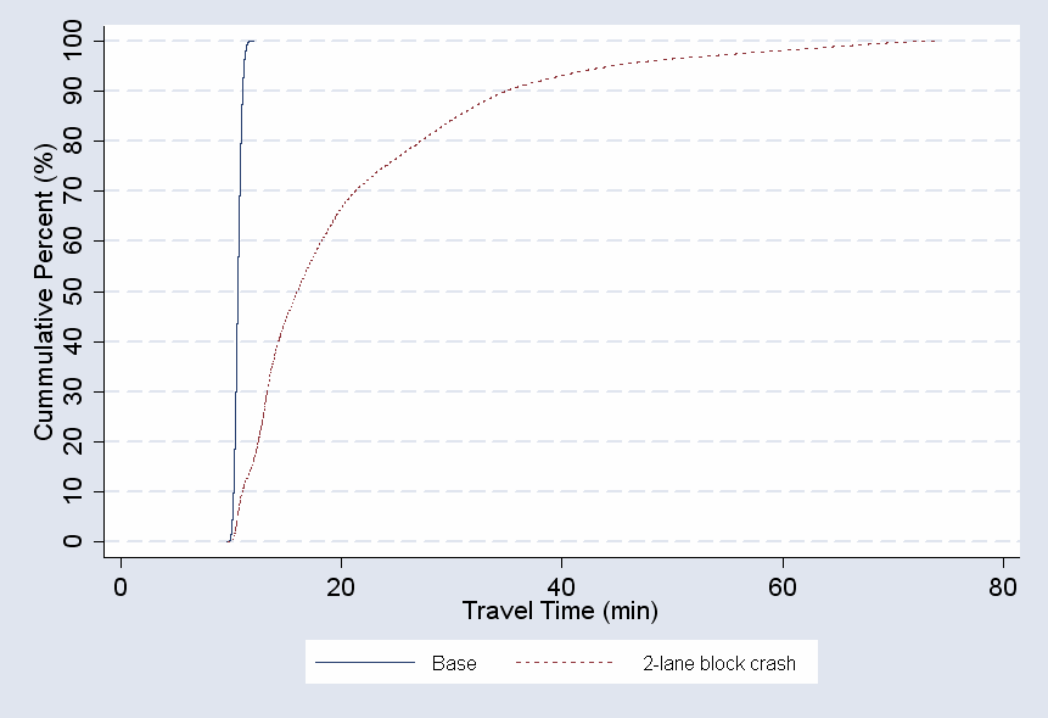

Figure 52: Change in travel time distribution (Base vs. two-lane blockage)

5.3.2 Travel Time Variation by Simulation Scenario

The changes in the tails of the travel time distributions were examined by comparing the location of the percentile values of the travel time in each simulation condition. Analyzing the change in travel time distribution in the right tail is relatively common because a traveler's expected travel cost is especially sensitive to the right tail of the travel time distribution—being late is more undesirable than being early (FHWA 2007; Small et al. 2005). Thus, a change in travel time distribution in the right tail can be more important than that in the opposite tail in measuring travel time uncertainty. However, the explanatory data comparison shown in Figure 50 to Figure 52 illustrates that the change in the travel time distribution between the *Base* and SEP conditions might occur more significantly in the left tail. Consequently, we used the 10th and 99th percentile travel time values in the *Base* condition as the reference values for investigating the change in travel time distribution on both tails.

Specifically, the 10th percentile travel time in the *Base* condition was used to measure the change in the proportion of the number of drivers whose travel time was faster (in the left tail), and the 99th percentile travel time in the *Base* condition was used to measure the change in travel time reliability (in the right tail). Travel time reliability is the probability that a trip between a given OD pair can be made successfully within an acceptable amount of travel time (Al-Deek and Emam 2006; Bates et al. 2001; Bell and Iida 1997; FHWA 2007; Lam and Small 2001; Lam and Wong 2003; Levinson and Zhang 2003; Rakha et al. 2006; Recker et al. 2005; Small et al. 2005; Sumalee and Watling 2003).

Although there are other proxy statistics to determine the change in travel time distribution, the 10th and 99th percentile travel time values in the *Base* condition were consistently used in analyzing the simulation results in order to meet the aim of this study, which is to compare the relative change in the travel time distribution imposed by the SEP. Especially, the 99th percentile travel time in the *Base* condition was selected to capture the change in travel time reliability between the *Base* and NR conditions as well as between the *Base* and SEP conditions, even though the 99th percentile travel time in the *Base* condition might be conservative in comparing the change in travel time reliability between the *Base* and NR conditions. Since the discussion of the measures for travel time uncertainty is necessarily brief, the interested reader can refer to a variety of references for additional information (Al-Deek and Emam 2006; Bates et al. 2001; Bell and Iida 1997; FHWA 2007; Ikhrata and Michell 1997; Lam and Small 2001; Levinson and Zhang 2003; Li et al. 2006; Noland and Polak 2002; Oh and Chung 2006; Rakha et al. 2006; Recker et al. 2005; Small et al. 2005; Turochy and Smith 2002).

The proportion of drivers whose travel time is less than the 99th percentile travel time in the *Base* condition—travel time reliability—is defined as:

$$R_i^m = \Pr(T_i^m \le \tau_R^m), \tag{76}$$

where R_i^m is the proportion of the number of drivers whose travel time is less than the 99th percentile travel time in the *Base* condition for trip direction *m* in the *i*th simulation state, τ_R^m is the 99th percentile travel time in the *Base* condition for trip direction *m*, and T_i^m is a continuous random variable for the travel time for trip direction *m* in the *i*th simulation state. Similarly, the proportion of the number of drivers whose travel time is less than the 10th percentile travel time in the *Base* condition (L_i^m) is:

$$L_i^m = \Pr(T_i^m \le \tau_L^m), \tag{77}$$

where τ_L^m is the 10th percentile travel time in the *Base* condition and the rest of the notation is as previously stated.

In order to test whether or not the difference in the sample proportions is statistically significant, the ordinary logit models were estimated. In the logit models for comparing R_i^m, the dependent variable was a binary variable which is 1 if the travel time of each vehicle is less than the 99th percentile travel time in the *Base* condition, and the independent variables were the indicator variables for the simulation states. The same independent variables were used in the logit models for comparing L_i^m, but the dependent variable was a binary variable which is 1 if the travel time of each vehicle is less than τ_L^m. In all models, the *Base* condition was considered consistently as a reference group as previously mentioned.

Table 52: Change in travel time distribution by simulation state and direction

	Variable	Change in the travel time distribution on the right tail		Change in the travel time distribution on the left tail	
	Direction	Northbound trips	Southbound trips	Northbound trips	Southbound trips
	Driver Group	% of Drivers < τ_R^{NB} [1]	% of Drivers < τ_R^{SB}	% of Drivers < τ_L^{NB} [2]	% of Drivers < τ_L^{SB}
Simulated network state	Base condition	99.00%	99.00%	10.00%	10.00%
	SEP condition	98.93% (0.930; 0.233)[3]	98.97% (0.961; 0.479)	2.75% (0.254; <0.001)	3.25% (0.302; <0.001)
	1-lane blockage condition	91.61% (0.110; <0.001)	82.81% (0.048; <0.001)	4.25% (0.399; <0.001)	4.85% (0.459; <0.001)
	2-lane blockage condition	0.17% (1.72E-05; <0.001)	12.61% (0.001; <0.001)	0% (N/A)	1% (0.091; <0.001)

[1] The proportion of the number of drivers whose travel time is less than the 99th percentile travel time in the *Base* condition.
[2] The proportion of the number of drivers whose travel time is less than the 10th percentile travel time in the *Base* condition.
[3] The estimated odds ratio and associated p-value are in parentheses.

Table 52 shows the estimates for the proportions by simulation state and direction, which were obtained from the simulation output results, as well as the associated odds ratios for the proportions, which were obtained by exponentiating the logit estimates. The insignificant odds ratio indicates that the proportions between the *Base* and the compared simulation state are not significantly different (i.e., $R_B^m = R_i^m; L_B^m = L_i^m$). The key findings are itemized below:

- The changes in the travel time distribution in the right tail are significant in the NR conditions as expected.
- Specifically, the travel time reliability significantly decreased in the NR conditions: the travel time reliability in the *two-lane blockage* condition (i.e., 0.17% or 12.61%) was remarkably less than those in the *Base* condition due to a serious breakdown, while the reduction in the travel time reliability in the *one-lane blockage* condition was small because of the relatively low demand during the non-peak-period.
- The change in the travel time distribution in the left tail in the NR conditions was also significant, which indicates that the change in travel time distribution in the NR conditions simultaneously occurred in both tails.
- Unlike the significant change in the travel time reliability in the NR conditions, the change in the travel time reliability in the SEP condition was insignificant (p-values: 0.233 and 0.479), suggesting that drivers can travel in the enforcement zone in the same acceptable amount of travel time regardless of the existence of the SEP, which is consistent with the findings in a prior study (Liu and Tate 2004).
- However, it is evident that the SEP contributes to reducing the proportion of faster drivers, which may eventually lead to the reduction in crashes by reducing the variance and mean travel speed in the enforcement zone. These results are congruous with the findings in previous studies (Liu and Tate 2004; Toledo et al. 2007).

In the next subsection, the change in the daily travel time uncertainty obtained as a byproduct of the SEP was estimated.

5.3.3 Daily Travel Time Uncertainty

The daily travel time uncertainty can be defined as a measure that shows how the travel time reliability during the non-peak period differs from the travel time reliability of other days during the same non-peak period. In order to estimate the daily travel time uncertainty, the probabilistic method assuming the most *n* probable system states was used as in prior studies (Al-Deek and Emam 2006; Sumalee and Watling 2003):

$$R(\mathbf{\Omega}_n) = \sum_{S_j \in \mathbf{\Omega}_n} \Pr(S_j) R(S_j), \tag{78}$$

where S_j is one of the simulation states, $\mathbf{\Omega}_n$ is the most *n* probable system states, which is a subset of all possible system states $\mathbf{\Omega}$, $R(S_j)$ is the travel time reliability for the system

state S_j, $\Pr(S_j)$ is the probability of the system state S_j, and $R(\mathbf{\Omega}_n)$ is the overall daily travel time reliability for a given period. The most *n* probable states are generally assumed in this method because it is difficult not only to enumerate all system states but also to obtain the reliability for all system states.

The simulation states described previously were used again for estimating the daily travel time uncertainty. Since the probabilities of the FF and NR conditions during with and without the SEP are different due to the reduction in crashes during the program period, the probabilities for the NR state were estimated:

$$\widehat{\Pr}\left(S_{NR} \mid \text{Before}\right) = \frac{\hat{\pi}}{D} > \widehat{\Pr}\left(S_{NR} \mid \text{Program}\right) = \frac{\hat{\lambda}}{D}, \tag{79}$$

where $\widehat{\Pr}\left(S_{NR} \mid \text{Before}\right)$ and $\widehat{\Pr}\left(S_{NR} \mid \text{Program}\right)$ are the probabilities of the NR state during the before and program period respectively, D is the number of days during the program period, $\hat{\pi}$ ($\hat{\lambda}$) is the estimates of crashes expected for the program period without SEP (with SEP).

In order to avoid overestimation of the change in the daily travel time uncertainty, we assumed that the NR conditions (the lane blockage states caused by crashes) were only related to the injury crashes, since the PDO crashes generally have relatively minor impacts on traffic (Ullman and Ogden 1996). In addition, the impact of the injury crashes on the network system, represented as one–lane block crash or two–lane block crash, was assumed to be the same during both periods. Thus, the daily travel time reliability is estimated for each crash state (i.e., one–lane block crash state or two–lane block crash state).

Table 53: Annual daily travel time unreliability (%)

Crash state	Direction	Unreliability (%)		
		Before period	Program period	Relative risk
1-lane blockage crash	Northbound trips	1.94;1.96[1]	1.58	1.23; 1.24
	Southbound trips	3.06;3.12	2.16	1.42; 1.44
2-lane blockage crash	Northbound trips	13.60;13.96	7.95	1.71; 1.76
	Southbound trips	12.01;12.33	7.05	1.70; 1.75

[1] The two estimates obtained from the BA study with traffic flow and the BA study with a comparison zone are represented respectively.

Table 53 shows the estimated annual daily travel time unreliability (1–reliability) by period and crash condition. The ratio of travel time unreliability between two periods is represented as the relative risk, which compares the risk of unreliable travel with and

without the SEP. The findings from comparing the travel time unreliability are summarized below:

- The daily travel time unreliability was consistently greater in the before period than in the program period.
- The risk of unreliable travel was at least 23% higher without the SEP than with the SEP, assuming the *one-lane blockage* condition.
- When assuming the *two-lane blockage* condition, the risk of unreliable travel was at least 70% greater without the SEP than with the SEP.
- These two scenarios represent a range of estimates depending on crash severity.

5.4 Change in Total Travel Time

In order to examine the overall effect of SEP and associated crashes on the SEP network, the total travel time estimated from the *j*th replication for the *i*th simulation state was used for comparison. The descriptive statistics for total travel time are summarized by simulation state in Table 54, which shows the unequal variances among states that often affect the statistical significance of estimates in the general linear model. Consequently, the homoskedastic variance assumption was examined by using the Brown-Forsythe test described in the previous section.

Table 54: Summary statistics for total travel time and the results of the BF test

Simulated network condition	N	Mean	Std. Dev.	F_{BF} (associated p-value; d.f.)
Base	30	7163.34	55.31	–
SEP	30	7175.92	48.88	0.08 (0.779; 1, 58)
1-lane blockage crash	60	7222.81	100.89	4.68 (0.033; 1, 88)
2-lane blockage crash	60	9168.79	809.79	32.65 (<0.001; 1, 88)
Total	180	7853.75	1044.21	40.56 (<0.001; 3, 176)

The four tests were conducted to detect heteroskedasticity among all states as well as between two states, in which the *Base* condition was always included as a reference group as previous. The test results in Table 54 show that variances in total travel time between the *Base* and NR conditions are not equal at α=0.05 (F_{BF}'s are 4.68 and 32.65 respectively), while the equal variance assumption between the *Base* and *SEP* conditions is insignificant at α=0.05, indicating that the dispersion of overall total travel time with and without the SEP is not significantly different. However, variances among all simulation conditions are not equal at α=0.05 (F_{BF}=40.56).

Since the group-wise heteroskedasticity was investigated, the generalized least square (GLS) estimation technique was used to estimate the expected total travel time for each simulation condition. For estimating the error term variances, the inverse of the sample variances by

simulation condition represented in Table 54 was directly used (see Equation (2)) , since replicate observations are made at each scenario (Greene 2003; Kutner et al. 2005).

Table 55: GLS estimation results for difference in total travel time with 95% CIs (veh-hours)

Pair	Difference in mean total travel time		
	Lower	Mean	Upper
SEP – Base	–14.01	12.59	39.18
1–lane Blockage Crash – Base	26.95	59.48	92.00
2–lane Blockage Crash – Base	1,798.18	2,005.46	2,212.74

Table 55 shows the GLS estimation results, in which the difference in mean total travel time between simulation states was estimated using the *Base* scenario as a reference group. The results show:

- The difference in the mean total travel time between the *Base* and SEP conditions is 12.59 vehicle-hours during the non-peak period. However, the difference is not significant (p-value=0.352), which might be attributed to the insignificant change in the travel time reliability between the *Base* and SEP state described in the previous subsection.
- Unlike the difference in the mean total travel time between the *Base* and SEP conditions, the mean total travel times of the NR conditions are significantly greater than the mean total travel time of the *Base* condition at α=0.05.
  - Specifically, the mean total travel time of the *two–lane blockage* condition is remarkably higher than that of the *Base* condition—between 1,798 vehicle–hours and 2,212 vehicle–hours.
  - The difference in mean total travel time between the *Base* and the *one-lane blockage* condition is relatively small.
- The GLS estimation results indicate that there is no significant change in the total travel time in the SEP condition, which is consistent with the finding that there is no change in the travel time reliability.
- In contrast, the NR conditions lead to a significant increase in total travel times.

Therefore, the total travel time savings is estimated using the difference in mean total travel times with and without the SEP in the NR conditions. The reduction in the injury crashes was used again with the assumption that the same impact of the injury crashes on the network system during both periods. Consequently, the total travel time savings resulting from the SEP was estimated:

$$TTS = \hat{\delta} \cdot \widehat{D}_M, \tag{80}$$

where *TTS* is total travel time savings (vehicle-hours) resulting from the SEP, $\hat{\delta}$ is the estimate of the reduction in the injury crashes in the previous chapter, and $\widehat{D}_M$ is the estimate of the increase in total travel time per crash in the NR conditions summarized in

Table 55. The annual total travel time savings by crash state is summarized in Table 56, and the results indicate that:

- The potential total travel time savings as a byproduct of the SEP was at least 569 vehicle-hours/year when assuming the *one-lane block crash* state and at least 37,981 vehicle-hours/year when assuming the *two-lane block crash* state.
- The large difference between the minimum total travel time savings by crash condition are attributed to the low traffic flow rate during the non-peak period.

Table 56: Total travel time savings (veh-hours/year)

Simulated network condition	BA study with traffic flow correction			EB BA study with time-varying κ		
	Lower	Mean	Upper	Lower	Mean	Upper
1-lane blockage crash	569	1256	1943	606	1336	2067
2-lane blockage crash	37981	42360	46738	40402	45060	49717

If a reasonable value of travel time savings is assigned to the estimates in Table 56, using say lower and upper estimates from Ozbay et. al (2006) of $15.00 to $20.00 per hour respectively, then mean estimates (using EB BA study results) range from a low of $20,040 to a high of $26,720 for a one-lane blockage crash. For a two-lane blockage crash, mean estimates of the value of travel time savings range from $675,900 to $901,200 per year.

Chapter 6 Conceptual Plan for Long-Term Deployment of Automated Freeway Speed Photo Enforcement in Arizona

This chapter presents a conceptual plan for deploying an automated freeway speed photo enforcement program in Arizona. It addresses the use of appropriate analytical methods, the identification of appropriate locations, performance measures, and benefit and cost assessments necessary to implement and evaluate a statewide program. Legislative, public outreach, and financial impacts and procedures of a statewide program shall be provided in a separate report by the City of Scottsdale, Arizona.

The broadening of a photo enforcement program in Arizona requires that two major activities be undertaken; implementation and evaluation. Implementation involves the selection of sites and installation of camera systems to enforce speeds over some future time horizon. Evaluation involves the proper collection of data and monitoring of installed systems so that effectiveness and impacts of the program can be accurately measured. These two major activities are discussed in turn.

Implementation of an Arizona Freeway Photo Enforcement Program

The following eight steps constitute the conceptual framework and action plan for implementing a statewide photo enforcement program. As a reminder, these steps do not include details on legislative, public outreach, and financial actions that must be considered.

1. *Identify candidate sites*. In cooperation with ADOT and DPS, identify and inventory candidate freeways, interstates, and highways within Arizona that qualify as suitable candidates for "freeway" photo enforcement. These candidate locations include all locations that meet the following conditions: 1) they are maintained by ADOT and enforced by DPS; 2) in cases where condition 1 is not met, a suitable arrangement between cooperating agencies is arranged; 3) sites are high-speed, limited-access multi-lane divided roadways posted at 65mph or greater; and 4) when condition 3 is not met, the ADOT and/or DPS has legitimate reason to add a facility to the list of candidate sites.
2. *Collect exposure, crash, and speed data on candidate sites*. As conveyed in the analysis portion of this report, ideal sites will reveal speeding behavior and higher than expected crash counts compared to a reference group of facilities. Since the sites will be road segments and not intersections, a segment will be defined as a homogenous segment of road, absent of major design and/or operational changes that will significantly affect safety. For example, a four-mile segment of SR 51 might be defined between major interchanges where the number of lanes is constant, pavement type is contiguous, and the roadside environment is homogenous.

The research team will need to make decisions as to what objective criteria should be used to define road segments, and these criteria should then be applied uniformly to identify a candidate list of road segments in Arizona. The criteria might be established in an iterative fashion as sites are examined.

Once road segments serving as candidate sites are determined, exposure, crash, and speed data must be collected for these segments. Segment data (e.g., number of lanes, median type, posted speed, etc.), along with exposure (i.e., VMT), crash, and speed data should be imported/managed in an electronic database for later steps in the process. Crash data should be culled to identify target crashes—i.e., crashes that occurred during free-flow traffic conditions and that are otherwise deemed to be preventable via automated photo enforcement. The team might also consider removing DUI and otherwise driver-impaired crashes from the remaining crashes, as these crashes may not be preventable via photo enforcement. The set of variables describing the site should be uniformly collected and stored, and should be based on their impact of expected safety (from the literature, etc.).

3. *Develop safety performance functions of candidate sites*. Data obtained in step 2 are used to develop safety performance functions for freeway segments in the state of Arizona. These safety performance functions should be modeled using negative binomial regression models, with target crashes (e.g., off-peak period crashes) as the dependent variable, and exposure, geometric, and operational variables as predictors. Models for functional classes of roadways can be estimated separately, or an indicator variable for functional class can be used in a single safety performance function model. If the latter is the case, interactions with main-effect variables should be considered with the functional class indicator. This step will produce a set of models that can predict the expected safety performance of candidate road segments. These models must also include an offset that accounts for segment length.

4. *Rank candidate sites*. The safety performance functions developed in step 3 are now used to rank order the candidate sites for safety effectiveness. There are two recommended options for accomplishing this. The first is to calculate the correction potential as the observed target crash count in the segment minus the expected count (based on safety performance function) across all sites. Sites with the largest correction potential will yield the largest positive differences between observed and expected crash counts. A second, more complicated method is based on the Empirical Bayes' approach, which corrects for possible regression to the mean effects of sites, and requires that the crash history of the sites is known to perform the calculation. The basic procedure is described in section 4.5 of this report.

   This step will produce a list of ranked sites, with the top sites representing the sites in Arizona with the highest potential for improvement from automated photo enforcement. After this statistical screening, the sites should be further screened

to make sure the sites possess the qualitative criteria for improvement; high prevalence of speeding and speed-related crashes.

5. *Conduct field investigations*. Field investigations of the top ranked sites are now required. Site visits should be systematically conducted by a qualified team of evaluators. This task will focus on assessing the operational characteristics associated with sites identified through statistical analysis as 'correctable'. The purpose here is threefold: to ensure that photo enforcement technologies are appropriate and/or feasible at the locations, to identify technology configurations that would be most appropriate/beneficial; and to rule out other operational features that could have led to the observed high accident frequencies (i.e., restricted sight distances, intensely used weaving section, excessive glare conditions, etc.), reducing the potential effectiveness of photo enforcement. This step will further reduce the list of candidate sites for treatment.

6. *Examine photo enforcement technology options.* There are various technological options for administering freeway photo enforcement. The type applied in Scottsdale essentially sets a small speed trap using highly precise double loop detectors to measure speeds. A second type uses a much longer speed trap—and measures travel time between two points (and matches license plates between locations). The first type is quite suitable when freeway interchanges are tightly spaced (e.g., every two miles), whereas the latter might be more suitable when access is severely restricted for long periods (e.g., many sections of Interstate 10 between Phoenix and Tucson). The appropriate mix of technologies should be identified for each of the top ranked sites.

7. *Conduct financial/cost analysis*. The selection and implementation of photo enforcement will likely proceed on a case-by-case basis. Task 6 resulted in a ranked list of candidate locations that offer the most potential for improvement. How many of the top-ranked sites that are selected for photo enforcement depends on a large number of financial, cost, and political factors, many of which cannot be predicted. For example, partnerships between local jurisdictions and the ADOT and DPS may significantly change the cost/financial constraints at a particular site. Nonetheless, the costs and anticipated benefits of photo enforcement programs at top sites must now be estimated. These costs may also include revenue forecasts, impact on the courts and legal system, etc., and will require detailed cost analysis and cooperation across affected agencies.

8. *Prepare site implementation plans*. Each selected site will need to have an implementation plan. Each plan will be different and will reflect the uniqueness of the site and affected jurisdictions and stakeholders. The common denominator among sites is that all will have been identified as a site with high potential for improvement given installation of photo enforcement. The implementation plans shall include phasing, design, build, financial, administration, legal, and oversight components. The City of Scottsdale should be able to provide an example of its implementation plan to serve as a template.

Of course a program of this magnitude and importance requires careful evaluation, so that the cost effectiveness of the safety investment can be determined in the future. The evaluation reflected in this report represents a significant and substantial effort in evaluation, and serves as a template for future evaluations.

The technical details on how to evaluate a photo enforcement program will not be repeated here for obvious reasons. However, a summary of the most critical aspects of a technical evaluation are provided. Due to lack of data in some cases, evaluation could not be conducted on the Loop 101 demonstration.

1. *Speed Impacts.* The SEP, of course, is expected to impact speeds. The most important speeds to monitor are free-flow (off-peak) upper percentile speeds. Since the programs necessarily detect (instantaneous) speeds, the equipment also serves as a reliable source for speeding data. It is important to consider the collection of speeds prior the program and prior to the functioning of equipment. If an alternative method for measuring speeds is used (e.g., radar, loops, laser, etc.) prior to the SEP, there needs to be time measurement overlap between the two devices (the camera speed detector and the alternate) so that they can be calibrated against each other. In addition, it is important to assess speeds upstream and downstream of the SEP with a comparable (or calibrated) measuring device so that potential spillover effects can be measured and assessed.

2. *Crash Impacts.* Obtaining complete and accurate crash records is important for assessment. High-profile crashes, usually serious injuries and fatalities, should be carefully tracked through media and legal sources, since these crashes often do not get entered into a database system as quickly as less serious crashes due to pending litigation. It is also important to be able to determine whether or not crashes are preventable by photo enforcement. For example, an unusually high number of DUI related crashes (in before or after periods) may need to be removed from the dataset in order obtain accurate results. Finally, crashes at comparison sites (e.g., sites identified in Step 1 of implementation) should be compiled to serve as comparison sites in an evaluation.

3. *Exposure, geometric, and weather data.* In order to reliably estimate the expected safety performance of facilities and to identify anomalous conditions, exposure (e.g., VMT), geometric (e.g., number of lanes, median type, etc.), and weather data (wet pavement, high winds, etc.) need to be collected at program and candidate sites.

Combined with a systematic evaluation approach, as described in this report, these three data collection efforts will provide the ability to effectively and accurately monitor and evaluate the safety effectiveness of a statewide freeway photo enforcement program on a case-by-case basis.

Chapter 7 Conclusions and Recommendations

This report presents the comprehensive analysis results of the speed enforcement camera demonstration program that was implemented on Loop 101 from January 2006 to October 2006. This study estimated the impacts of the SEP on traffic safety, speed, speeding behavior, and travel time. The analyzed SEP is in Scottsdale, Arizona, and is the first fixed-camera photo enforcement program on a freeway in Arizona and possibly in the United States. The following conclusions were drawn from a variety of detailed statistical analyses, site visits, logical reasoning, and simulation analysis:

Impact of the SEP on Speeding Behavior and Speed

The speeding behavior was analyzed by comparing the speeding detection frequency during the *before*, *program*, *after*, and *reactivation* periods, collected at the six enforcement camera locations, and the impact on speed was compared by analyzing the mean speeds during the *before* and *program* periods. The findings from the comparison are summarized below:

1. Speeding detection frequency (speeds ≥ 76 mph) increased by a factor of 10.5 times after the SEP was temporarily terminated. During this termination the cameras were "bagged" and advertising and news media advertised the end of the program.
2. The detection frequency for the *reactivation* period in 2007 is not statistically different than that for the *program* period in 2006, indicating that the activation of the SEP contributed to reducing drivers' speeding behavior.
3. The Scottsdale Loop 101 SEP appears to be an effective deterrent to speeding in excess of 75 mph, as evidenced by the significant increase in speeding when the cameras were deactivated.
4. The SEP not only reduced the average speed at the enforcement camera sites by about 9 mph, but also contributed to reducing the speed dispersion at the enforcement camera sites. Thus, as prior research has revealed, both the prerequisites for crash reduction (safety improvement) are met with the SEP.
5. The reduction in the mean and variance of speed resulting from the SEP depends on traffic flow: the reduction increased as traffic flow decreased due to the well known relationship between speed and traffic flow. Thus, the magnitude of speed effects of the SEP is inversely related to traffic flow.

Impact of the SEP on Safety

The impact of the SEP on safety was analyzed by comparing the observed number of crashes with the SEP to the expected number of crashes without the SEP. The expected number of crashes was carefully estimated by accounting for the change in traffic flow,

trend effect, and regression-to-the-mean phenomenon simultaneously. The estimation results are summarized below:

1. The total number of target crashes was reduced by estimates of 54%. In addition, the total number of injury crashes was reduced by about 48%, and the total number of PDO crashes decreased by about 56%.
2. All but rear-end crash types appear to have been reduced. Although the changes in safety for rear-end crashes were inconsistent among evaluation methods (and their assumptions), the decrease in rear-end crashes was not significant. We conclude that rear-end crashes were unaffected by the SEP or increased slightly, depending on the particular analysis method and associated assumptions.
3. Swapping of crash types is common for safety countermeasures—many countermeasures exhibit the 'crash swapping' phenomenon observed in this study (left-turn channelization, red-light cameras, conversion of stop signs to signals, etc.) Thus, it is quite expected to see varying magnitudes of reductions across crash categories, and even some increases are possible.
4. The total estimated SEP benefits range from an estimated $16.5 million to $17.1 million per year, depending on the analysis type and associated assumptions.
5. Consequently, this study revealed that the speed enforcement camera is a promising countermeasure to reduce crashes in Arizona, which is also consistent with findings in other countries.

Impact of the SEP on Travel Times

The impact of the SEP on travel times and travel time uncertainty was estimated by simulating network traffic conditions with and without the SEP. Travel time impacts from changes in average travel speeds and non-recurrent congestion (by-products of the SEP and its impact on crashes) are estimated by simulating the enforcement zone within the broader Loop 101 freeway network in Scottsdale. The following conclusions were drawn from the simulation analysis results:

1. The SEP shifted the distribution of the travel time of the enforcement zone to the right by significantly reducing the number of faster drivers (by at least a 67.5% decrease in the proportion of the number of faster drivers), while travel time reliability remains the same regardless of the existence of the SEP.
2. The significant change in travel time distribution in the left tail (fast drivers) was a primary factor in reducing the variance and mean speed, which may ultimately lead to a reduction in crash frequency in the enforcement zone during the *program* period.
3. There is no significant difference in the total free-flow travel time with and without the SEP, suggesting that drivers can travel in the enforcement zone in the same acceptable amount of travel time regardless of the existence of the SEP
4. The insignificant difference in total free-flow travel time with and without the SEP conditions led to total travel time savings, which resulted from the reduction in crash frequency. The reduction was at least 569 vehicle-hours/year when

assuming the *one-lane block crash* state and at least 37,981 vehicle-hours/year when assuming the *two-lane block crash* state.

5. Speed enforcement on the Loop 101 not only improved safety but also improved mobility through travel time savings, improved travel time reliability, and reduced travel time uncertainty. The annual benefit of travel time savings ranges from a low of $20,040 (one-lane blockage crash assuming $15/hr value of travel time savings) to a high of $901,200 (two-lane blockage crash assuming $20.00/hr of travel time savings).

Recommendations

The following actions are recommended to maximize the impacts of speed enforcement cameras and to improve the study results. Although the SEP is not a panacea to reduce speeding-related crashes, the SEP may be a promising countermeasure given the following considerations,

1. An "ideal" site for SEP exhibits relatively high rates of speed and corresponding severity of crashes prior to implementation. The crash history of a site should be used to aid in selection, and sites that reveal a 'worse than average' safety record should be identified as candidate sites. A statistical model that predicts the expected safety performance of sites should be developed to help identify candidate sites, and predictors should include exposure and some important geometric features.
2. Design of SEP sites should consider the element of surprise to drivers and should aim to minimize it. For example, the placement of cameras in close proximity to high information load locations (e.g., on- and off-ramps, underpasses, billboards, weaving sections, directional signs, etc.) should be avoided. Placement of cameras in sight-restricted locations should be avoided. Efforts should be made to increase driver expectation of speed enforcement camera locations.
3. Photo enforcement technology that measures average speeds (instead of effectively instantaneous speeds) over a long section of freeway (e.g., five miles) may offer some operational advantages over the currently used technology, including reduced sudden braking (and subsequent rear-end accidents).
4. Spillover effects are more likely in a dispersed system of enforcement zones compared to a concentrated location.
5. Further evaluation (of future programs) is needed to enable the continued knowledge and improvement of safety performance of SEPs.
6. In future evaluations, additional speed data may enable the assessment of spillover effects. Currently, the extent and magnitude of spillover effects of the SEP are uncertain.

References

1. Abbess, C., Jarrett, D., and Wright, C. C. (1981). "Accidents at blackspots: estimating the effectiveness of remedial treatment, with special reference to the 'Regression-to-Mean' effect." *Traffic Engineering and Control*, 22(10), 535-542.
2. ADOT. (2006). "Arizona motor vehicle crash facts 2005." Arizona Department of Transportation.
3. Al-Deek, H. M., and Emam, E. B. (2006). "Computing travel time reliability in transportation networks with multistates and dependent link failures." *Journal of Computing in Civil Engineering*, 20(5), 317-327.
4. Bates, J., Polak, J., Jones, P., and Cook, A. (2001). "The valuation of reliability for personal travel." *Transportation Research Part E: Logistics and Transportation Review*, 37(2-3), 191-229.
5. Bell, M. G. H., and Iida, Y. (1997). *Transportation network analysis*, John Wiley & Sons, New York.
6. Blincoe, L., Seay, A., Zaloshnja, E., Miller, T., Romano, E., S.Luchter, and R.Spicer. (2002). "Economic impact of motor vehicle crashes, 2000." National Highway Traffic Safety Administration.
7. Caliper. (2006a). "TransModeler user's guide: Chapter 1. TransModeler basics." Caliper Corporation, 1-22.
8. Caliper. (2006b). "TransModeler user's guide: Chapter 7. Microscopic model and parameters." Caliper Corporation, 135-237.
9. Cameron, A. C., and Trivedi, P. K. (1998). *Regression analysis of count data*, Cambridge University Press.
10. Campbell, D. T., and Kenny, D. A. (1999). *A primer on regression artifacts*, The Guilford Press, New York.
11. Carlin, B. P., and Louis, T. A. (2000). *Bayes' and empirical Bayes' methods for data analysis*, Chapman & Hall/CRC, New York.
12. Champness, P., and Folkman, L. (2005). "Time and distance halo effects of an overtly deployed mobile speed camera." *The Australasian Road Safety Research, Policing and Education Conference Proceedings*.
13. Chen, G., Meckle, W., and Wilson, J. (2002). "Speed and safety effect of photo radar enforcement on a highway corridor in British Columbia." *Accident Analysis and Prevention*, 34(2), 129-138.
14. Cheng, W., and Washington, S. P. (2005). "Experimental evaluation of hotspot identification methods." *Accident Analysis & Prevention*, 37(5), 870-881.
15. Chu, L., Liu, H. X., and Recker, W. "Evaluation of potential ITS strategies under non-recurrent congestion using microscopic simulation." *Transportation Research Board 83rd Annual Meeting Washington, D.C.*, Washington, D.C.

16. Cunningham, C. M., Hummer, J. E., and Moon, J. (2005). "An evaluation of the safety affects of speed enforcement cameras in Charlotte, North Carolina." Institute for Transportation Research and Education, North Carolina State University.

17. Elvik, R. (1997). "Effects on accidents of automatic speed enforcement in Norway." *In Transportation Research Record: Journal of the Transportation Research Board, No. 1595*, 14-19.

18. Elvik, R., and Vaa, T. (2004). *The handbook of road safety measures*, Elsevier Science, Ltd. , Oxford. United Kingdom.

19. FHWA. (2007). "Travel time reliability: making it there on time, all the time."

20. Garber, N. J., and Ehrhart, A. A. (2000). "Effect of speed, flow, and geometric characteristics on crash frequency for two-lane highways." *In Transportation Research Record: Journal of the Transportation Research Board, No. 1717*, 76-83.

21. Garber, N. J., and Gadiraju, R. (1989). "Factors affecting speed variance and its influence on accidents." *In Transportation Research Record: Journal of the Transportation Research Board, No. 1213*, 64-71.

22. Garber, N. J., Miller, J. S., Sun, X., and Yuan, B. (2006). "Safety impacts of differential speed limits for trucks and passenger cars on rural interstate highways: A modified empirical Bayes' approach." *Journal of Transportation Engineering*, 132(1), 19-29.

23. Goldenbeld, C., and van Schagen, I. (2005). "The effects of speed enforcement with mobile radar on speed and accidents: An evaluation study on rural roads in the Dutch province Friesland." *Accident Analysis and Prevention*, 37(6), 1135-1144.

24. Greene, W. H. (2003). *Econometric analysis*, Prentice Hall, Upper Saddle River, New Jersey.

25. Griffin, L. I., and Flowers, R. J. (1997). "A discussion of six procedures for evaluating highway safety projects." Texas Transportation Institute, Texas A&M University, College Station.

26. Ha, T., Kang, J., and Park, J. (2003). "The effects of automated speed enforcement systems on traffic flow characteristics and accidents in Korea." *ITE Journal*, 73(2), 28-31.

27. Harwood, D. W., Bauer, K. M., Potts, I. B., Torbic, D. J., Richard, K. R., Rabbani, E. R. K., Hauer, E., and Elefteriadou, L. (2002). "Safety effectiveness of intersection left- and right-turn lanes." Federal Highway Administration, Washington, D.C.

28. Hauer, E. (1992). "Empirical Bayes' approach to the estimation of "unsafety": The multivariate regression method." *Accident Analysis & Prevention*, 24(5), 457-477.

29. Hauer, E. (1996). "Statistical test of difference between expected accident frequencies." *In Transportation Research Record: Journal of the Transportation Research Board, No. 1542*, 24-29.

30. Hauer, E. (1997). *Observational before-after studies in road safety: Estimating the effect of highway and traffic engineering measures on road safety*, Pergamon, Elsevier Science Ltd. , Oxford, U.K.

31. Hauer, E., Ahlin, F. J., and Bowser, J. S. (1982). "Speed enforcement and speed choice." *Accident Analysis and Prevention*, 14(4), 267-278.

32. Hauer, E., Harwood, D. W., Council, F. M., and Griffith, M. S. (2002). "Estimating safety by the empirical Bayes' method: A tutorial." *In Transportation Research Record: Journal of the Transportation Research Board, No. 1784*, 126-131.

33. Hauer, E., and Persaud, B. (1983). "Common bias in before-and-after accident comparisons and its elimination." *In Transportation Research Record: Journal of the Transportation Research Board, No. 905*, 164-174.

34. Hauer, E., and Persaud, B. N. (1987). "How to estimate the safety of rail-highway grade crossings and the safety effects of warning devices." *In Transportation Research Record: Journal of the Transportation Research Board, No. 1114*, 131-140.

35. Hess, S. (2004). "Analysis of the Effects of Speed Limit Enforcement Cameras: Differentiation by Road Type and Catchment Area." *In Transportation Research Record: Journal of the Transportation Research Board, No. 1865*, 28-34.

36. Hess, S., and Polak, J. (2003). "Effects of speed limit enforcement cameras on accident rates." *In Transportation Research Record: Journal of the Transportation Research Board, No. 1830*, 25-33.

37. Hines, W. W., Montgomery, D. C., Goldsman, D. M., and Borror, C. M. (2003). *Probability and statistics in engineering*, John Wiley & Sons, New York.

38. Horiguchi, R., and Kuwahara, M. (2005). "The art of the utilization of traffic simulation models: How do we make them reliable tools?" Simulation approaches in transportation analysis: recent advances and challenges, R. Kitamura and M. Kuwahara, eds., Springer Science.

39. Ikhrata, H., and Michell, P. (1997). "Technical report of Southern California Association of Governments' Transportation performance indicators." *In Transportation Research Record: Journal of the Transportation Research Board, No. 1606*, 103-114.

40. Joksch, H. C. (1993). "Velocity change and fatality risk in a crash: A rule of thumb." *Accident Analysis and Prevention*, 25(1), 103-104.

41. Kelton, W. D., Sadowski, R. P., and Sturrock, D. T. (2004). *Simulation with ARENA*, McGraw-Hill, New York.

42. Kloeden, C. N., Ponte, G., and McLean, A. J. (2001). "Travelling speed and the risk of crash involvement on rural roads." *CR 204*, Road Accident Research Unit, Adelaide University.

43. Kutner, M. H., Nachtsheim, C. J., Neter, J., and Li, W. (2005). *Applied Linear Statistical Models*, McGraw-Hill Irwin, New York.

44. Kweon, Y.-J., and Kockelman, K. M. (2005). "Safety effects of speed limit changes: Use of panel models, including speed, use, and design variables." *In Transportation Research Record: Journal of the Transportation Research Board, No. 1908*, 148-158.

45. Lam, T. C., and Small, K. A. (2001). "The value of time and reliability: measurement from a value pricing experiment." *Transportation Research Part E: Logistics and Transportation Review*, 37(2-3), 231-251.

46. Lam, W. H. K., and Wong, G. C. K. (2003). "A macroscopic approach to evaluate the effect of incident on travel time reliability of a highway." *Journal of the Eastern Asia Society for Transportation Studies*, 5, 1065-1074.

47. Lamm, R., and Kloeckner, J. H. (1984). "Increase of traffic safety by surveillance of speed limits with automatic radar devices on a dangerous section of a German Autobahn: A long-term investigation." *In Transportation Research Record: Journal of the Transportation Research Board, No. 974*, 8-16.

48. Lave, C., and Lave, L. (1998). "Fuel economy and auto safety regulation: Is the cure worse than the disease?" Essays in transportation economics and policy, J. Gomez-Ibanez, W. B. Tye, and C. Winston, eds., Brookings Institution Press, Washington, D.C., 257-289.

49. Lave, C. A. (1985). "Speeding, coordination, and the 55 mph limit." *The American Economic Review*, 75(5), 1159-1164.

50. Levinson, D., and Zhang, L. (2003). "Travel time variability after a shock: The case of the Twin Cities ramp meter shut off." The Network Reliability of Transport, Pergamon, San Diego, 385-402.

51. Levy, D. T., and Asch, P. (1989). "Speeding, coordination, and the 55 mph limit: Comment." *The American Economic Review*, 79(4), 913-915.

52. Li, R., Rose, G., and Sarvi, M. (2006). "Using automatic vehicle identification data to gain insight into travel time variability and its causes." *In Transportation Research Record: Journal of the Transportation Research Board, No. 1945*, 24-32.

53. Liu, R., and Tate, J. (2004). "Network effects of intelligent speed adaptation systems." *Transportation*, 31(3), 297-325.

54. Lord, D. (2006). "Modeling motor vehicle crashes using Poisson-gamma models: Examining the effects of low sample mean values and small sample size on the estimation of the fixed dispersion parameter." *Accident Analysis & Prevention*, 38(4), 751-766.

55. Lord, D., and Persaud, B. N. (2000). "Accident prediction models with and without trend: Application of the generalized estimating equations procedure." *In Transportation Research Record: Journal of the Transportation Research Board, No. 1717*, 102-108.

56. Moore, V. M., Dolinis, J., and Woodward, A. J. (1995). "Vehicle speed and risk of a severe crash." *Epidemiology*, 6(3), 258-262.

57. National Highway Traffic Safety Administration. (2005). "Traffic safety facts: Speeding." NHTSA's National Center for Statistics and Analysis.

58. Noland, R. B., and Polak, J. W. (2002). "Travel time variability: a review of theoretical and empirical issues." *Transport Reviews*, 22(1), 39-54.

59. Oh, J.-S., and Chung, Y. (2006). "Calculation of travel time variability from loop detector data." *In Transportation Research Record: Journal of the Transportation Research Board, No. 1945*, 12-23.

60. Oh, J.-S., and Jayakrishnan, R. (2002). "Emergence of private advanced traveled information system providers and their effect on traffic network performance." *In Transportation Research Record: Journal of Transportation Research Board, No. 1783*, 167-177.

61. Ozbay, K., et. al "Theoretical derivation of value of travel time and demand elasticity: Evidence from New Jersey Turnpike Toll Road." *In Transportation Research Record: Journal of the Transportation Research Board, No. 1985*, 248-256.

62. Pilkington, P., and Kinra, S. (2005). "Effectiveness of speed cameras in preventing road traffic collisions and related casualties: Systematic review." *British Medical Journal*, 330(7487), 331-334.

63. Przyborowski, J., and Wilenski, H. (1940). "Homogeneity of results in testing samples from Poisson series: With an application to testing clover seed for dodder." *Biometrika*, 31(3/4), 313-323.

64. Rakha, H. A., El-Shawarby, I., Arafeh, M., and Dion, F. "Estimating path travel-time reliability." *Transportation Research Board 86th Annual Meeting*, Washington, D.C.

65. Recker, W., Chung, Y., Park, J., Wang, L., Chen, A., Ji, Z., Liu, H., Horrocks, M., and Oh, J.-S. (2005). "Considering risk-taking behavior in travel time reliability." *California PATH Research Report UCB-ITS-PRR-2005-3*, INSTITUTE OF TRANSPORTATION STUDIES.

66. Retting, R. A., and Farmer, C. M. (2003). "Evaluation of speed camera enforcement in the District of Columbia." *In Transportation Research Record: Journal of the Transportation Research Board, No. 1830*, 34-37.

67. Roberts, C. A., and brown-Esplain, J. (2005). "Technical evaluation of photo speed enforcement for freeways." *ADOT-AZ-05-596*, AZTrans: The Arizona Laboratory for Applied Transportation Research.

68. Roess, R. P., Prassas, E. S., and McShane, W. R. (2004). *Traffic engineering*, Pearson Prentice Hall, London.

69. Sharma, S. L., and Datta, T. K. (2007). "Investigation of "Regression-to-Mean" effect in traffic safety evaluation methodologies." Transportation Research Board 86th Annual Meeting, Washington, DC,.

70. Shin, K., and Washington, S. P. (2007a). "The impact of red light cameras on safety in Arizona." *Accident Analysis and Prevention*, 39, 1212-1221.

71. Shin, K., and Washington, S. P. "Investigating the regression to the mean effect in traffic safety study." *Research in Interdisciplinary Science and Engineering*, Arizona State University, Tempe, Arizona.

72. Sisiopiku, V. P., and Patel, H. (1999). "Study of the impact of police enforcement on motorists's speeds." *In Transportation Research Record: Journal of the Transportation Research Board, No. 1693*, 31-36.

73. Skabardonis, A., Petty, K., Noeimi, H., Rydzewski, D., and Varaiya, P. P. (1996). "I-880 field experiment: Data-base development and indident delay estimation procedures." *In Transportation Research Record: Journal of Transportation Research Board, No. 1068*, 204-212.

74. Skszek, S. L. (2004). "Actual speeds on the roads compared to the posted limits." Arizona Department of Transportation.

75. Small, K. A., Winston, C., and Yan, J. (2005). "Uncovering the distribution of motorists' preferences for travel time and reliability." *Econometrica*, 73(4), 1367-1382.

76. Solomon, D. (1964). "Accidents on main rural highways related to speed, driver, and vehicle." Federal Highway Administration, Washington, D.C.

77. Stuster, J., Coffman, Z., and D., W. (1998). "Synthesis of safety research related to speed and speed management." FHWA.

78. Sumalee, A., and Watling, D. (2003). "Travel time reliability in a network with dependent link modes and partial driver response." *Journal of the Eastern Asia Society for Transportation Studies* 5, 1686-1701.

79. Synder, D. (1989). "Speeding, coordination, and the 55 mph limit: Comment." *The American Economic Review*, 79(4), 922-925.

80. Toledo, T., Albert, G., and Hakkert, S. "A simulation-based evaluation of the impact of active speed limiters on traffic flow and safety." *Transportation Research Board 86th Annual Meeting*, Washington, D.C.

81. Toledo, T., Koutsopoulos, H., Ben-Akiva, M., and Jha, M. (2005). "Microscopic traffic simulation: Models and application." Simulation approaches in transportation analysis : recent advances and challenges, R. Kitamura and M. Kuwahara, eds., Springer Science.

82. Transportation Research Board. (2000). *Highway capacity manual*, Washington, D.C.

83. Turochy, R. E., and Smith, B. L. (2002). "Measuring variability in traffic conditions by using archived traffic data." *In Transportation Research Record: Journal of the Transportation Research Board, No. 1804*, 168-172.

84. Ullman, G. L., and Ogden, M. A. (1996). "Analysis of major freeway incidents in Houston, Texas." *In Transportation Research Record: Journal of Transportation Research Board, No. 1544*, 221-227.

85. Vaa, T. (1997). "Increased police enforcement: effects on speed." *Accident Analysis and Prevention*, 29(3), 373-385.

86. Waard, D., and Rooijers, T. (1994). "An experimental study to evaluate the effectiveness of different methods and intensities of law enforcement on driving speed on motorways." *Accident Analysis and Prevention*, 26(6), 751.

87. Washington, S. P., Karlaftis, M. G., and Mannering, F. L. (2003). *Statistical and econometric methods for transportation data analysis*, Chapman & Hall/CRC, New York.

88. Washington, S. P., and Shin, K. (2005). "The impact of red light cameras (automated enforcement) on safety in Arizona." *FHWA-AZ-05-550*.

89. Wicks, D. A., and Lieberman, E. B. (1980). "Development and testing of INTRAS : A microscopic freeway simulation model vol.1. program design, parameter calibration and freeway dynamics component development." KLD Associates, Inc.

90. Winkelmann, R. (2003). *Econometric analysis of count data*, Springer, New York.

91. Wong, S. C., Sze, N. N., Lo, H. K., Hung, W. T., and Loo, B. P. Y. (2005). "Would relaxing speed limits aggravate safety?: A case study of Hong Kong." *Accident Analysis and Prevention*, 37(2), 377-388.

92. Yang, Q., and Morgan, D. "A hybrid traffic simulation model." *Transportation Research Board 85th Annual Meeting*, Washington, D.C.